Greenhouse Gas Fluxes from Forest Soils and Trees

by

Scott L. Pitz

A dissertation submitted to the Johns Hopkins University in conformity with the requirements for the degree of Doctor of Philosophy

Baltimore, Maryland

February, 2019

Abstract

Forests are major sources of terrestrial methane (CH_4) and carbon dioxide (CO_2) fluxes but not all surfaces within forests have been accounted for and measured. Stem respiration is a well-known source of CO_2, but more recently tree stems have been shown to be sources of CH_4 in wetlands and upland habitats. I established a study transect along a natural moisture gradient, with one end anchored in a forested wetland, the other in an upland forest with a transitional zone at the midpoint. Stem and soil fluxes of CH_4 and CO_2 were measured using static chambers during the 2013 and 2014 growing seasons, from May to October. Measurable CH_4 fluxes from tree stems were not always observed, but every individual tree in my experiment released measurable CH_4 flux at some point during the study period. Automated, high frequency stem flux measurements indicate that stem temperature or transpiration may be driving CH_4 fluxes. These results indicate that tree stems represent overlooked sources of CH_4 in forested habitats and warrant investigation to further refine CH_4 budgets and inventories.

Soil respiration is one of the largest annual fluxes of carbon to the atmosphere and tropical rainforests have some the highest soil respiration rates of any ecosystem. I measured soil respiration in a tropical rainforest in eastern Ecuador using traditional chamber-based methods and newer, unproven gradient methods. The gradient methodology has the potential to provide continuous soil respiration measurements, greatly reducing uncertainty in global soil respiration estimates, but it did not work well in the wet, high clay soils found at my site. Further refinement of the gradient method is required before it can be usefully deployed in soil respiration studies.

Acknowledgements

I would like to thank Katalin Szlavecz and Anand Gnanadesikan for being my advisors and tireless supporters. I would also like to thank my family and friends. I couldn't have done this without you.

I would also like to thank Chih-Han Chang, Xu Yang, Michael Bernard, Lijun Xia, Jerry Burgess, Andrew Peresta, Blanca Bernal, Justin Meschter, Lisa Schile, Doug Carlson, Jayant Gupchup, Andreas Terzis, Razvan Musaloiu-E, Alex Szalay, Jong Hyun Lim, Jay O'Neill, Dennis Whigham, Adam Langley, Geoffrey Parker, Jacob Rode, Adam Dec, Andy Sample, Kyle King, Peter Houlihan, Renato Valencia, Alvaro Pérez, Andrea Narvaez, the staff at Yasuni Research Station, the staff of EPS, and the staff at SERC. Thank you.

Contents

List of Tables

List of Figures

1. Introduction

Anthropogenic activities are drastically changing the composition of important greenhouses gases in Earth's atmosphere. By changing the concentration of greenhouse gases, Earth's radiative balance is altered, allowing for more infrared heat to be trapped in the atmosphere, land and oceans, leading to a general warming of the planet. Carbon dioxide (CO_2) and methane (CH_4) are considered to be the most important anthropogenic greenhouse gases, responsible for 1.82 W m^{-2} and 0.48 W m^{-2} of radiative forcing, respectively (IPCC 2013). Both CO_2 and CH_4 have more than doubled from preindustrial levels. Methane, in particular, is a potent greenhouse gas with a global warming potential of 30 and has an atmospheric lifetime of 8-10 years. Etminan et al. (2016) found that radiative forcing from CH_4 could be 25% higher than previously calculations, illustrating the need to better understand the sources, sinks and uncertainties of CH_4.

Methane sources and sinks can be calculated using a top-down or bottom-up approach. Top-down approaches use atmospheric observations and inversion models to estimate optimal surface fluxes. Bottom-up models use process-based models to estimate emissions and can incorporate empirical knowledge about fluxes. Using bottom-up methodology, the total annual CH_4 sources from 2000-2009 have been estimated to be from 678 Tg CH_4 yr^{-1} (Kirschke et al. 2013) to 719 Tg CH_4 yr^{-1} (Saunois et al. 2016a). Those estimates are the ensemble values, with other bottom-up models projecting total annual sources as low as 542 Tg CH_4 yr^{-1} (Kirschke et al. 2013) to as high as 861 Tg CH_4 yr^{-1} (Saunois et al. 2016a). Top-down approaches tend to result in smaller magnitude sources and sinks.

Natural and anthropogenic sources of CH_4 are comparable in size. From 2000-2009, using bottom-up methodology, estimated that total natural CH_4 sources were 347 Tg CH_4 yr^{-1} and total anthropogenic sources were 331 Tg CH_4 yr^{-1}. Natural sources of CH_4 are natural wetlands, wildfires,

lakes, termites, CH_4 seeps, and others. Anthropogenic sources can be domesticated ruminants, rice paddies, landfills, fossil fuels, and biomass burning.

The origin of CH_4 can be broken down into three types; biogenic, thermogenic, and pyrogenic. Biogenic, thermogenic, and pyrogenic CH_4 can have both natural and anthropogenic sources. Biogenic methane is produced by methanogens, specifically archaea, in anoxic conditions (Conrad 2007). Archaea can be found in wetland soils and the stomachs of ruminants. Thermogenic methane is created by high temperature chemical reactions of organics. Natural geologic methane seeps and drilling for petroleum can release thermogenic CH_4 to the atmosphere. Pyrogenic methane is created by incomplete combustion of organic matter. Both natural and man-made fires produce pyrogenic CH_4.

There are two ways that CH_4 can be removed from the atmosphere; reactions with hydroxyl radicals (OH) and consumption by methanotrophic bacteria in upland soils. Depending on the methodology, total sinks in the last 20 years have been estimated to be as low as 514 Tg CH_4 yr^{-1} and as high as 785 Tg CH_4 yr^{-1} (Kirschke et al. 2013). The majority of CH_4, approximately 92-96%, is removed from the atmosphere by reactions with hydroxyl radicals (OH), which occur primarily in the troposphere.

The remainder of CH_4 is removed by bacteria in unsaturated, oxic, upland soils. Methanotrophic bacteria consume CH_4 that has diffused into the soil from the atmosphere and require oxygen for metabolism. Other than temperature and nutrient availability, one of the major controls on CH_4 consumption is soil water content which varies through time. Therefore, CH_4 consumption rates will vary through time and if soil water content increases enough to block sufficient oxygen diffusion, a normally oxic soil can become a source of CH_4. The converse is also true of wetland soils, illustrating the ongoing need to better model and observe soil water content on a global scale. Median estimates of global soil uptake since 2000 are 28-36 Tg CH_4 yr^{-1} (Kirschke et al. 2013, Saunois et al. 2016a) but with a range of 9-47 Tg CH_4 yr^{-1} (Curry 2007). These median estimates represent 4-8% of total CH_4 sinks.

With CH_4 sources greater than sinks, the concentration in the atmosphere has been generally increasing since the late 18th century. Atmospheric CH_4 concentration had averaged 695±40 ppb from 1000 to 1800 A.D. but began increasing steadily 200 years ago (Etheridge et al. 1998). Over the last several decades, however, the growth rate of CH_4 concentration has not been as steady as other greenhouse gases such as CO_2 and nitrous oxide (N_20) (Dlugokencky et al. 2011). The growth rate of CH_4 in the atmosphere was exceptionally high from the 1940's through the 1970's (Etheridge et al. 1998) but began slowing in the early 1980's (Dlugokencky et al. 1998). It is believed this accelerating rate from 1940 to 1980 can be explained by increasing development, industrial activity and anthropogenic emissions. The decrease in growth rate since 1980, however, cannot be easily explained.

The most enigmatic period of atmospheric CH_4 concentrations was from 1999 until early 2007. During this eight-year period, atmospheric CH_4 concentrations, which had been growing for 200 years, did not significantly change. This period is often referred to as the "CH_4 hiatus". A variety of plausible but sometimes contradictory explanations have been put forth to explain the CH_4 hiatus. Some studies have suggested that a decrease in natural sources was responsible, specifically decreased emissions from wetlands, northern peatlands, and drier soils (Spahni et al. 2011, Nisbet et al. 2016). Other studies have indicated that decreased emissions of CH_4 from the fossil fuel industry caused the hiatus (Aydin et al. 2011). Isotopic CH_4 evidence may support the theory that decreased natural gas production during and after the collapse of the Soviet Union resulted in the hiatus (Schaefer et al. 2016).

While the reasons for the CH_4 hiatus are still being debated, since 2007 atmospheric CH_4 concentrations have begun to rise again. In 2014 the global atmospheric CH_4 concentration increased more than 12 parts per billion (ppb), which is the largest year over year increase in more than 25 years (Nisbet et al. 2016). Mounting isotopic evidence seems to indicate that the increase in the growth rate of atmospheric CH_4 since 2007 have been caused by changes in the contributions of biogenic CH_4 (Simpson et al. 2012, Schwietzke et al. 2016). And because of the increased growth of CH_4 since 2007,

and the reduced growth of anthropogenic CO_2 in the last several years (Le Quere et al. 2015), CH_4 is playing a growing role in climate change (Saunois et al. 2016b). The recent increases in CH_4 have set Earth's atmosphere on a path that is incompatible for all Representative Concentration Pathways (RCP) except RCP8.5, the highest pathway of increased radiative forcing.

The biogeochemical community's inability to explain both the CH_4 hiatus and atmospheric methane's shift towards biogenic sources has led to a reinvestigation of ecosystems, processes, and assumptions. Saunois et al. (2016a) found that uncertainties in natural emissions were higher than uncertainties for anthropogenic emissions, indicating that further study and measurement is required to reduce budget uncertainties. These large and persistent uncertainties in natural emissions have led to efforts to refine measurements of known sources and sinks of CH_4 (Schwietzke et al. 2016) but to also look for novel sources of CH_4 emissions.

While nearing the end of the CH_4 hiatus, data from the SCIMACHY instrument aboard the ENVISAT satellite revealed disagreements between models of CH_4 emissions and direct observations of column CH_4 concentrations from space, particularly over tropical forests (Frankenberg et al. 2005). Above tropical forests, concentrations of CH_4 were consistently higher than predictions from bottom-up models. Later, the differences were found to be smaller than initially reported (Frankenberg et al. 2008), biasing the satellite measurements high due to previously unknown spectroscopic interaction between water vapor and CH_4. But even after measurements were corrected, satellite derived CH_4 concentrations were higher relative to models, indicating there may be an unaccounted source of CH_4 in tropical forests.

Shortly after Frankenberg et al. (2005) reported mismatches between modeled and measured CH_4 concentrations, Keppler et al. (2006) reported CH_4 emissions from both fresh and dried *Fraxinus* and *Fagus* leaves under aerobic conditions. Using net primary productivity (NPP) as a basis to scale CH_4

emissions, they produced a global estimate of 62-236 Tg CH_4 yr^{-1} from leaves and litter, which is approximately 10-33% of total annual CH_4 sources. Unknown sources that high would require a complete re-accounting of CH_4 sources. A global estimate of CH_4 emissions from leaves would likely be more accurate using leaf biomass and sunlight intensity (Megonigal and Guenther 2008). Keppler et al. (2006) posited that CH_4 anomalies in the tropics observed by Frankenberg et al. (2005) could be the same novel leaf emissions they had documented. While the global estimate was received skeptically, subsequent studies have shown that live leaves and leaf litter do emit CH_4 from UV degradation of pectin (Keppler et al. 2008, Vigano et al. 2008).

Another potential novel source that may explain satellite observed tropical CH_4 anomalies are tank bromeliads (Martinson et al. 2010), which harbor methanogens and emit CH_4 from standing water and leaves. Carmichael et al. (2014) categorized tank bromeliads and the methanogens that they provide habitat for as cryptic wetlands. This illustrates that many wetland plants and the microbial communities they associate with are poorly understand from a biogeochemical prospective.

For nearly 40 years it has been known that CH_4 can be released from herbaceous plants in wetlands (Dacey and Klug 1979) through porous tissue known as aerenchyma. Along with ebullition and diffusion, herbaceous plant mediated emissions are recognized as one of the three main sources of CH_4 in wetlands. It has been estimated that 90% of CH_4 emissions from rice cultivation is mediated by the rice plant itself (Mayer and Conrad 1990). While herbaceous plants are accepted as CH_4 sources, with the exception of a few studies (Pulliam 1992, Vann and Megonigal 2003), not until recently has any attention been paid to the potential of wetland trees as emitters of CH_4.

Approximately 60% of wetlands are forested (Matthews and Fung 1987), so determining tree stems as a potential emitting surface should be a priority. Terazawa et al. (2007) demonstrated that significant amounts of CH_4 could be emitted from the stems of temperate wetland trees in a floodplain

with shallow groundwater. They also found that emissions decreased with height indicating that the source of CH_4 may be belowground production in the soil or groundwater. In a short study, Gauci et al. (2010) found a similar pattern of decreasing stem fluxes with increasing stem height in a mature wetland alder stand and notably, the fluxes were in the same order of magnitude as the soil surface CH_4 fluxes. It was suggested that the CH_4 was originating from belowground and could be exiting the stem through lenticels via aerenchyma tissue. Aerenchyma is primarily associated with herbaceous plants but has been reported in trees exposed to flooding (Kozlowski 1997), particularly tropical trees (De Simone et al. 2002). In a tropical peat wetland, stem CH_4 emissions were found to be higher than soil CH_4 emissions and it was estimated that as much as 87% of the CH_4 emissions were coming from tree stems (Pangala et al. 2013). In a yearlong study of a temperate wetland, it was estimated that over 30% of CH_4 could be emitted from tree stems (Pangala et al. 2015) and significant differences were seen between the two species that were monitored. It should be noted that several studies have looked for diurnal cycles in wetland CH_4 fluxes but have not observed them (Pangala et al. 2014, Terazawa et al. 2015). The sampling frequency in the two studies was between 6 and 12 measurements per day which may not be frequent enough to measure diurnal variation.

In addition to the previously mentioned field studies, controlled laboratory experiments focused on wetland trees have shown that CH_4 and other gases can be diffused through woody tissue (Rusch and Rennenberg 1998, Rice et al. 2010, Pangala et al. 2014). With consistent and mounting evidence that wetland tree stems are sources of CH_4, the next logical step is to test if tree stems in drier habitats are also emitting CH_4.

Trees in upland forests have been shown to have sources of CH_4 contained within their stems. Over a century ago elevated CH_4 concentrations were reported from in-situ measurements of tree stems (Bushong 1907). This has been confirmed more recently by several studies (Zeikus and Ward 1974, Covey et al. 2012). Some measured concentrations of CH_4 from tree stems are above 10,000 ppm. Covey

et al. (2012) modelled stem CH_4 emissions but did not directly measure fluxes. Beyond assumed or modeled stem emissions from high internal concentrations due to heart rot, it is possible that the same mechanisms that have been proposed for the stem CH_4 emissions in wetlands could result in emissions in upland forests with drier soils. But few studies have attempted to replicate the methodologies in upland forests that Terazawa et al. (2007) and Gauci et al. (2010) used in wetland forests.

Upland forests are assumed to be sinks of CH_4 (Dutaur and Verchot 2007) because their soils are dry enough to promote net methanotrophic activity. Measuring CH_4 flux in soils quantifies the net CH_4 activity but CH_4 production and CH_4 consumption are occurring in both wet and dry soils. Methanogenic archaea are pervasive in both anoxic and oxic soils (Angel et al. 2012), meaning that CH_4 can be produced if conditions are favorable. Beyond stem emissions from high internal concentrations due to heart rot, it is possible that the same mechanisms that have been proposed for the stem CH_4 emissions in wetlands could result in emissions in upland forests with drier soils.

Soil moisture is the major driver of belowground oxygen availability. In a wetland, soil moisture measurements likely reflect conditions throughout the soil profile, but in an upland forest, surface conditions do not represent the steeper, more variable, vertical soil moisture gradient.

A majority of tree root biomass lies in the top 30 cm of the soil, where the soil is mostly oxic and the soil moisture is lower relative to the deeper soil profile. But some roots can utilize relatively deep groundwater, deeper than 5m and as much as 25m (Jackson et al. 1999). If the groundwater contains dissolved CH_4, it is possible that CH_4 could be transported through woody tissue aboveground, bypassing oxic soil layers where it would normally be consumed by methanotrophic bacteria. Upland tree roots that are shallow in the soil may also be near anoxic microsites. These microsites can be local sources of CH_4 (von Fischer and Hedin 2002, 2007). This CH_4 could be entrained in the transpiration stream and transported aboveground, ultimately being emitted from stems and leaves.

With mounting evidence that multiple novel or overlooked sources of CH_4 can be emitted from a biome, forest, or even a single plant, some have suggested that vegetation should be included in global budgets (Carmichael et al. 2014). Consequently, in a recent review of the CH_4 budget, fluxes from trees and non-wetland plants are starting to be considered in global budgets (Saunois et al. 2016a).

Traditional methods of characterizing greenhouse gas fluxes are systematically missing some surfaces that could be significant emitters in natural ecosystems. The second and third chapters of this thesis address the potential of tree stems to emit CH_4 in a temperate deciduous forest. The second chapter investigates trees and soils in an upland forest during one field season and looks for drivers that may explain the timing and magnitude of these fluxes. An automated system was constructed to make high frequency CH_4 flux measurements on several trees and determine if diurnal fluxes could be observed.

The third chapter explores stem and soil CH_4 fluxes from trees along a natural moisture gradient during two growing seasons, 2013 and 2014. A transect was established with one end in a forested wetland and the other in an upland forest. Variables such as trees species, soil moisture, groundwater depth were studied.

While CH_4 is a potent greenhouse gas and its relative sources are poorly constrained, CO_2 is currently responsible for over three times more radiative forcing than CH_4 (IPCC 2013). Of the various annual fluxes of CO_2 to the atmosphere, soil respiration is one of the largest and is growing. It was estimated that global soil respiration was 98 ± 12 Pg C yr^{-1} in 2008 and during the time period of 1989 to 2008, soil respiration has been increasing by 0.1 Pg C yr^{-1} (Bond-Lamberty and Thomson 2010b). The atmosphere currently contains over 850 Pg of carbon (at 400 ppmv), meaning that every year the equivalent of more than 10% of atmospheric CO_2 cycles through soils via soil respiration. Anthropogenic emissions of carbon were recently estimated to be 9.8 ± 0.5 Pg C yr^{-1} in 2014 (Le Quere et al. 2015)

which indicates that soil respiration is approximately 10 times higher than anthropogenic emissions and the uncertainty for global soil respiration is larger than the sum of human emissions. Therefore, if human emissions can have an effect on the atmosphere, small changes in soil respiration also have effect on atmospheric CO_2 concentrations.

Based on a recent database of soil respiration studies (Bond-Lamberty and Thomson 2010a), only 10% of data is collected in the tropics due to a heavy bias towards temperate biomes. But it has been estimated that two thirds of global soil respiration is emitted from the tropics (Bond-Lamberty and Thomson 2010b) and one quarter of global soil respiration is from broadleaf tropical rainforests forests (Raich et al. 2002). Studying tropical forests may be one way to create better estimates of global soil respiration and reduce its uncertainty.

Soil respiration is most often measured using open bottom chambers that are placed on the soil surface. To determine the soil efflux, after the chamber is closed, the rate of CO_2 accumulation in the headspace can be converted into a mass flux. Some of the advantages of using chambers are that they are small, portable, relatively inexpensive and deployable to remote sites.

While the chamber method is the most commonly used in soil respiration studies, it has its drawbacks. The chamber distorts the natural CO_2 concentration gradient between the soil and air while taking a measurement (Davidson et al. 2002). Measurements are often infrequent because they are limited by time and labor. Automated system can improve the sampling rate but can often only collect measurements once an hour, which may not be fast enough to understand some soil processes (Lee et al. 2004), and are used in only a fraction of all soil respiration studies.

The gradient method involves measuring CO_2 concentrations at several depths in the soil and estimating soil CO_2 efflux using diffusion-based models (Penman 1940, Marshall 1959, Moldrup et al. 2000). These models use parameters such as soil moisture, soil temperature, bulk density, and soil

texture to calculate the effective diffusivity. In the last two decades, ruggedized CO_2 sensors that can be placed into the soil, allow for long term and continuous measurements to be made. These sensors measure CO_2 in-situ via diffusion into a small absorption cavity as opposed to physically withdrawing a soil-air sample from the subsurface and introducing it into an analyzer. The gradient method does not change the soil-to-atmosphere CO_2 gradient like the chamber method can. The soil CO_2 sensors can also provide additional information about the soil CO_2 depth profile.

The gradient method still has some limitations. While the disturbance to the soil is less than the chamber method, the presence of the CO_2 probes will still change the soil environment (Maier and Schack-Kirchner 2014). The gradient method measures a small area of the soil, and because soil respiration is heterogenous, more replicates may be required than other methods to characterize a particular study site. The diffusion models used to estimate soil respiration are largely empirical and were validated on high sand and silt soils. Therefore, the diffusion models may not accurately extrapolate to other soil textures. The tropics generally have higher clay contents due to increased weathering. Only one study has used the gradient method in a tropical forest (Vargas and Allen 2008).

The fourth chapter presents measurements of soil respiration in a tropical broadleaf rainforest using both the chamber and gradient methods. The study site was not a seasonally wet rainforest but soil respiration was measured during the historically driest and wettest months of the year to capture how differences in soil moisture may affect soil respiration. Because of the wet, high clay soils at the study site, there may need to be more validation studies in clay soils to refine the gradient method before it can be usefully deployed in tropical environments.

2. Temperate Forest Methane Sink Diminished by Tree Emissions

Abstract

Global budgets ascribe 4-10% of atmospheric methane (CH_4) sinks to upland soils and have assumed until recently that soils are the sole surface for CH_4 exchange in upland forests. Here we report that CH_4 is emitted from the stems of dominant tree species in a temperate upland forest, measured using both the traditional static-chamber method and a new high-frequency, automated system. Tree emissions averaged across 68 observations on 17 trees from May-Sep were 1.59±0.88 µmol CH_4 m^{-2} h^{-1} (mean±95% CI), while soils adjacent to the trees consumed atmospheric CH_4 at a rate of -4.52±0.64 µmol CH_4 m^{-2} h^{-1} ($P<0.0001$). High-frequency measurements revealed diurnal patterns in the rate of tree stem CH_4 emissions. A simple scaling exercise suggested that tree emissions offset 1-6% of the growing season soil CH_4 sink and may have briefly changed the forest to a net CH_4 source.

2.1. Introduction

Upland (free-drained) soils are estimated to consume 20-45 Tg methane (CH_4) per year (Topp and Pattey 1997, Dutaur and Verchot 2007, Kirschke et al. 2013, Schlesinger 2013), a sink comparable to the rate of CH_4 accumulation in the atmosphere and, therefore, capable of influencing the radiative forcing caused by this potent greenhouse gas. Global CH_4 budgets, Earth system models, and carbon accounting policies have generally assumed that the role of upland forests can be determined by measuring the rate of CH_4 fluxes at the soil surface. This assumption is problematic in forests where soils but not whole trees can be enclosed in gas flux chambers, the most common technique for quantifying upland CH_4 fluxes. A variety of evidence now makes it clear that all biological surfaces in upland forests have the potential to exchange CH_4. These include reports of novel sources of CH_4 emissions in nominally upland ecosystems (Keppler et al. 2006, Martinson et al. 2010, Lenhart et al. 2012), eddy flux

evidence of hot spots or hot moments of forest CH_4 emissions (do Carmo et al. 2006, Shoemaker et al. 2014) and elevated CH_4 concentrations in tree stems (Bushong 1907, Zeikus and Ward 1974, Covey et al. 2012).

Despite significant advances in identifying novel sources of CH_4 in upland forests, the consequences for upland forest CH_4 budgets have been highly speculative due to a lack of *in situ* observations of CH_4 emissions across surfaces other than soils. Abiotic emissions driven by UV radiation (Keppler et al. 2008, Megonigal and Guenther 2008), fungal emissions from wood surfaces (Lenhart et al. 2012) and microbial emissions from wood cores (Zeikus and Ward 1974, Wang et al. 2016) have been measured in laboratory settings. Emissions from living tree stems were modeled from CH_4 concentration gradients and estimates of gas diffusion constants (Covey et al. 2012). Until recently it was difficult to judge whether these potential upland CH_4 sources are quantitatively important because there were no direct, *in situ* emissions data other than from tropical forest tank bromeliads (Martinson et al. 2010). This changed recently with direct CH_4 flux measurements from the living stems and shoots of three temperate forest tree species – *Populus davidiana*, *Carya cathayensis* and *Larix gmelinii* -- in China (Wang et al. 2016); the stems and shoots of *Pinus sylvestris* in a European boreal forest (Machacova et al. 2016); the stems of several hardwood species in a temperate hardwood forest in eastern North America (Warner et al. 2017); and stems of *Fagus sylvatica* in a temperate European forest (Maier et al. 2017).

Representation of CH_4 emissions from upland ecosystems has been acknowledged in global models and budgets (Saunois et al. 2016a) but remains limited by *in situ* flux measurements from non-soil surfaces. The global contributions of CH_4 from abiotic production, fungi and epiphytes are difficult to estimate, but are expected to be too small to adequately explain the potential source-sink imbalance of 8-46 Tg yr^{-1} (Kirschke et al. 2013). Coarse woody debris is a source of CH_4 emissions from termites and microorganisms that may be significant (Carmichael et al. 2014, Covey et al. 2016, Warner et al. 2017).

Living tree stems are potentially a large CH_4 source in upland forests (Covey et al. 2012, Machacova et al. 2016, Wang et al. 2016, Warner et al. 2017), and are known to be a significant CH_4 source in floodplain forests (Terazawa et al. 2007, Terazawa et al. 2015) wetland forests (Pulliam 1992, Gauci et al. 2010, Pangala et al. 2013). In floodplain and wetland forests, the source of tree-emitted CH_4 has been assumed to be biological production in saturated soils with subsequent transport through aerenchyma tissue or transpiration. But in upland forests there is evidence that the CH_4 emitted from living tree stems is produced biologically in wood (Bushong 1907, Zeikus and Ward 1974, Covey et al. 2012, Wang et al. 2016). Distinguishing between sources (e.g. wood, soil) is critical for global CH_4 models.

Our objectives were to quantify CH_4 emissions from tree stems in an upland temperate forest and to evaluate whether soil moisture, tree species and tree activity regulate the size and timing of emissions. We hypothesized that upland trees emit CH_4 from stems; soils are a source of stem-emitted CH_4; and stem emissions offset a meaningful fraction of net CH_4 consumption by soils.

2.2. Materials and Methods

Study Site

This study was conducted in a mature, temperate, deciduous, upland forest located at the Smithsonian Environmental Research Center near Annapolis, Maryland, USA. The site is in a 226 ha forested watershed drained by a second-order stream (watershed 101 in Correll et al. (2000)). It presently has a closed canopy and very little understory (Yesilonis et al. 2016). The dominant species include *Liriodendron tulipifera* L., *Quercus* spp., *F. grandfolia Ehrh*, and *Carya* spp. (Brush et al. 1980). Mean rainfall is 1001 mm, mean annual temperature is 12.9°C, and the soils are well-drained fine sandy loams or sandy loams classified as Typic Hapludults (Yesilonis et al. 2016).

Table 2-1: Tree Species and relative elevations of stems and groundwater wells. Minimum (min) and maximum (max) depth to water table was estimated from the water table depth below the soil surface at the well located closest to each tree, and the elevation of the tree in relation to that well.

ID	Tree Species	DBH (cm)[†]	Wetland Type[‡]	Elevation Above Well 2 (m)	Min Water Table Depth (m)	Max Water Table Depth (m)
12001	*Fagus grandifolia*	56.1	FACU	5.132	3.33	4.03
12002	*F. grandifolia*	56.2	FACU	0.419	0.65	1.62
12003	*F. grandifolia*	53.0	FACU	2.270	2.50	3.47
12006	*F. grandifolia*	44.9	FACU	0.936	1.17	2.14
12008	*F. grandifolia*	31.4	FACU	5.113	3.32	4.01
12010	*Lireodendron tulipifera*	31.8	FACU	6.009	4.21	4.91
12011	*Carya tomentosa*	22.8	None	5.360	3.56	4.26
12012	*F. grandifolia*	55.9	FACU	6.907	5.11	5.81
12013	*Quercus velutina*	65.8	None	7.445	6.01	6.23
12014	*Q. michauxii*	65.9	FACW	6.887	5.09	5.79
12015	*Acer rubrum*	17.0	FAC	6.271	4.47	5.17
12016	*L. tulipifera*	71.1	FACU	6.256	4.82	5.04
12017	*F. grandifolia*	47.1	FACU	7.658	6.22	6.44
12018	*Liquidambar styraciflua*	34.8	FAC	8.123	6.69	6.91
12019	*L. styraciflua*	27.2	FAC	6.000	4.56	4.79
12020	*L. styraciflua*	21.9	FAC	8.962	7.48	7.70
12021	*L. tulipifera*	92.6	FACU	7.473	6.04	6.26
Well 2				0.000	0.29	1.20
Well 3				4.749	2.95	3.65
Well 4				6.928	5.45	5.67

[†] DBH = diameter at breast height of the main tree stem.

[‡] Wetland type is from the USDA classification database. Abbreviations are Facultative Upland (FACU, usually occur in non-wetlands), Facultative Wetland (FACW, usually occurs in wetlands), Facultative (FAC, occurs in wetlands and non-wetlands), and species without a USDA Wetland Status (None).

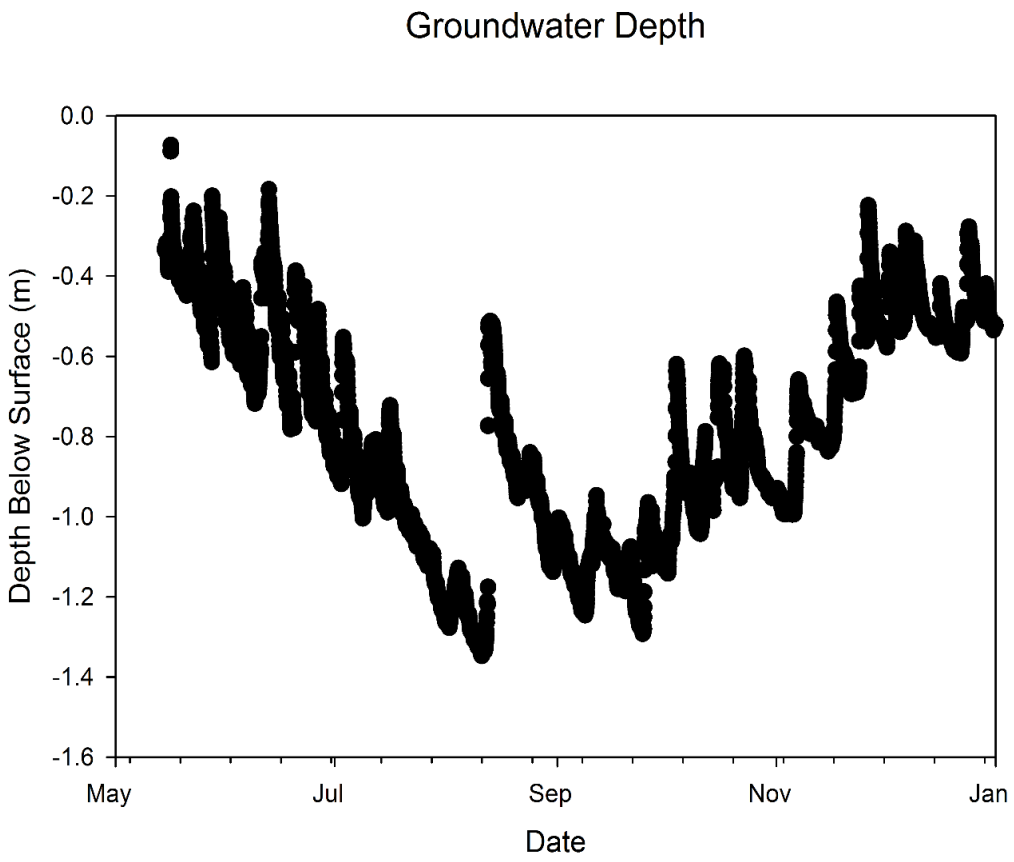

Figure 2-1: Depth to groundwater in Well 2 recorded by a continuous logger groundwater data logger during the study period in 2014. The water level is relative to the ground surface. Well 2 was at the lowest elevation in the transect, and closest to the forested wetland boundary; all of the trees in the study were at a higher elevation than this well.

A transect 120 m in length was established along a south-facing slope with a 5% grade, with an elevation difference between endpoints of 7 m. The depth to groundwater across the transect varied from 3.3-7.7 m below the soil surface (Table 2-1); three of the *F. grandifolia* trees in the study grew at a relatively low elevation where the water table ranged from 0.7 to 3.5 m (Table 2-1). Water depth was recorded using a groundwater elevation logger (Aqua Troll 200, In-Situ Inc., Fort Collins, Colorado, USA). Elevations were surveyed with a laser-based total station (Topcon Positioning Systems Inc., Livermore, California, USA) capable of millimeter precision. The tree species in the study were *L. tulipifera*, *F. grandifolia*, *Carya tomentosa* (Lam.) Nutt., *Quercus velutina* Lam., *Quercus michauxii* Nutt., *Acer rubrum* L. and *Liquidambar styraciflua*.

Flux Measurements

Seventeen trees were fitted with opaque acrylic chambers, as seen in Figure 2-2 (Ryan 1990). Each tree was paired with a soil gas flux chamber within 1 m of the base. Stem chambers were permanently fixed at 30-60 cm above the soil and secured with elastic shock cord. An airtight seal between the chamber and the stem was created with closed-cell neoprene foam, sealed with non-VOC dental impression material (Examix^{TM}, GC America, Alsip, IL, USA). Soil rings were constructed from 30.5 cm-diameter schedule 80 PVC pipe buried 5 cm into the soil surface. Chambers were mounted a minimum of one week before taking flux measurements, and remained in place for the duration of the study.

Gas concentrations were measured using a portable Off-Axis Integrated Cavity Output Spectroscopy (OA-ICOS) instrument (Los Gatos Research, Los Gatos, CA, USA). The instrument measures

Figure 2-2: Example of the two types of flux chambers used in the study. Left: seventeen trees were fitted with manual chambers that remained in place and open between flux measurements over the course of a growing season (May-Sep). Fluxes were measured by securing a lid over the chamber and measuring concentrations for 5-10 min. Right: an automated version of the same chamber design.

CH_4 in a range of 0.01-100 ppm with a precision of 0.002 ppm at 0.5 Hertz, and CO_2 in a range of 200-20000 ppm with a precision of 0.3 ppm. The closed system drew headspace gas from the chamber, measured CH_4 concentration non-destructively, then returned the gas to the chamber. Each flux was measured over 5-10 min and generated ≥150 observations (Figure 2-3).

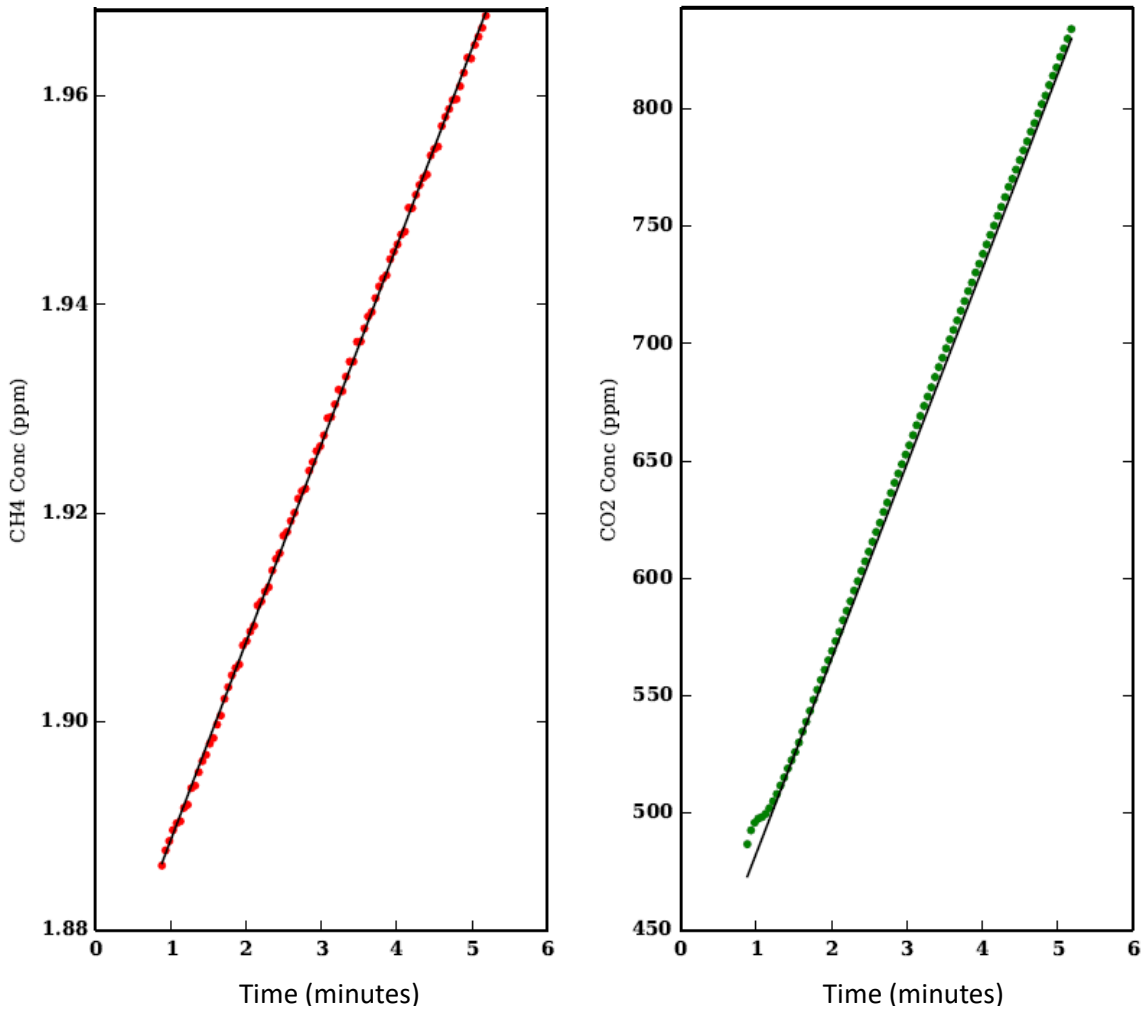

Figure 2-3: Example of a single CH_4 and CO_2 flux measurement showing the sensitivity of the Off-Axis Integrated Cavity Output Spectroscopy (OA-ICOS) instrument and the number of observations used for subsequent regression analysis to determine the flux rate.

Stem and soil CH_4 and CO_2 flux rates were measured monthly from May to Sep 2014 for a total of five campaigns. In the first campaign (22-23 May), fluxes were measured once on seven individual trees. In the second campaign (20 Jun) a set of 10 completely different trees were measured, such that

there was no overlap between the individual trees measured in the May and Jun campaigns. Thereafter, all 17 trees (Table 2-1) were measured once during each of the final three campaign (i.e. Jul 8-10, Aug 20-29 and Sep 17-22). Each tree measurement was paired with a single measurement of soil CH_4 and CO_2 flux taken the adjacent soil chamber. The full dataset consists of four measurements (one on each of four different campaigns) for every tree-soil pair. There were 68 tree observations and 68 soil observations for a total of 136 flux measurements.

Both CO_2 and CH_4 were quantified from ≥150 concentration observations. We removed the first 20% of the observations to eliminate artifacts caused by closing the lid, estimated the slope using linear regression, and calculated gas flux by following equation:

$$\boldsymbol{F = \frac{d[CH_4]}{dt} \times \frac{PV}{ART}}$$

where F is the flux in μL m^{-2} h^{-1}, P is atmospheric pressure, T is temperature, R is the universal gas constant, A is the collar surface area and V is the volume of the air enclosed by the chamber. Air temperature was measured by the OA-ICOS unit on gas circulating between the unit and the chamber. Atmospheric pressure was based on a nearby weather station (<1 km).

We constructed an automated system for high-frequency tree CH_4 flux measurements to gain insights on the source and mechanism of CH_4 emissions from upland trees. The system was installed on two new trees that had not been measured previously. The elevation of the trees was similar to those at the highest elevation in the transect study, and separated by about 300 m. During a three-day period (28-31 Jul 2014) CH_4 and CO_2 fluxes were measured at 45 min intervals from the trunk of a single *L. tulipifera* at three heights above the soil surface (75, 165 and 245 cm) and a single *F. grandifolia* at one height (75 cm). Automated measurements were made using the same chamber design (Figure 2-2), modified with a lid that was opened and closed by pneumatic cylinders and solenoids controlled by an

Arduino Mega microcontroller. The manifold sampled from one chamber at a time in a closed loop for eight minutes, flushing with ambient air for three minutes between measurements.

Statistical Analyses

The slope of gas concentration per time (≥150 observations in each case) was determined by linear regression analysis using the SAS® procedure Proc Reg. We used two criteria to determine whether the slopes were statistically significant. The first was to reject regressions with P-values ≥0.05 and assign them a flux of zero. Although this approach is statistically defensible, with ≥150 observations the analysis detected small but statistically significant fluxes, including two cases in which the regression relationship was significant (P<0.05) but explained <10% of the variation (R^2<0.10). The second criterion was based on a graphical analysis of the distribution of R^2 values (Figure 2-4), in which we arbitrarily assigned R^2<0.80 as the threshold below which fluxes were set equal to zero. Flux data were analyzed separately using the two criteria, recognizing that the R^2-based criterion was more conservative. Based on the criterion that fluxes with R^2<0.80 were not reliably different than zero, and taking account of chamber volume, the smallest detectable CH_4 consumption rate was -0.36 μmol m^{-2} h^{-1}, and the smallest detectable production rate was 0.03 μmol m^{-2} h^{-1}.

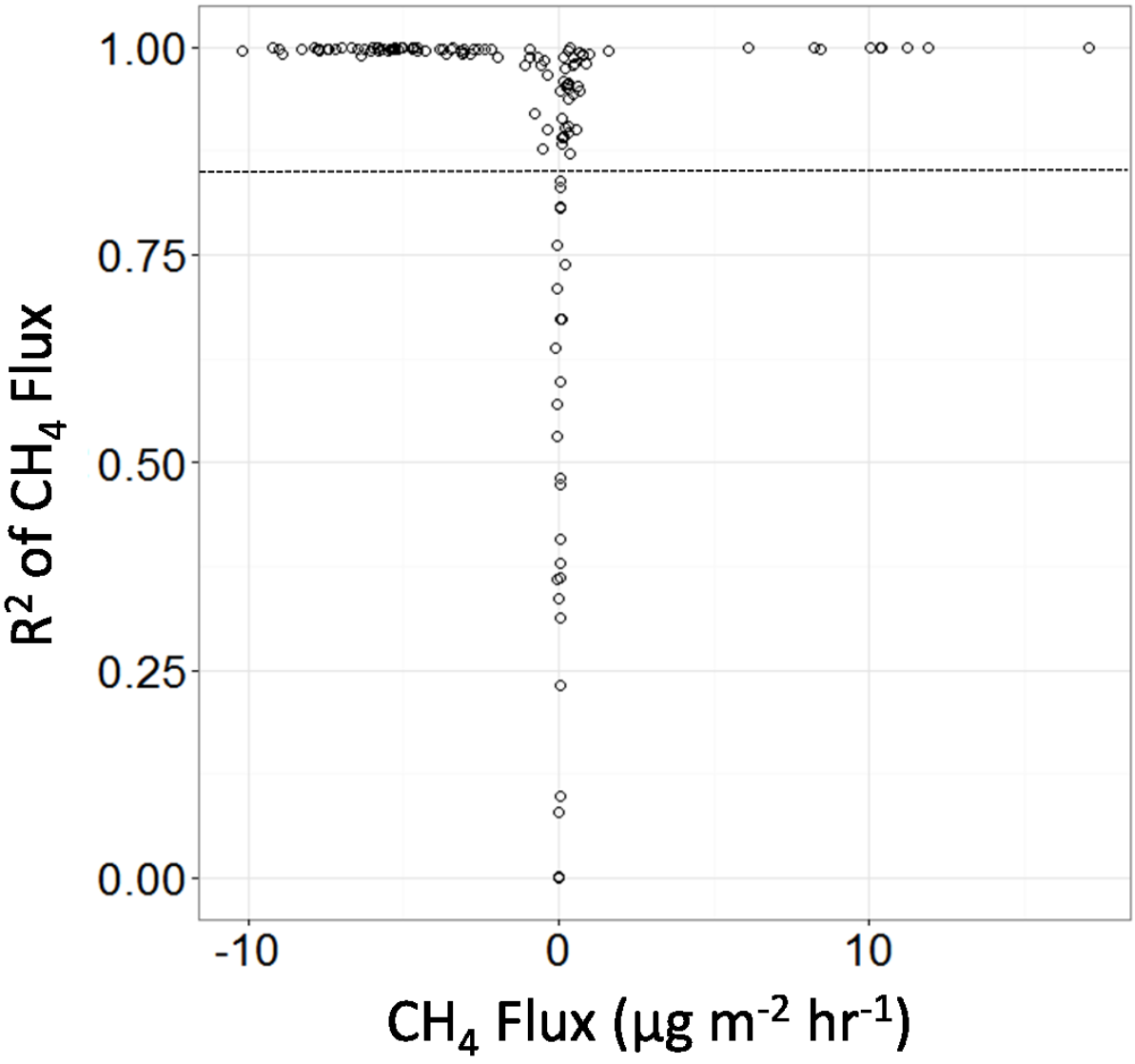

Figure 2-4: The distribution of regression R^2 values as a function of the rate of CH_4 flux. The horizontal dashed line represents R^2 = 0.80

The SAS procedure Proc Univariate was used to calculate means and 95% confidence intervals, and to perform a sign test of the hypothesis that fluxes were significantly different than zero at α=0.05. The sign test is two-tailed and non-parametric. It was chosen because soil and tree flux data were occasionally non-normal (Kolmogorov-Smirnov test); however, the outcomes of this non-parametric test and a parametric t-test were always the same. The non-parametric Kruskal-Wallis test was used to test for differences in CH_4 emissions across species using SAS Proc NPAR1WAY; *C. tomentosa* was excluded

due to an absence of variability (all fluxes were zero). SAS Proc CORR calculated Pearson correlations between CH_4 and CO_2 emissions from the automated system. CH_4 flux percentile distributions were calculated in SigmaPlot® 12.0. The timing of peak flux in diurnal cycles of CH_4 and CO_2 emissions were quantified by non-linear least squares using the Curve Fitting package of MATLAB R2106b (MathWorks, Inc.).

Ecosystem Scaling Exercise

We performed a simple scaling exercise to estimate the fraction of soil CH_4 consumption that is offset by stem emissions. A simple approach was adopted because tree flux rates did not relate to measured explanatory variables including tree species, diameter, soil moisture content, soil temperature or air temperature ($P>0.05$). Although such relationships may exist, sample sizes in this study were too small to support a more complex approach to scaling.

Linear interpolation was used to calculate the average CH_4 flux during each of four time-intervals between flux campaigns, then multiplied by number of days in the interval to estimate total tree emissions and total soil consumption. This approach assumes that factors affecting CH_4 fluxes changed linearly between consecutive sample events and does not attempt to model changes that occurred between sample events. The approach can either over- or underestimate actual fluxes if there is was a bias for high or low fluxes between samples. The conservative estimates of flux (i.e. $R^2 \geq 0.80$) were used for these calculations. The totals were scaled to ground area by calculating stem surface area as a function of soil surface area using data from an adjacent 16 ha forest research plot (Anderson-Teixeira et al. 2015). The trees in this study were chosen because they fell along a transect line, not because they were a representative sample of the 16 ha plot. Nonetheless, the seven species in the study are 74% the stems and 75% of the basal area in the 16 ha plot, with *F. grandifolia*, *L. tulipifera*, and

L. styraciflua representing >60% of the stems and 64% of the basal area. Three meters is a reasonable estimate because we show that CH_4 emissions were still occurring at 2.5 m on two trees, and there are similar observations in the wetland tree literature (Pangala et al. 2013). Stem surface area to a height of 3 m is 13% of the soil surface area, therefore total tree CH_4 emissions were multiplied by 0.13 to yield tree emissions per unit ground area.

2.3. Results and Discussion

Using the criterion that fluxes with P-values <0.05 were significant, 65 of the 68 tree CH_4 flux observations were highly significant (P<0.001), and three were statistically indistinguishable from zero (P>0.05). Each of the seven upland tree species in the study was capable of emitting CH_4, namely *F. grandifolia*, *L. tulipifera*, *C. tomentosa*, *Q. velutina*, *Q. michauxii*, *A. rubrum*, and *L. styraciflua*. In six cases, the fluxes indicated low rates of CH_4 consumption (< -0.07 μmol m^{-2} h^{-1}) by tree stems. Using the more conservative criterion that fluxes with R^2<0.80 are indistinguishable from zero, 46 of the 68 observations were greater than zero, all of which were positive fluxes to the atmosphere. All of the soil flux regression models had P-values <0.001 and R^2>0.80. Soil CH_4 fluxes generally showed net CH_4 consumption from the atmosphere as expected in an upland forest, with one exception in which the flux was positive (Figure 2-5). Thus, different terrestrial-atmosphere interfaces (soils versus tree stems) in an upland forest tended to simultaneously act as either a CH_4 sink (soils) or a CH_4 source (stems), each counteracting the influence of the other on net ecosystem CH_4 emissions.

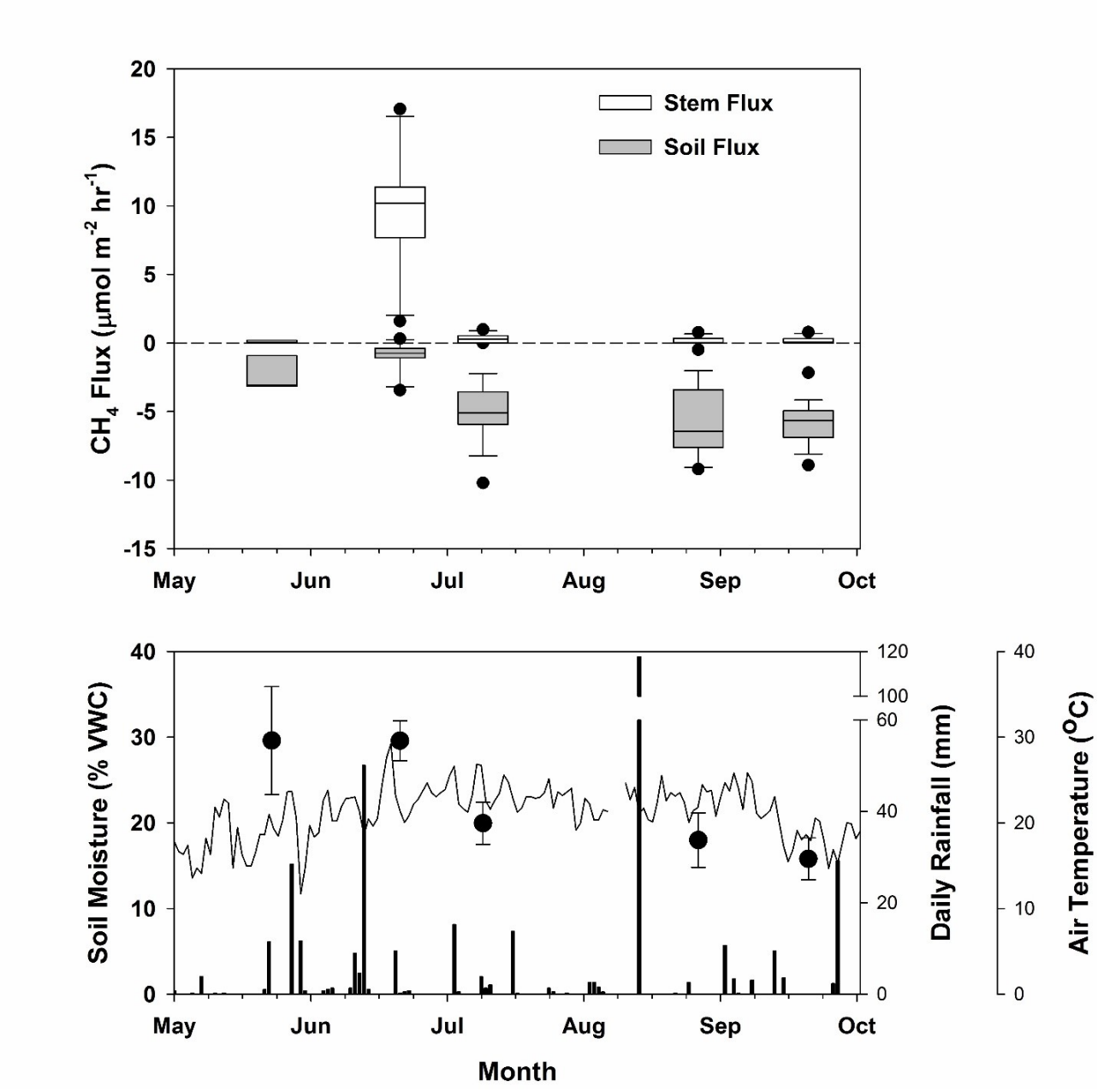

Figure 2-5: Upper panel: CH_4 fluxes across tree stems and soil surfaces in an upland (freely drained) forest. Lower panel: Corresponding soil moisture as percent of volumetric water content (VWC, filled circles), daily total rainfall (bars), and daily mean air temperature (solid line). CH_4 fluxes are plotted as box plots with box boundaries that represent 25th, 50th (median) and 75th percentiles; whiskers are 90th and 10th percentiles; and points are outliers. VWC is plotted as mean±95% CI. Sample sizes for CH_4 and VWC were n=7 in May, n=10 in Jun, and n=17 on all other dates.

Soil CH_4 flux averaged over the growing season was -4.52 ± 0.64 μmol m^{-2} soil h^{-1} (mean ± 95% CI), which is similar to the global average for temperate forest soils of -4.07 μmol m^{-2} h^{-1} (Dutaur and Verchot 2007). Stem flux averaged 1.59 ± 0.88 μmol m^{-2} stem h^{-1} ($p \leq 0.0001$). These averages and errors were the same whether calculated using the more relaxed or conservative criteria for assigning fluxes a value of zero, reflecting the fact that the highest rates of flux also had high R^2 values (Figure 2-4). For this reason, we restrict discussion from here forward to the more conservative estimates. Tree emissions were positive and significantly greater than zero in Jun (9.53±2.87), Jul (0.33±0.16), Aug (0.19±0.13) and Sep (0.19±0.13) ($p \leq 0.002$), but not in May (0.09±0.10) ($P=0.13$; all units μmol m^{-2} stem h^{-1}). Soil fluxes were significantly different from zero ($p \leq 0.02$) for all months.

Of the 46 stems with the highest CH_4 emissions ($R^2>0.80$), 45 were paired with a soil that was a net CH_4 sink. These data and those from a second North American temperate forest (Warner et al. 2017), two temperate upland forests in Asia (Wang et al. 2016), a boreal forest in Europe (Machacova et al. 2016) and observations of super-ambient CH_4 concentrations inside temperate forest tree stems (Covey et al. 2012), collectively suggest that the size of the CH_4 sink ascribed to upland forests has been overestimated.

This study and that of Warner et al. (2017) were similar in many respects. They were conducted at roughly the same time (2014 growing season), using similar methods (static chambers, Los Gatos OA-ICOS gas analyzer), similar sampling effort (16-17 trees measured 1-2 times per month), and on four of the same tree species. Climate is similar between the sites because they are at the same elevation (near sea level) and separated by 100 km, and both forests are on loamy soils classified as Typic Hapludults. Average tree stem CH_4 emissions over the growing season in Warner et al. (2017) (0.40±0.18 μmol CH_4 m^{-2} h^{-1}) were comparable to the present study when the Jun data are excluded (0.23±0.23 μmol CH_4 m^{-2} h^{-1}), suggesting that tree CH_4 emissions may be similar when stratified by species, climate and soil characteristics under most conditions. However, stem CH_4 emissions in the present study rose an order

of magnitude in the Jun sample (9.53±2.87 μmol m^{-2} h^{-1}), a "hot moment" event of uncertain duration that was not observed by Warner et al. (2017). Because both studies sampled emissions over short time periods (minutes) at long intervals (2-4 weeks), we cannot state whether the difference between studies is real or a limitation of the sampling designs. Regardless, the transient increase in stem CH_4 emissions observed in the present study is an illustration of the potential for high temporal variation in this process.

A small but growing collection of upland tree CH_4 emission studies indicates substantial spatial and temporal variability that must be resolved in order to account for tree emissions in upland forest CH_4 budgets. A three-month study of the conifer *P. sylvestris* reported median rates of stem CH_4 emissions that were 1-2 orders of magnitude lower than those in the present study (0.01 to 0.001 μmol m^{-2} h^{-1}), with lower rates in a dry plot under cloudy conditions than a wet plot under sunny conditions (Machacova et al. 2016). At the high extreme is a *P. davidiana* forest where annual average rates ranged 5.3-6.4 μmol m^{-2} h^{-1} (Wang et al. 2016), suggesting sustained rates comparable to the high Jun rate in the present study. Average rates from the present study (1.59 ± 0.88 μmol m^{-2} stem h^{-1}), a nearby temperate forest (Warner et al. (2017); 0.40±0.18 μmol CH_4 m^{-2} h^{-1}) and a high emitting site in a European temperate forest (1.87±3.31 μmol CH_4 m^{-2} h^{-1} (Maier et al. 2017) fall between these extremes, but toward the upper end of the range. An important step toward improved experimental designs and scaling exercises is to understand the sources of this variability.

There were no statistical relationships between tree CH_4 emissions and stem diameter, soil moisture, air temperature or soil temperature that could be used for scaling fluxes ($P>0.05$), consistent with the results of Warner et al. (2017) in a similar forest. In contrast, stem emissions were positively correlated to temperature in a *P. davidiana* forest (Wang et al. 2016), perhaps because relatively high summer emissions and low winter emissions produced a wider range of rates. Previous studies reported that much of the variation in stem CH_4 emissions is related to tree species (Covey et al. 2012, Wang et al.

2016, Warner et al. 2017). In the present study there were no significant differences across all species (P=0.07); however, for the species with the largest sample sizes -- *F. grandifolia* (n=28), *L. styraciflua* (n=12) and *L. tulipifera* (n=12) -- there were significant differences (P=0.04), with *F. grandifolia* supporting lower rates than the other species (Figure 2-7). Such differences may be linked to characteristics such as stem morphology or disease resistance (Warner et al. 2017).

In the present study, there was variation across individuals and time that was not clearly related to species. Of the 17 trees in the transect study, five individuals contributed 84% of the cumulative CH_4 emitted from all stems (May-Sep fluxes scaled to stem diameter). The five trees belonged to four species -- *F. grandifolia*, *L. tulipifera*, *Q. velutina* and *Q. michauxii* -- each of which contributed 12-23% of the total. Other than *C. tomentosa* of which there was just one stem, every species contributed >10% of cumulative stem CH_4 emissions. About half of the individuals (8 of 17) were consistent emitters with measurable fluxes (i.e. $P<0.05$ and $R^2>0.80$) during every sample event, while the remainder emitted CH_4 intermittently on three dates (2 individuals), two dates (3 individuals), or one date (2 individuals). Two individuals never emitted significant amounts of CH_4. A similar result was reported in a study of 10 *F. grandifolia* stems across two Central European forests where nearly all stem CH_4 was emitted by a single tree (Maier et al. 2017). It is clear that robust estimates of stem CH_4 emissions at the stand scale will require a combination of large sample sizes and high-frequency measurements, and improved techniques such as eddy covariance flux capable of quantifying small fluxes over large areas.

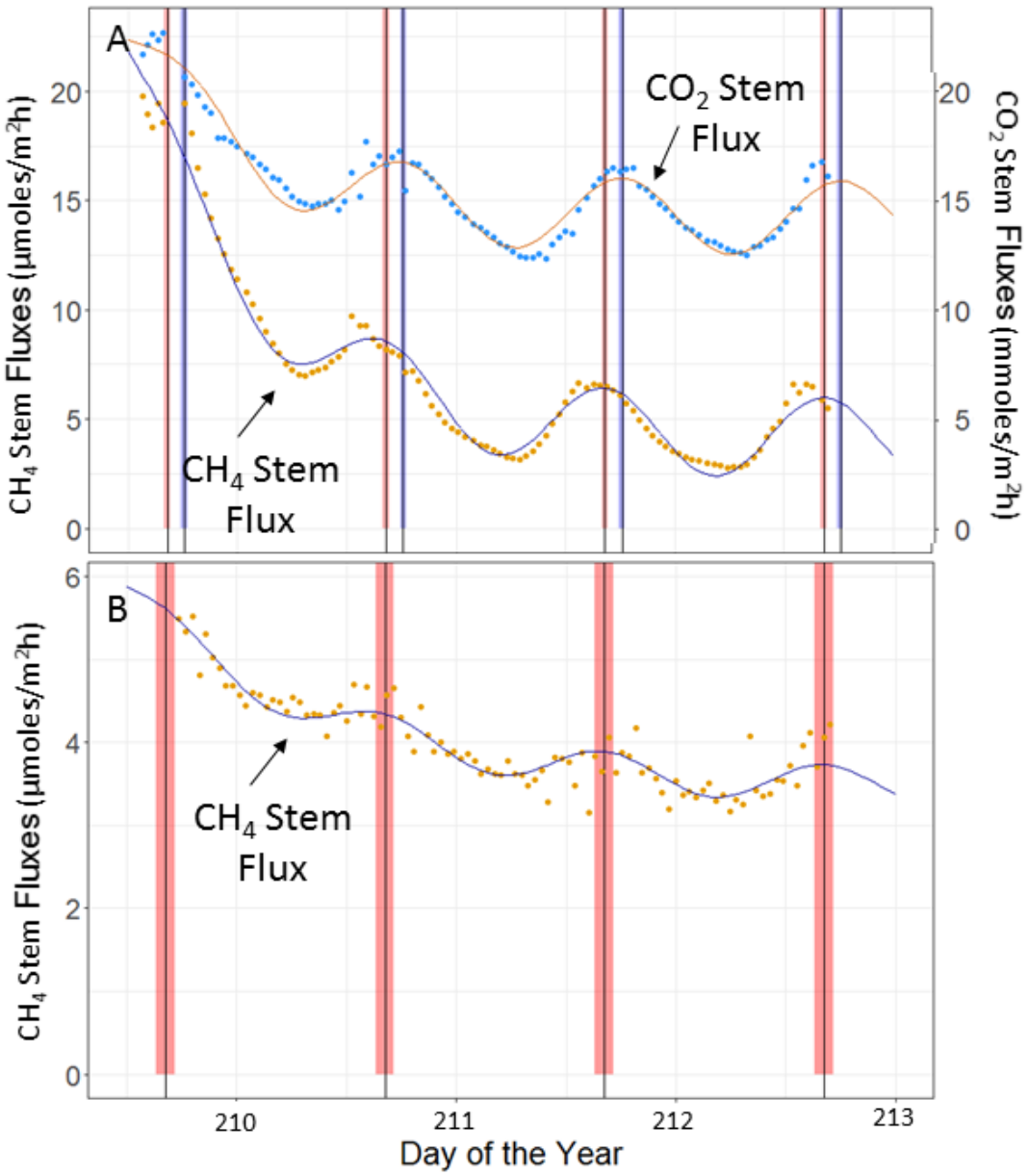

Figure 2-6: Data and curve fitting results from the 75 cm height chambers on the L. tulipifera (A) and the F. grandifola (B). (A) Data and fitted curves from stem CO_2 and CH_4 fluxes. Vertical black lines mark the mean time of peak flux during the measurement period with stem CH_4 fluxes leading stem CO_2 fluxes. Shaded areas are the 95% CI for the mean time of peak fluxes for CH_4 (red) and CO_2 (blue). Note that the Y-axes differ in units. (B) Data and fitted curve from the CH_4 stem fluxes from the F. grandifola. The stem CO_2 fluxes from F. grandifola at 75 cm did not show a discernible diurnal cycles and was not plotted. The vertical black lines mark the mean time of peak flux during the measurement period and red shaded areas are the 95% CI for the mean time of peak fluxes. The 95% CI is wider than the L. tulipifera at the same height but the mean peak times differ by only eight minutes.

Despite empirical evidence of several potential CH_4 sources in living upland trees, there is no evidence in this study or previous studies that can definitively assign the CH_4 emitted from trees to an *in*

situ source. Potential sources include microbial production inside the tree stem (Zeikus and Ward 1974, Covey et al. 2012, Wang et al. 2016), on stem bark (Lenhart et al. 2015) and in subsurface soils (Megonigal and Guenther 2008), and abiotic, UV-driven production by leaves and other tree surfaces (Keppler et al. 2008). UV-driven CH_4 production was not a source in the present study because emissions were measured in opaque chambers. Fungi on tree stems are unlikely to be an important source because reported rates are far less than those observed here (Lenhart et al. 2015). In the present study, evidence against a soil CH_4 source (thus consistent with a wood source) is the fact that stem emissions were not statistically related to soil moisture, soil temperature or water table depth ($P>0.05$). Also, a rise in the water table in late Aug (Figure 2-1) did not increase Aug emissions (Figure 2-5). The trees in this study were not surveyed for rot or wet wood (e.g.Wang et al. (2016)), but surveys of Atlantic coast temperate forest tree stems show that super-ambient internal CH_4 concentrations are commonplace and reflect an internal source (Covey et al. 2012).

Soils are a potential source of tree CH_4 consistent with some observations in this study (Megonigal and Guenther 2008). Methane transport via transpiration is consistent with declining CH_4 emissions with increasing height on the same tree (Figure 2-8). This pattern is expected for a soil CH_4 source (Terazawa et al. 2007, Gauci et al. 2010, Pangala et al. 2013, Pangala et al. 2015), while an internal (wood) source is expected to peak at a height well above the base (Covey et al. 2012). We observed the same pattern in stem CO_2 emissions (Figure 2-8) and found that CO_2 and CH_4 were correlated ($r=0.35$, $p<0.01$); similar observations have been observed for stem CO_2 emissions and interpreted as soil CO_2 entrained in the tree transpiration stream (Teskey et al. 2008). Second, a soil source CH_4 is expected to respond to changes in soil water content. Although we did not detect a statistical relationship between soil moisture content and stem CH_4 emissions, there were two instances when high emission rates followed a precipitation event. The first was the Jun sample in the transect study when all 10 individuals emitted CH_4 at rates one order of magnitude higher than in other months.

The Jun sample occurred during a period of high volumetric soil moisture content (>30%) and warm soil temperatures compared to mid-May when water content was also high (Figure 2-5). The combination of warm temperatures and high soil water content may have simultaneously increased CH_4 production and decreased methanotrophy due to O_2 limitation, as evidenced by the fact that soil CH_4 uptake rates were also lowest in Jun (Figure 2-5). The second instance was in the three-day record of automated flux measurements when rates in two individuals declined with time (Figure 2-9, Figure 2-6); this occurred during a rain-free period following a damp period (2 mm rain over 5 days) and may reflect the influence of declining soil water content.

We observed striking differences in diurnal patterns of stem CH_4 emissions for the two individuals fitted with automated flux chambers (Figure 2-9). The relatively subtle diurnal variation in the *F. grandifolia* tree compared to the *L. tulipifera* tree (Figure 2-6) may reflect different CH_4 sources, different axial and radial stem diffusion rates, or different sinks (e.g. CH_4 oxidation), all of which influence stem CO_2 emissions (Teskey et al. 2008). Sorz and Hietz (2006) found that O_2 diffusion rates tend to increase in the order: conifers > ring-porous species > diffuse-porous species, but both *L. tulipifera* and *F. grandifolia* are diffuse-porous. With just one stem of each species, the differences may

simply reflect characteristics of these particular individuals. However, mean CH_4 emissions were also higher in *L. tulipifera* in the well replicated transect study (Figure 2-7).

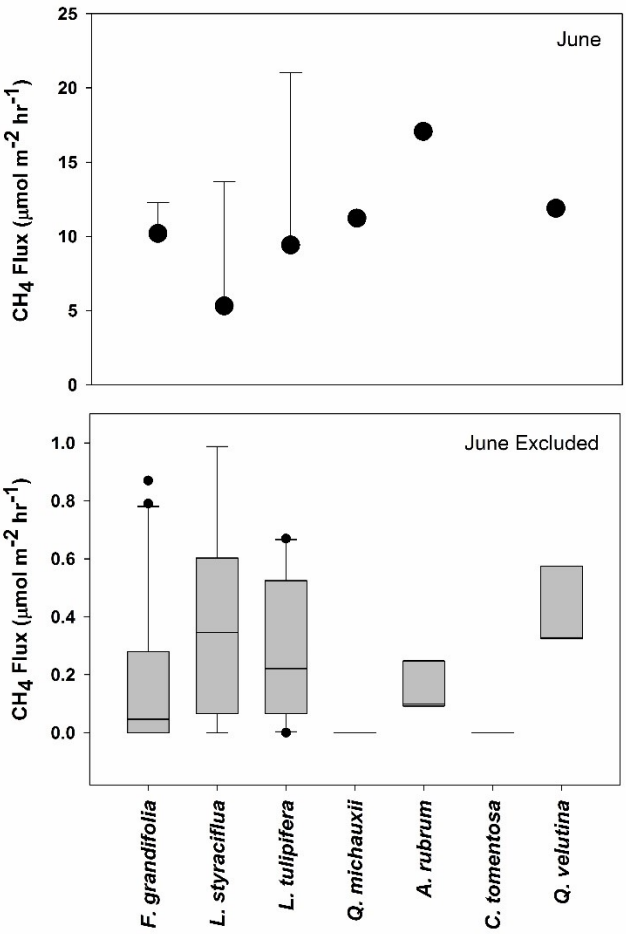

Figure 2-7: Upland tree CH_4 emissions from May-Oct 2014 as a function of species. Upper panel: Jun emissions plotted as mean±95% CI. Lower panel: Fluxes for other months (Jun excluded) plotted as box plots with box boundaries that represent 25th, 50th (median) and 75th percentiles; whiskers are 90th and 10th percentiles; and points are outliers. Sample sizes for each species from left (F. grandifolia) to right in the upper panel were n=2, 3, 2, 1, 1, 0, 1; in the lower panel samples sizes were n=26, 9, 10, 3, 3, 4, 3.

High frequency flux measurements and time series analysis have the potential to be powerful analytical tools to disentangle tree CH_4 sources and transport pathways. The *L. tulipifera* fit with an automated chamber showed a diurnal cycle with peak emissions in late afternoon (CH_4=1620 h,

CO_2=1813 h; Table 2-2). The timing of this CH_4 peak falls between peak sap flux density (1200 h) and near the transpiration-driven minima in tree diameter (1630 h) measured one year later on the same *L. tulipifera* tree (Herrmann et al. 2016). Long-term records of near-continuous CH_4 emissions combined with knowledge of the kinetics of gas and heat transfer in trees will help to infer CH_4 sources.

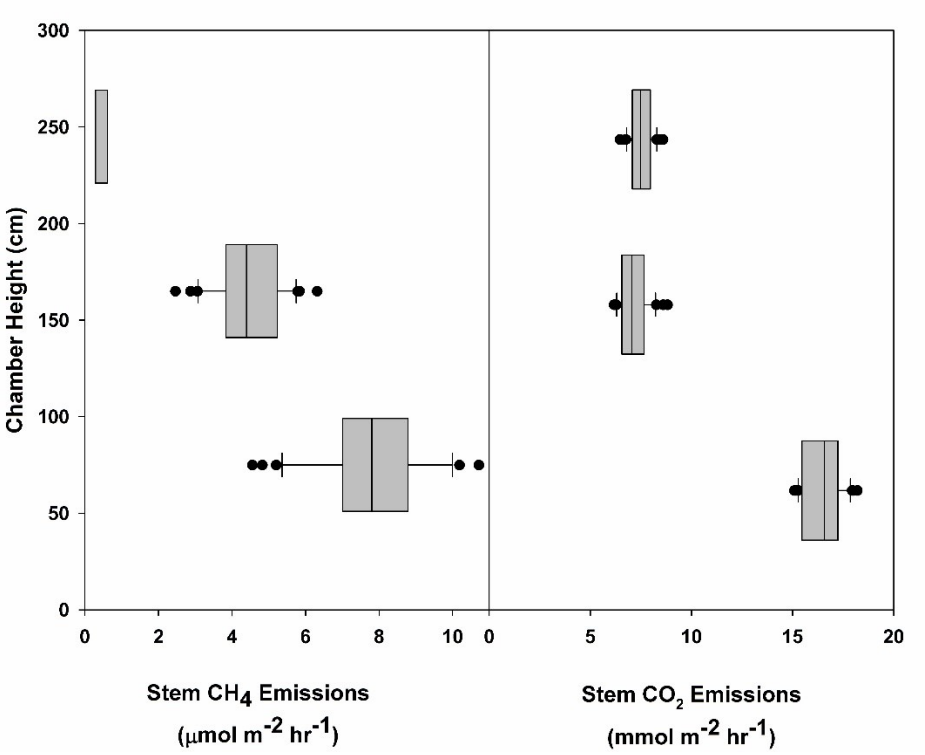

Figure 2-8: Vertical profiles of CH_4 and CO_2 emissions from a L. tulipifera stem on day of the year 210 of 2014. Chambers were mounted at heights of 75, 165 and 245 cm. Sample sizes were 32-33 observations per for each box plot except CH_4 at 245 cm where n=3. Fluxes are plotted as box plots with box boundaries that represent 25th, 50th (median) and 75th percentiles; whiskers are 90th and 10th percentiles; and points are outliers.

The consequences of our observations for upland forest CH_4 budgets are difficult to judge because of the limited sample size of soils, trees, tree species and tree surface types (i.e. trunks only).

Nonetheless, it is useful to estimate the balance of soil CH_4 consumption and tree CH_4 emissions because *in situ* tree and soil CH_4 fluxes have been measured simultaneously in only three other upland

Tree Species	Gas	Chamber Height (cm)	Peak Flux (hours)†	r^2	Adjusted r^2	RMSE
L. tulipifera	CH_4	75	16:20 (15:59, 16:42)	0.98	0.98	0.598
L. tulipifera	CH_4	165	16:08 (15:43, 16:31)	0.98	0.98	0.450
F. grandifola	CH_4	75	16:12 (15:11, 17:14)	0.87	0.86	0.203
L. tulipifera	CO_2	75	18:13 (17:53, 18:33)	0.95	0.95	0.526
L. tulipifera	CO_2	165	17:11 (16:34, 17:47)	0.82	0.81	1.200
L. tulipifera	CO_2	245	17:41 (17:07, 18:14)	0.89	0.88	0.890

†Mean with 95% confidence intervals in parentheses. Diurnal cycles were fit to the equation: $y = a \cdot e^{-\lambda t} + b \cdot \cos(2\pi \cdot (t-\delta)) + c$, where a is the exponential coefficient, λ is the exponential decay constant, t is the time in decimal days, c is the exponential asymptote, b is the harmonic coefficient, and d is the phase shift in decimal days from zero (midnight). The exponential term ($y = a \cdot e^{-\lambda t} + c$) detrended the data. The harmonic function [$\cos(2\pi \cdot (t-\delta)$] returned the phase shift, which is the average time of day during which peak flux rates occur. The equation was fit using nonlinear least squares within the Curve Fitting package from MATLAB R2106b (The MathWorks, Inc., Natick, MA, USA).

Table 2-2: Statistical analysis of diurnal CH_4 and CO_2 fluxes for two trees. Data from chambers at two heights on a L. tulipifera and one height on a F. grandifola. Heights and gases that did not show statistically significant diurnal patterns are not included (i.e. CH_4 from L. tulipifera at 245 cm; CO_2 from F. grandifolia at 75 cm).

forests (Machacova et al. 2016, Wang et al. 2016, Warner et al. 2017). A simple scaling exercise suggests that upland tree emissions offset 6% of the soil sink over the May-Sep growing season, much of which occurred in a single Jun event of uncertain duration when this forest may have become a transient net source of CH_4 at a rate of 2.14 μmol m^{-2} soil h^{-1}. A more conservative approach is to eliminate the Jun sample from the calculation, in which case tree emissions offset 1% of the soil sink. The range of estimates from our study (1-6%) brackets the only other estimate (3.5%) for a North American temperate forest (Warner et al. 2017). Both estimates are far lower than an estimate from a temperate deciduous forest in China where tree emissions offset 63% of soil CH_4 sink (Wang et al. 2016), but higher than a dry *P. sylvestris* site where the offset was 0.8% (Machacova et al. 2016). This wide

range of estimates suggests that upland tree CH_4 emissions are highly variable and illustrates the need for new sampling and scaling strategies for quantifying local, regional and global upland forest CH_4 dynamics. The sampling challenge may be greater depending on whether small stems and leaves emit significant amounts of CH_4 (Machacova et al. 2016), consume CH_4 (Sundqvist et al. 2012), or have neither effect (Wang et al. 2016), all of which have been observed. It should be noted that while the degree to which stem emissions offset the soil sink is highly uncertain, in all cases upland soils remained net sinks for atmospheric CH_4.

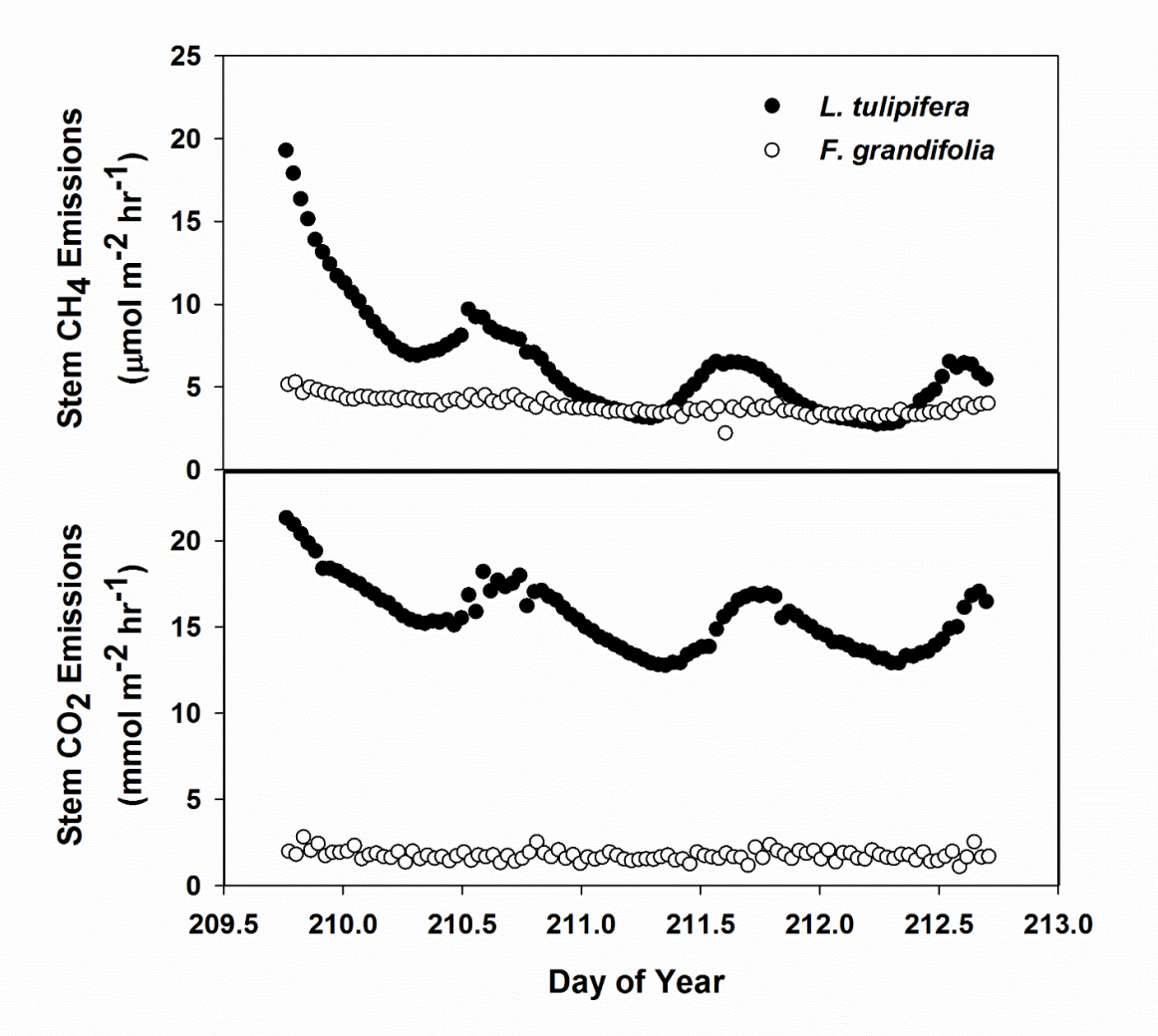

Figure 2-9: CH_4 and CO_2 emissions from a L. tulipifera (filled circles) and a F. grandifolia (open circles) at 75 cm above the soil surface. Note that the Y axes for the two gases are scaled differently.

2.4. Conclusions

We propose that upland forests are smaller CH_4 sinks than previously estimated due to stem emissions. A simple and conservative scaling exercise suggests that tree stem CH_4 emissions offset 1-6% of annual CH_4 consumption by soils, and that under some conditions may be large enough to briefly change an upland temperate forest from a net sink to a source. These data support a small but growing body of evidence that suggest that upland forests are not uniform consumers of CH_4 and that the role of stem emissions in the CH_4 budget of upland forests is highly variable in space and time. Our data demonstrate that stem emissions may have a diurnal component, which points to soils as a source of CH_4 and transpiration as a possible driver of CH_4 fluxes in some temperate forest species. On the contrary, the absence of correlations with soil water content or water table depth are consistent with a microbial source inside these trees. Distinguishing between these potential sources is a challenge and an important step towards scaling upland tree CH_4 fluxes.

Acknowledgments

This chapter was published in the journal New Phytologist (Pitz and Megonigal 2017). This study was supported by the DOE Terrestrial Ecosystem Science program (grant DE-SC0008165) and NSF-ERC MIRTHE (EEC-0540832). The authors would like to thank Geoffrey Parker for the forest plot data and surface area estimates. S.P. thanks Katalin Szlavecz for her mentorship. We thank Lisa Schile for her assistance and advice. We would also like to thank Adam Langley for helping us in the early phases of this project and the entire GCReW and Soil Ecology Labs. Flux data are presented in the supporting information and will be archived at the Smithsonian Environmental Research Center. Requests for the unprocessed data can be made to the corresponding authors.

3. Methane fluxes from tree stems and soils along a habitat gradient

Abstract

Forests are major sources of terrestrial CH_4 and CO_2 fluxes but not all surfaces within forests have been measured and accounted for. Stem respiration is a well-known source of CO_2, but more recently tree stems have been shown to be sources of CH_4 in wetlands and upland habitats. A study transect was established along a natural moisture gradient, with one end anchored in a forested wetland, the other in an upland forest and a transitional zone at the midpoint. Stem and soil fluxes of CH_4 and CO_2 were measured using static chambers during the 2013 and 2014 growing seasons, from May to October. Mean stem CH_4 emissions were 68.8 ± 13.0 μg m^{-2} h^{-1} (mean ± standard error), 180.7 ± 55.2 μg m^{-2} h^{-1} and 567.9 ± 174.5 μg m^{-2} h^{-1} for the upland, transitional and wetland habitats, respectively. Mean soil methane fluxes in the upland, transitional and wetland were -64.8 ± 6.2 μg m^{-2} h^{-1}, 7.4 ± 25.0 μg m^{-2} h^{-1} and 190.0 ± 123.0 μg m^{-2} h^{-1}, respectively. Measurable CH_4 fluxes from tree stems were not always observed, but every individual tree in our experiment released measurable CH_4 flux at some point during the study period. These results indicate that tree stems represent overlooked sources of CH_4 in forested habitats and warrant investigation to further refine CH_4 budgets and inventories.

3.1. Introduction

Atmospheric methane (CH_4) concentrations have increased from 700 ppb to over 1800 ppb since the beginning of the industrial revolution and presently contribute 0.7 W m^{-2} or 25% of radiative forcing (IPCC 2013). Although the net balance of CH_4 sources and sinks is well constrained compared to trace gases other than CO_2, the relative contributions of individual sources and sinks are less certain (Kirschke et al. 2013, Saunois et al. 2016a). Such uncertainty has made it difficult to explain phenomena such as changes in the globally averaged atmospheric growth rate and isotopic concentration of CH_4 (Aydin et al. 2011, Nisbet et al. 2016) and exposed the limits of our current mechanistic understanding of CH_4 cycling.

In response, the past decade has been a period of prospecting for novel CH_4 sinks and sources that might better describe CH_4 cycle dynamics.

Wetlands have always been considered a source of CH_4, which is emitted across both the soil-atmosphere interface and plant surfaces (Dacey and Klug 1979). Emission from herbaceous wetland plants is facilitated by aerenchyma tissue which allows rapid rates of gas exchange between soils and the atmosphere, supporting aerobic respiration but also diffusion and mass flow of CH_4 past oxic zones at the soil surface.

While whole-ecosystem (plant and soil) CH_4 emissions have been measured extensively in wetlands dominated by herbaceous plants (Dacey and Klug 1979, Conrad 2007), such data are generally lacking from woody plants such as trees because their large stature makes plant flux measurements difficult. Early studies demonstrated CH_4 emissions from woody wetland tree roots (Pulliam 1992, Rusch and Rennenberg 1998), and seedlings (Vann and Megonigal 2003, Garnet et al. 2005), but field measurements to quantify tree CH_4 emissions were conducted only in the last decade (Terazawa et al. 2007, Gauci et al. 2010, Pangala et al. 2015). The results indicate that tree-mediated CH_4 emissions have been overlooked and may account for 60-87% of total CH_4 efflux in tropical wetlands (Pangala et al. 2013) and 20% in temperate wetlands (Gauci et al. 2010). Given that forested wetlands represent 53% of total wetlands (Fung et al. 1987), these numbers are significant, yet have not been included global earth systems models and budgets (Saunois et al. 2016a).

Upland forests have been generally considered net sinks of CH_4 based upon the assumption that the only surface in a forest that interacts with CH_4 is the soil. Studies have shown that CH_4 can be produced inside upland trees (Bushong 1907, Zeikus and Ward 1974, Covey et al. 2012), however, few *in situ* direct measurements have attempted to quantify net fluxes from trees (Machacova et al. 2016, Wang et al. 2016, Maier et al. 2017, Pitz and Megonigal 2017, Warner et al. 2017) . Wang et al. (2016)

estimated that tree CH_4 flux was sufficient to offset the soil sink by 5-10% on an annual basis. Machacova et al. (2016) suggested that depending on soil moisture, Scots pine CH_4 emission account up to 35% of soil uptake. Clearly, tree-atmosphere trace gas interactions cannot be ignored and have to be included in calculating CH_4 budgets in forested ecosystems.

The processes by which CH_4 is produced and emitted to the atmosphere through trees are poorly understood. Data are insufficient for developing a generalized conceptual model of tree CH_4 emissions that captures the wide range of species, ecosystems, and conditions. Studies in wetland forests generally show a positive relationship between tree emission rates and water table depth (Terazawa et al. 2007, Gauci et al. 2010, Pangala et al. 2015), suggesting that CH_4 produced under saturated, anaerobic conditions in groundwater becomes entrained in the transpiration stream or diffuses into plant tissue, where it is transported and eventually emitted to the atmosphere. In contrast, a more diverse set of mechanisms have been proposed in upland forests, including non-soil CH_4 sources such as UV-driven aerobic production (Keppler et al. 2008, Vigano et al. 2008) and anaerobic biological production in trunks associated with heart rot (Covey et al. 2012) or non-structural carbohydrates (Covey et al. 2016). Megonigal and Guenther (2008) hypothesized that groundwater is also a source of CH_4 emitted by upland forest tree species. In this case, deep roots growing in CH_4-rich groundwater or anoxic soil microsites could entrain CH_4 and transport it to the atmosphere, bypassing the oxic soil horizons where it would otherwise be consumed by methanotrophs. A growing list of studies indicates that a variety of plant-mediated CH_4 sources exist and that all ecosystems contain some surfaces that have the potential to emit CH_4.

Gradient studies can reveal insights into some of these processes as they vary across wetland and upland forests, but studies reported thus far have focused on only one habitat. In this study, we conducted the first CH_4 flux measurement along a soil moisture gradient from wetland to upland at the

same location. The close proximity of upland and wetland allows potentially confounding variables such as climate, past land use, and, to some extent, plant community composition to be kept constant. We directly measured CH_4 fluxes from soils and stems from a variety of tree species that are common in mid-Atlantic deciduous forests.

The goals of this study were to: (1) quantify CH_4 emissions from trees growing across a soil moisture gradient in a temperate forest ecosystem, (2) compare the relative contribution of soils and trees in upland and wetland forests, and (3) relate these fluxes to environmental factors. We also report stem and soil CO_2 fluxes because CO_2 emissions from stem respiration are relatively well understood and thus help to interpret the pattern of CH_4 fluxes.

3.2. Methods

Study site

The study was conducted at the Smithsonian Environmental Research Center (SERC), a property of 1072 hectares (2,650 acres) on the western shore of Chesapeake Bay in Maryland. Much of the site is forested with smaller areas of brackish tidal wetlands and farmland. Forests have been recovering for 70-150 years from different land use and disturbance histories such as logging, wind damage, and agricultural abandonment (Higman 1968, Yesilonis et al. 2016), with small patches that have no known history of land use. Our main study plot was in an upland forest that was most likely grazed before the Civil War and then abandoned (Higman 1968). Today the forest is dominated by Tulip poplar (*Liriodendron tulipifera),* American beech *(Fagus grandfolia),* and several species of oaks *(Quercus spp.),* and hickories *Carya spp.* The species composition is typical of the mature stage of a Tulip poplar association (Brush et al. 1980, Brown and Parker 1994) with a closed canopy and very little understory.

Mean rainfall is 1146 mm and mean annual temperature is 13.0°C (D. Correll, T. Jordan, and J. Duls, unpublished data). The mean annual maximum temperature is 19.0°C and the mean minimum temperature is 8.0°C (NCDC database, Annapolis Police Bar Station).

Soils at SERC are predominately fine sandy loams or sandy loams. Physical and chemical characteristics of surface soils reflect past land use history, forest age and non-native earthworm activity (Yesilonis et al. 2016). Our transect crossed three soil associations, with the upland and transitional sections in the Collington-Annapolis series and the Collington-Wist-Westphalia series, respectively. Soils in the wetland section transect were in the Widewater-Issue series (Natural-Resources-Conservation-Service 2016)

We established an approximately 150 m long transect along a soil moisture gradient (location: 38.8878, -76.5624). The elevation difference between the two end points of the transect was approximately 6 m. Based upon soil characteristics, elevation, and water table depth we divided the transect into three habitat types: upland (100 m), transitional (25 m) and wetland (25 m). Thirty-two trees selected for the study belonged to nine species (Table 3-1). Based upon stem counts, these nine species make up 80% of the mature stand adjacent to the transect (Parker and Tibbs 2004). *Liquidambar styraciflua* (sweetgum) occurred in all three habitat types, with the remaining species present in one or two habitats.

Stem and Soil Chambers, and Flux Measurements

Tree and soil measurements were made between May and November in 2013 and between May and September in 2014 using the closed chamber technique. A total of 32 trees were fitted with opaque rectangular chambers modified from Ryan (1990), originally designed to measure stem respiration. In

Table 3-1: Tree species used in the stem flux measurements at the Smithsonian Environmental Research Center

Latin name	**Common name**	**Number**	**DBH[a] (cm)** Mean ± SD	**Range of DBH (cm)**	**Habitats found[b]**	**Wetland designation[c,d]**
Fraxinus pennsylvanica	Green ash	4	24.7 ± 4.7	17.8 – 28.5	W	FACW
Liquidambar styraciflua	Sweetgum	8	39.6 ± 14.3	21.9 – 62.5	U, T, W	FAC
Carya tomentosa	Mockernut hickory	1	22.8	--	U	NI
Fagus grandifolia	American beech	8	45.1 ± 14.4	16.1 – 56.2	U, W	FACU
Liriodendron tulipifera	Tulip poplar	4	60.7 ± 26.7	31.8 – 92.6	U, T	FACU
Quercus velutina	Eastern black oak	1	65.8	--	U	NI
Quercus michauxii	Swamp chestnut oak	3	60.4 ± 18.4	39.9 – 75.5	U, T	FACW
Carpinus caroliniana	American hornbeam, Ironwood	1	12.5	--	W	FAC
Acer rubrum	Red maple	2	31.1 ± 14.6	17.0 – 46.2	U, W	FAC

[a]DBH: Diameter at breast height
[b] U: upland; T: transitional; W: wetland
[c] Indicator status: FACW: facultative wetland; FAC: facultative; FACU: facultative upland; NI: no indicator assigned.
[d] Source: Tiner and Burke (1995)

2013, 21 chambers were installed across the transect. In 2014, 10 additional trees were fitted with chambers in order to expand the upland section of the transect. Each tree was paired with a soil gas flux chamber placed within 1 m of the base. Sampling rounds differed among habitats with the upland habitat sampled more frequently in 2014 than the other two habitats, because our main interest was to quantify upland CH_4 stem fluxes. Rectangular stem chambers were constructed of acrylic, permanently fixed to stems 30-60 cm above the soil, and were secured to the stem using elastic shock cord. Each chamber was 28 cm in height with varying depths and widths depending on the tree size. To create an airtight seal, closed-cell neoprene foam was placed between the chamber edge and the stem, and sealed with dental mold to create a non-VOC seal (Examix^{TM}, GC America, Alsip, IL, USA). Soil flux chambers were constructed out of 30.5 cm-diameter (12") schedule 80 PVC pipe, machined into a 10-cm high ring and placed 5 cm into the soil surface. All chambers were in place for a minimum of one week before taking flux measurements, and once mounted they remained in place for the duration of the study.

In the two years of study we used two different instruments to analyze the gas samples from the headspace of the flux chambers. Gas samples from the headspace of the flux chambers were analyzed by gas chromatography (GC) in 2013 and by a more accurate and precise portable Off-Axis Integrated Cavity Output Spectroscope (OA-ICOS) (Ultra-Portable Greenhouse Gas Analyzer, Los Gatos Research, Mountain View, CA, USA) in 2014. The two instruments provided different amounts of data for each flux which required a different approach, described below, for the statistical analysis.

In 2013, gas concentrations in air samples were determined using a gas chromatograph. After closing the chamber lid, 12 mL samples were withdrawn by syringe at 0, 15, 30, 45, and 60 minutes. The air samples were immediately transferred from the syringe to a 12 mL, nitrogen-flushed Exetainers (Labco, UK). The gas samples were analyzed for CH_4 and CO_2 on a Varian GC-450, equipped with a flame

ionization detector (FID) and a thermal conductivity detector (TCD). The FID had a precision of 0.120 ppm for CH_4 and the TCD had a precision 5 ppm for CO_2.

In 2014, gas concentrations were measured using a portable OA-ICOS. The instrument is capable of measuring CH_4 within a range of 0.01-100 ppm with a precision of 0.002 ppm at 0.5 Hertz. The OA-ICOS can also measure CO_2 in a range of 200-20000 ppm with a precision of 0.3 ppm. The OA-ICOS was used as a closed system: headspace gas was drawn from the chamber, measured non-destructively for CH_4 and CO_2 concentration, and returned to the flux chamber as described in Baird et al. (2010). Changes in CH_4 and CO_2 concentration were measured over periods of approximately 5-30 minutes, during which the system generated ≥150 observations.

In 2013, five concentration data points were collected for each flux measurement. We occasionally dropped a concentration data point for two reasons; soil CH_4 ebullition or poor quality data from the GC. If a data point was dropped due to poor quality data from the GC, both CH_4 and CO_2 data had to support that conclusion. The slope of gas concentration change over time was determined by linear regression (SAS® procedure Proc Reg). In every case, the slope was based on ≥4 observations. For a slope to be determined as a quality data point, the R^2 had to be greater than 0.90. If the R^2 of a slope was less than 0.90, then the slope and flux was considered to be zero.

In 2014, the OA-ICOS provided concentration data at a rate of 0.5 Hertz which required us to use a slightly different treatment of the data. When calculating the slope of gas concentration change over time, we ignored the first 20% of the observations, as those may produce false readings associated with closing the lid. The slope of gas concentration change was determined as described above (SAS® procedure Proc Reg). In every case, the slope was based on ≥120 observations.

Gas flux was calculated using the following equation:

$$F = \frac{d[CH_4]}{dt} \times \frac{PV}{ART}$$

where F is the flux in μg m^{-2} hr^{-1}, P is atmospheric pressure, T is temperature, R is the universal gas constant, A is the collar surface area and V is the volume of the air enclosed by the chamber. Air temperature was measured by the OA-ICOS unit on gas circulating between the unit and the chamber. Atmospheric pressure was based on a nearby weather station (<1 km). Flux units are reported in μg m^{-2} h^{-1} or mg m^{-2} h^{-1} to allow for direct comparison with stem flux data published by others.

Environmental Data

Soil moisture was measured using a FieldScout TDR (Spectrum Technologies Inc., Aurora, Illinois, USA). Soil temperature was measured with a digital thermometer at 10 cm. Weather data was collected on site from the SERC weather station (Campbell Scientific, Utah, USA).

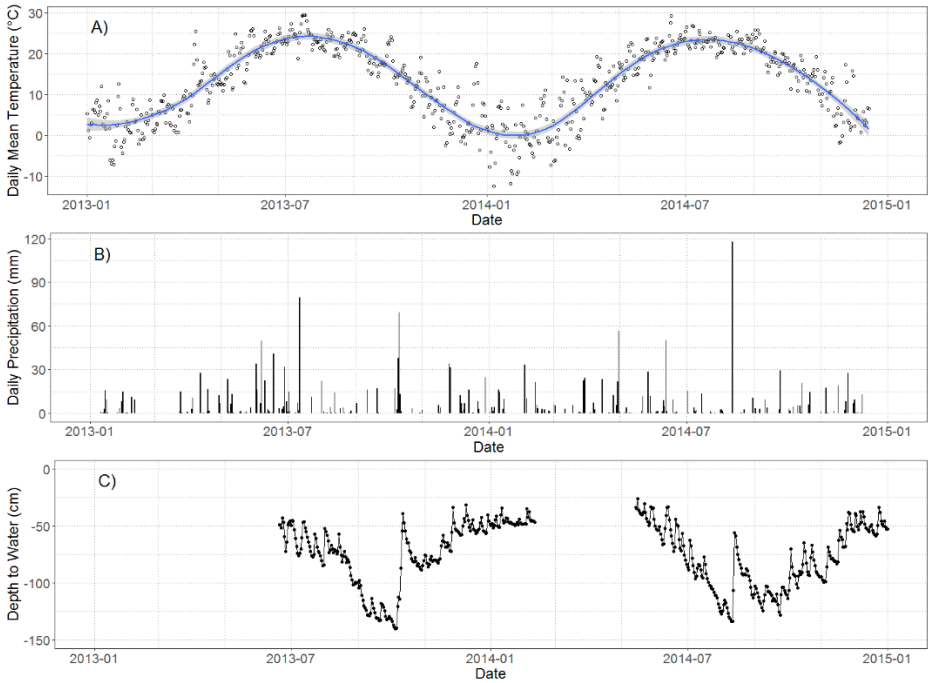

Figure 3-1: Daily mean air temperature (A), daily precipitation (B) and groundwater elevation (C) at the SERC study site during 2013 and 2014. A continuous groundwater elevation data logger was placed in a well (Well 2) within the transitional habitat; groundwater elevation in the three other wells located within the study site were recorded manually (see Methods). The water table elevation data logger was removed for three months in the winter of 2014.

Water table depth or groundwater elevation along the transect was monitored using several monitoring wells. Four 5.08 cm diameter wells were installed (three in 2013, and one was added in 2014). One was installed in the wetland, one in the transitional zone, and two in the upland. The fourth well was added to the upland in 2014 when new trees were added to the transect. Wells were constructed of 5.08 cm PVC and screened with 152 cm sections of PVC with 0.25 mm slot size. Number #1 sand was used as a screen pack. Water table depth was recorded manually during each sampling event using a water level meter (Model 102 Water Level Meter, Solinist, Georgetown, Ontario, Canada). Well #2 in the transitional was monitored during the growing seasons in 2013 and 2014 (Figure 3-1C) using a groundwater elevation logger (Aqua Troll 200, In-Situ Inc., Fort Collins, Colorado, USA).

Statistical analysis

All statistical analyses on flux data were conducted using R v3.1.2 (R Core Team 2014), except gas fluxes that were calculated using SAS. Methane flux rates were Box-Cox transformed after increasing all values until the minimum value in the data set was 10 $\mu g\ m^{-2}\ h^{-1}$ to avoid negative values after log transformation. Means and standard errors presented in the text, figures, and tables were calculated using non-transformed data. *P*-values below 0.05 were considered significant; those between 0.05 and 0.1 were considered marginally significant. In this paper we report data on CH_4 and CO_2 fluxes from three habitat types (upland, transitional, and wetland) in 2013 and 2014. Upland stem and soil CH_4 flux data from 2014 were reported in Pitz and Megonigal (2017) but were combined in the present study for statistical analysis.

The mean CH_4 and CO_2 fluxes were calculated for each tree and the respective soil chambers and analyzed for the effects of habitats using analysis of variance (ANOVA) followed by the Tukey's HSD test for multiple comparisons. Mixed effect models were conducted using the lme4 package to evaluate

the correlations between environmental factors and stem CH_4 flux, soil CH_4 flux, stem CO_2 flux, and soil CO_2 flux. Sampling round and tree identity were treated as random effects. Fixed effects included were habitat for all analyses, tree species and diameter at breast height (DBH) for stem fluxes, DTW, soil moisture and soil temperature for CH_4 fluxes, and soil moisture and soil temperature for CO_2 fluxes. These factors were evaluated in the models following the above order. Likelihood ratio tests were used to access significant differences between nested models, and were followed by the Tukey's HSD test for multiple comparisons using the multcomp package (Hothorn et al. 2008).

3.3. Results

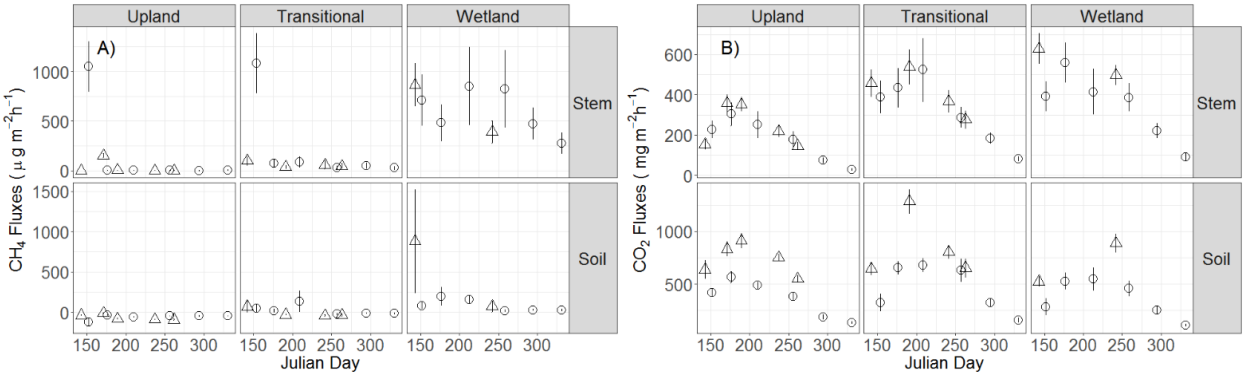

Figure 3-2: Temporal changes of stem and soil CH_4 (A) and CO_2 (B) fluxes in the three habitat types. Data for 2013-2014 are combined. 2013 fluxes are represented by circles and 2014 fluxes are represented by triangles. Error bars are standard error. Note the different scales.

A total of 470 flux measurements were made during the study, 235 measurements of tree stems and 235 of soils. Every tree stem emitted measurable CH_4 at least once during the two seasons of monitoring. Net CH_4 production was detected in all but two stem CH_4 measurements. Stem CH_4 fluxes ranged from -8.1 to 1900 μg m^{-2} h^{-1} in the upland habitat, -16.4 to 2146.2 μg m^{-2} h^{-1} in the transitional habitat and -157.1 to 3757.6 μg m^{-2} h^{-1} in the wetland habitat of the transect (Figure 3-2A). Soil was generally a CH_4 sink in the upland where 97% of the measurements showed net consumption, and a source in the wetland where 80 % of the measurements showed net production. The transitional segment of the transect fell in between, with 74% of the measurements demonstrating net consumption (Figures 2A). Soil CH_4 fluxes ranged from -309.3 to 68.1 μg m^{-2} h^{-1} in the upland habitat, -

167.4 to 651.4 μg m^{-2} h^{-1} in the transitional habitat and -33.3 to 4726.9 μg m^{-2} h^{-1} in the wetland habitat of the transect. (Figure 3-2A, Figure 3-5B). Neither stem nor soil CH_4 fluxes exhibited a seasonal trend; rather high fluxes compared to average values were few and episodic (Figure 3-2A). Stem and soil CO_2 fluxes were consistently positive and three orders of magnitude higher than CH_4 fluxes (Figure 3-2B). Both stem and soil CO_2 fluxes showed a seasonal trend with high values in the growing season and gradually declining values in the fall (Figure 3-2B).

Combining all stem CH_4 measurements by habitat yielded mean (±SE) rates of 68.8 ± 13.0 μg m^{-2} h^{-1} (upland), 180.7 ± 55.2 μg m^{-2} h^{-1} (transitional) and 567.9 ± 174.5 μg m^{-2} h^{-1} (wetland). Stem CH_4 fluxes were significantly different in the three habitat types ($F_{2, 29}$ = 5.80, P = 0.0076), and were higher in wetlands than in uplands (P = 0.006, Tukey's HSD test) (Figure 3-3A). Mean soil CH_4 fluxes were -64.8 ± 6.2 μg m^{-2} h^{-1} (upland), 7.4 ± 25.0 μg m^{-2} h^{-1}, (transitional) and 190.0 ± 123.0 μg m^{-2} h^{-1} (wetland). ANOVA showed significant differences in soil CH_4 flux among the three habitats types ($F_{2, 29}$ = 20.08, P < 0.001), and significantly higher fluxes in wetland and transitional (P < 0.001 and P = 0.012, respectively) than in upland (Figure 3-3A).

Stem CO_2 fluxes were only marginally affected by habitat types ($F_{2, 29}$ = 2.88, P = 0.073). Contrary to CH_4, stem and soil CO_2 fluxes showed opposite trends across habitats. Soil CO_2 fluxes were significantly affected by habitat ($F_{2, 29}$ = 4.90, P = 0.015), and were higher in upland than in wetland and transitional habitats (P = 0.011) (Figure 3-3B). The significant effect of habitat was further supported by the mixed effect models (Table 3-2).

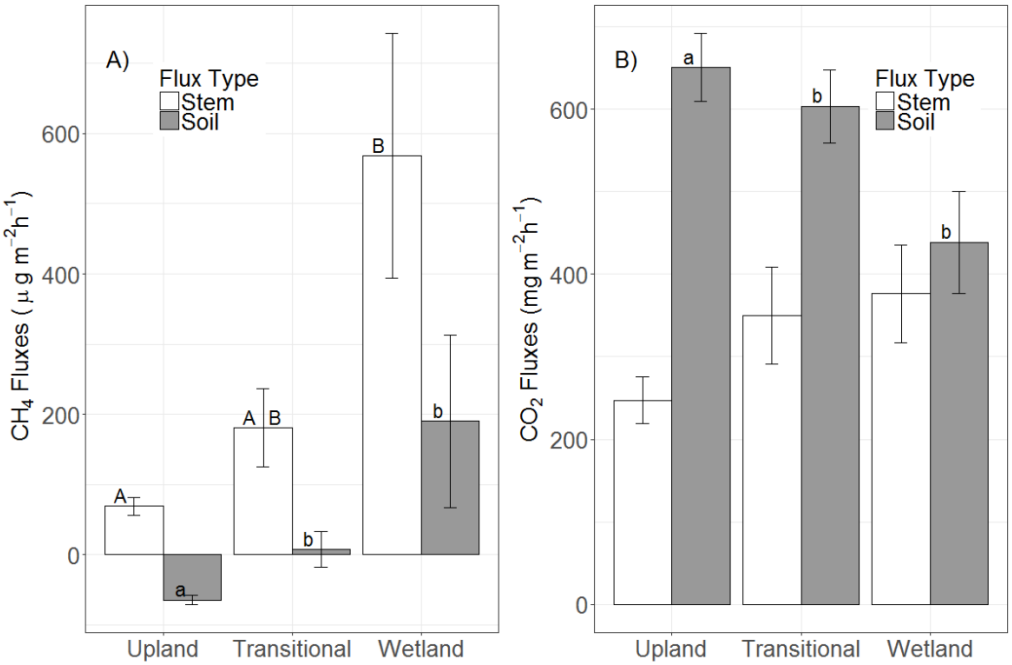

Figure 3-3: Mean (± SE) stem and soil flux for CH_4 (A) and CO_2 (B) in the three habitat types at the SERC study site. Means with different letters are significantly different (Tukey's HSD, $p<0.05$). Tests for stem and soil were run separately, and differences are indicated by upper and low case letters, respectively. Note the different units for CH_4 and CO_2 flux.

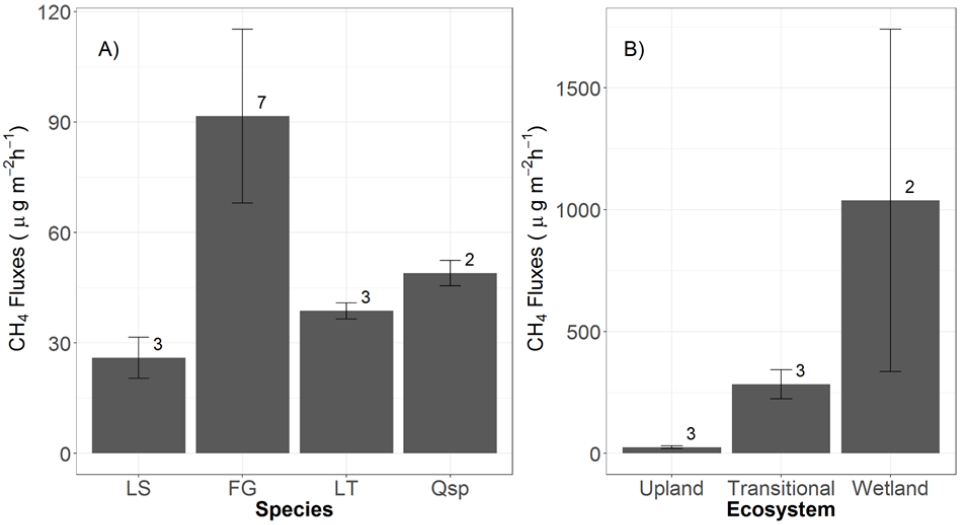

Figure 3-4: Species and habitat effects on stem methane fluxes. A: Four species in one habitat (upland); B: One species (Liquidambar styraciflua, sweetgum) in three habitats. The species codes are LT (Liriodendron tulipifera, tulip poplar), FG (Fagus grandifolia, beech), LS (Liquidambar styraciflua, sweetgum), and Qsp (Quercus sp., oak). Weighted mean (± SE) flux is shown (see Methods). Number of trees is shown on top of each column

Table 3-2: Results of mixed effect models testing the effects of habitat, tree species, diameter at breast height (DBH), depth to water table (DTW), soil moisture, and soil temperature on methane and CO_2 fluxes. Both significant ($P < 0.05$) and marginally significant ($0.05 < P < 0.1$) effects were kept in the models; ↓, significant negative effects; - variables not analyzed; ns, non-significant variables excluded from the model.

	Habitat		**Tree species**		**DBH**		**DTW**		**Soil moisture**		**Soil temperature**	
	χ^2	*P*	χ^2	*P*	χ^2	*P*	χ^2	*P*	χ^2	*P*	χ^2	*P*
Stem CH_4	19.81	<0.001	10.02	0.075	4.18	0.041	14.21	↓<0.001	ns	ns	4.03	0.045
Soil CH_4	22.31	<0.001	-	-	-	-	49.51	↓<0.001	ns	ns	7.91	0.005
Stem CO_2	13.33	0.001	ns	ns	7.17	0.007	-	-	107.72	<0.001	67.67	<0.001
Soil CO_2	4.68	0.096	-	-	-	-	-	-	76.30	<0.001	56.32	<0.001

The range of stem CH_4 fluxes varied greatly by tree species. We detected the highest emissions from green ash and sweetgum, and the lowest from oak and ironwood (*Carpinus caroliniana)*. Tree species identity was significant even after taking into account the confounding effect of habitat (Table 3-2), and comparing stem fluxes only in the upland habitat. On the other hand, habitat effects are clearly shown for stem CH_4 fluxes for sweetgum, the only tree species found in all three habitat types (Figure 3-4B).

Although there was a positive correlation between soil moisture and CH_4 flux in the upland soil (Figure 3-5B), soil moisture in general was not a significant variable in the mixed effects model (Table 3-2). Soil moisture co-varies with habitat and DTW, and was added to the model as the last of these three variables.

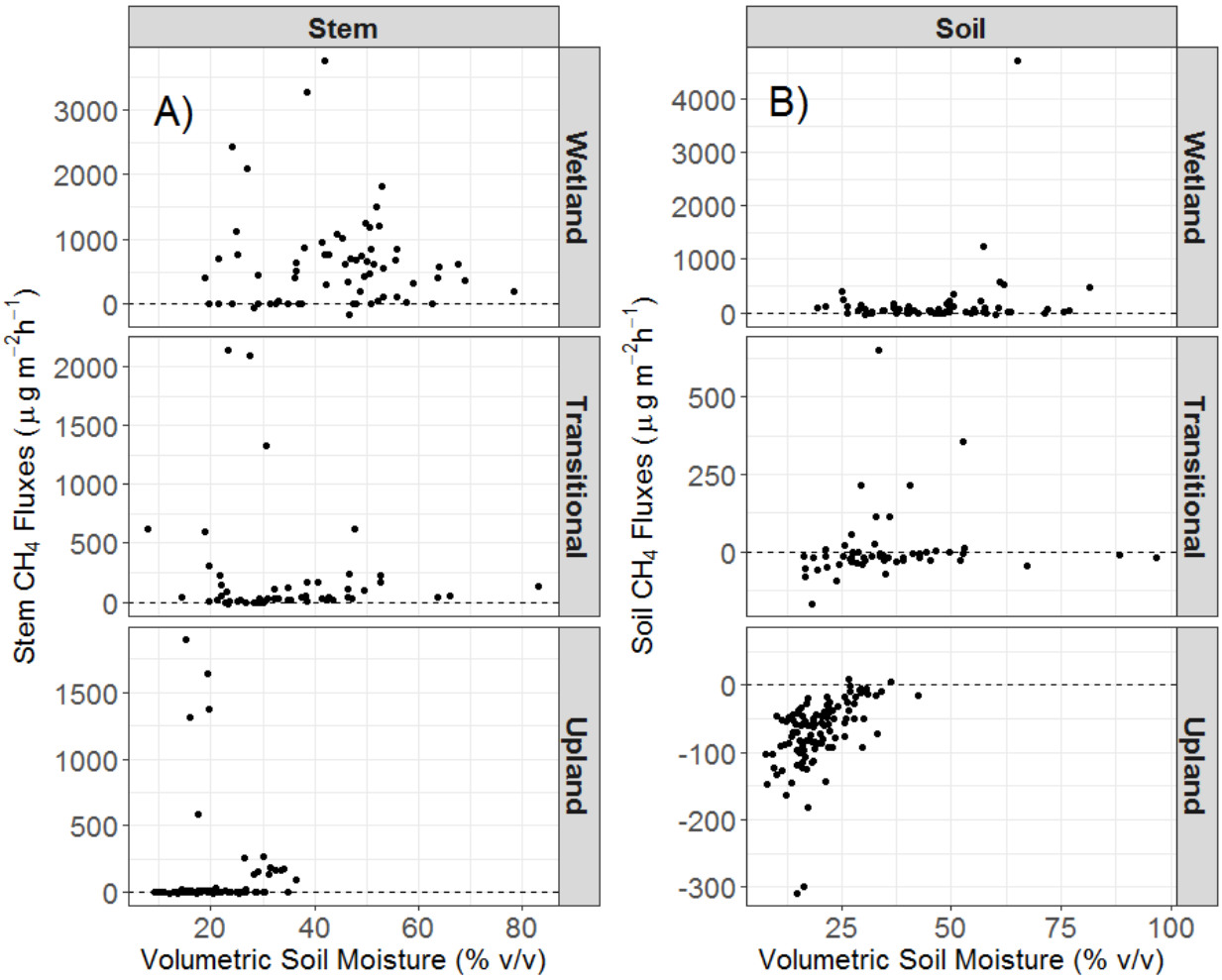

Figure 3-5: Soil moisture versus fluxes. Correlation between methane flux and soil moisture in the three habitats at SERC. Data for 2013-2014 are combined. Left panels: stem fluxes; right panels: soil fluxes. Note the different scales on the y axes.

3.4. Discussion

The present study is the first that simultaneously explores stem and soil trace gas fluxes along a soil moisture gradient (wetland, transitional and upland habitats) in close proximity to one-another. Habitat type is clearly the main driver of both CO_2 and CH_4 fluxes, but appears to more strongly affect the latter. To tease out the subset of abiotic and biotic factors that locally determines trace gas fluxes remains challenging.

We found large differences in the amount of CH_4 emitted from individual trees and from different species. Our data support other studies that report species differences in wetland (Pangala et al. 2015) and upland forests (Wang et al. 2016, Pitz and Megonigal 2017). Aspects of wood anatomy and tree physiology such as wood vessel structure, wood specific density, lenticel density, transpiration rates and sap flow rates may contribute to species level differences. While it has been shown that wood specific density and lenticel density affect stem CH_4 fluxes in wetland trees (Pangala et al. 2013, Pangala et al. 2014), it is unclear how these other factors contribute to interspecific CH_4 flux differences in upland trees. Among the four tree species we examined in the upland ecosystem, *Quercus* spp. have ring-porous vessel structure while the other three species are diffuse-porous. We did not detect any patterns that distinguish these morphological types. Future studies should incorporate these potential drivers into the experimental design.

The mixed effect model found stem CH_4 emissions to be positively related to DBH. This contrasts with Pangala et al. (2013) and Pangala et al. (2015) who found small diameter wetland trees emitted more CH_4 per unit area of stem than larger trees. There was little overlap between the DBH range of those studies (7.5-19.8 cm) and ours (16.1-92.6 cm). The mean stem diameter across all habitats in our study was 42.3 cm (Table 1), with only four trees out of 31 having DBH < 20 cm. Differences in root morphology and biomass between small and large trees may explain the contrasting results. Older and bigger trees have larger and deeper root systems and more likely have deep roots that tap into anaerobic soils or groundwater, both being potential sources of CH_4. Other potential CH_4 sources such as heart-rot and non- structural carbohydrates would result in a positive relationship between tree diameter and fluxes (Covey et al. 2012, Covey et al. 2016). Regardless of the mechanism, the data highlight the importance of tree size especially when scaling up plot-level studies to ecosystem-level estimates (Pangala et al. 2015, Covey et al. 2016). Future studies should address multiple tree size classes on a given species within one study site.

In the temperate region, stem CH_4 flux from trees has been shown to be related to temperature-dependent CH_4 production processes. In wetland forests, Pangala et al. (2015) reported a correlation between stem CH_4 emission and temperature, water-table depth, and CH_4 concentration in pore water. They concluded that CH_4 flux was driven by CH_4 production in water-logged wetland soil. By sampling a nearby spring, Wang et al. (2016) concluded that groundwater was not a source of CH_4 in an upland forest; rather, they attributed stem CH_4 flux to *in-situ* CH_4 production in the heartwood. The trees in the present study were arranged along an upland-to-wetland gradient of groundwater depth. Our results showed a strong negative correlation between stem CH_4 flux and the depth to groundwater, and is consistent with a belowground CH_4 source hypothesis previously proposed for wetland trees (Pangala et al. 2015). We measured high stem CH_4 fluxes in the wetland habitat where soil CH_4 production is consistently high and lower but still positive stem CH_4 fluxes from upland trees even when adjacent soils are net CH_4 consumers. The observation that co-located upland soils act as CH_4 sinks while trees act as sources suggests that trees may provide a flux pathway through the woody tissue that bypasses the methanotrophs in the oxic soil layers (Megonigal and Guenther 2008).

Methane transport in plants can be via diffusion or transpiration (Megonigal and Guenther 2008, Pangala et al. 2014). The latter process has a strong diurnal pattern, suggesting that transpiration-driven CH_4 fluxes should exhibit a diel cycle. Pangala et al. (2014) reported only a weak positive relationship between emissions and transpiration, and Terazawa et al. (2015) did not observe diurnal patterns. Both studies concluded that diffusion is the major driver of stem CH_4 emissions. In an upland forest stand near our transect, Pitz and Megonigal (2017) demonstrated a strong diurnal pattern in stem CH_4 flux for American beech and tulip poplar, with a two-fold diurnal difference for the latter. This indicates that transpiration may play a significant role in stem emissions. Clearly, high frequency measurements for longer periods are necessary to reveal the relative importance of transpiration and diffusion in different habitats.

Soil moisture is considered a major driver of belowground biogeochemical processes, and is thus often reported as an abiotic variable. Usually soil moisture measurements reflect only the surface conditions. In a wetland, such data reflects conditions throughout the soil profile, but in the upland, surface conditions do not represent the steeper, more variable, vertical soil moisture gradient. Soil moisture was not a significant variable in our model of stem CH_4 fluxes (Table 3-2), which is consistent with root uptake from groundwater and transpiration as a mechanism for gas transport.

Soil CO_2 efflux decreased from upland to wetland, while stem respiration showed the opposite pattern (Figure 3-3). Biological and physical processes may simultaneously explain this result. Lower soil CO_2 emissions in the wetland coincided with near-continuous flooding, which can be explained by several mechanisms. Flooding can decrease CO_2 respiration of stems by suppressing overall tree growth, and from roots by lowering both growth and root:shoot ratio (Megonigal et al. 1997). Similarly, flooding decreases microbial respiration both by suppressing overall microbial respiration and by lowering the CO_2:CH_4 ratio (Megonigal et al. 2004, Yu et al. 2008). Because stem CO_2 emissions were similar in the wetland and transitional zones, the most likely biological explanation for lower soil CO_2 emissions in the wetland is a decrease in microbial respiration as opposed to lower plant respiration. A purely physical explanation is that high soil moisture in the transitional and wetland habitats reduced gas diffusion rates through soil pore spaces (Davidson et al. 1998, Suseela et al. 2012, Moyano et al. 2013) favoring diffusion through woody tissues. These explanations are not mutually exclusive and may both have a role in explaining the cross-habitat patterns of soil and stem CO_2 emissions.

Tree CH_4 emission rates have now been measured in a variety of forest ecosystems (Table 3-3). Although the number of studies are few, it is noteworthy that during the growing season, the highest mean emissions from upland (190 μg m^{-2} hr^{-1} (Covey et al. 2012) and wetland stems (567.9 μg m^{-2} hr^{-1} in the present study) are within the same order of magnitude. The observation that upland trees have the

Table 3-3: Tree stem CH_4 flux comparisons from field experiments

Reference	**Climatic region**	**Ecosystem**	**Tree species**	**Chamber Method**	**CH_4 flux range (chamber height)** $\mu g\ m^{-2}\ h^{-1}$	**CH_4 flux (mean ± SD)** $\mu g\ m^{-2}\ h^{-1}$
Terazawa et al. 2007	Temperate	Floodplain	*Fraxinus mandshurica* var. *japonica*	partial circumference	164-212[m] (15 cm) 76-118[m] (70 cm)	176 97
Gauci et al. 2010	Temperate	Wetland	*Alnus glutinosa*	full circumference	3.22 – 126.5 (30 cm)	56.7 ± 52.7
Covey et al. 2012	Temperate	Upland	Various	modeled from internal concentration	4.24 – 181.3 (NA)	190 ± 34
Pangala et al. 2013	Tropical	Wetland	Various	full circumference	0.00 - 219 (35 cm)	103 ± 66
Pangala et al. 2015	Temperate	Wetland	*Alnus glutinosa* *Betula pubescens*	full circumference	161-182[m] (35 cm) 177-217[m] (35 cm)	172 ± 8 196 ± 15
Terazawa et al. 2015	Temperate	Floodplain	*Fraxinus mandshurica* var. *japonica*	partial circumference	59-1514 (15 cm)	337 ± 419
Wang et al. 2016	Temperate	Upland	*Populus davidiana*	full circumference	0-200 (30 cm)	85.3 (upper plot) 103.1 (lower plot)
Machacova et al. 2016	Boreal	Upland	*Pinus sylvestris* L.	full circumference	NA (20 cm)	0.005[med]
Warner et al. 2017	Temperate	Upland	Various	partial circumference	56[b] (130 cm)	6.3 ± 12
Maier et al. 2017	Temperate	Upland	*Fagus sylvatica*	full circumference	0-200 (40, 120, 200 cm)	30 ± 53
Present study	Temperate	Upland	Various	partial circumference	-8.1 – 1900 (45 cm)	68.8 ± 53.6
	Temperate	Transitional	Various	partial circumference	-4.0 – 2150 (45 cm)	180.7 ± 135.2
	Temperate	Wetland	Various	partial circumference	8.6 – 3760 (45 cm)	567.9 ± 523.5

SD: standard Deviation (SD) not always available
m: mean of measurements, not an individual measurement
med: median
NA: not available
b: maximum value

potential to emit CH_4 at rates comparable to wetland trees suggests the need for detailed mechanistic studies of CH_4 sources and sinks across all forest ecosystems.

Soil trace gas fluxes generally show high spatiotemporal variability and are often cited as examples for biogeochemical hotspots and hot moments (McClain et al. 2003, Hagedorn and Bellamy 2011, Ullah and Moore 2011). In such situations a single measurement can be several orders of magnitude higher than the mean (Kuzyakov and Blagodatskaya 2015). Our data also show high variability, especially in the wetland where soils and stems consistently emit CH_4. In this habitat, the coefficient of variation for soil flux (1.94) is twice as much as stem flux (0.92). Traditional soil trace gas measurement methods capture processes only in a small area, with large variations among individual measurements due to the existence of biogeochemical hot spots in a highly heterogeneous landscape. For a single tree, soil conditions around individual roots are highly heterogeneous, the entire root system spreads over a much larger area, and thus integrates widely varying conditions both vertically and horizontally (Schenk and Jackson 2002). Across all habitats pairwise measurements of stem CH_4 fluxes consistently exceeded soil CH_4 fluxes on an area basis, suggesting that the base of tree stems are a localized hot spot relative to the soil. In a few instances, we also recorded hot moments with extremely high (an order of magnitude higher than the mean) stem CH_4 fluxes (Figure 3-2). It is important not to discard such data as outliers, even though data analysis becomes more challenging. Recent advances of continuous field trace gas measurement technology will allow high frequency sampling and thus to better characterize the sources, sinks and drivers of CH_4 fluxes in forests.

Despite the heightened interest following Keppler et al. (2006), to date only a handful studies convincingly documented trees as CH_4 sources (Table 3-3). Six of those, including our study, attempted to quantify CH_4 flux from live upland trees, and five directly measured stem fluxes in the field. Different studies report their data using incompatible approaches, including different methodologies to scale up

data. Studies have been conducted under different climatic conditions, from tropical rainforests to boreal forests. Chambers were closed from 6 minutes to 6 hours for each measurement. The position of chambers above the ground, which has been shown to affect flux rates (Pangala et al. 2013), varied from 15 cm to 200 cm. One issue that we address here is the variations in stem flux chamber design used in direct field measurements. Some studies (Terazawa et al. 2007, Terazawa et al. 2015), ours included, employed a chamber that is mounted one side of a tree (i.e. partial-circumference design). The advantages of this design are that it allows measurements on large trees, maximizes the surface to volume ratio, allowing for relatively short measurement times. The design suited our goal of measuring emissions from a wide range of tree sizes and detecting small fluxes in upland forests. However, this type of chamber does not capture radially variation in emissions around the circumference of the tree and is difficult to fit on small trees. Other studies (Gauci et al. 2010, Pangala et al. 2013) have used a chamber that completely encloses the stem (i.e. full-circumference design). This chamber style results in a lower surface to volume ratio and may result in longer measurement times but it is well suited for small diameter stems. Recently Siegenthaler et al. (2016) developed a full-circumference design using low permeability, flexible material that significantly improves surface to volume ratios. This chamber style may ideally address some field, habitat, and tree diameter constraints. A systematic comparison between chamber styles and recommendations of standardized chamber designs and protocols will allow for interpretation and synthesis of stem flux measurements.

3.5. Conclusion

Forests cover about 30 % of the global land surface (FAO 2016) and are important sinks of atmospheric carbon (IPCC 2013). The present and other studies indicate that upland trees emit CH_4 and thus have to be incorporated into forest carbon cycling models. Our data support a below ground CH_4

source, but this pathway probably works simultaneously with other mechanisms, such as CH_4 derived from internal microbial sources. Our study highlighted the many biotic and abiotic factors that influence tree mediated CH_4 fluxes. Future studies should focus on teasing apart the roles of tree size and species identity (physiology, wood structure, rooting depth), and a multitude of above- and belowground environmental factors. Using high frequency measurements (Pitz and Megonigal 2017) will help determine drivers on diurnal, seasonal and annual scales, and identify hot moments. Considering evidence that the global warming potential of CH_4 is dramatically higher when being consumed from the atmosphere than emitted (sustained global warming potential of uptake = 203 versus emission = 45 over 100 years) (Neubauer and Megonigal 2015), systems such as upland forests where CH_4 is simultaneously produced and consumed are particularly important to evaluate from a whole-system perspective.

Acknowledgements

This chapter was published in the journal Biogeochemistry (Pitz et al. 2018). This study was supported by grants from the Department of Energy (DE-SC0008165), the National Science Foundation (ACI-1244820, EAGER NEON EF-1550795, ERC-MIRTHE EEC-0540832), and the Department of Earth and Planetary Sciences Summer Field funds. We thank Jess Parker, Anand Gnanadesikan, Lisa Schile, and members of the GCREW Lab for their advice and useful suggestions throughout the study. We are thankful for all the help that Mike Bernard, Jacob Rode, Adam Dec, Andy Sample and Kyle King provided in the field. Anand Gnadadesikan and two anonymous reviewers provided helpful comment on earlier versions of the manuscript.

4. Soil Respiration in a Tropical Rainforest

4.1. Introduction

Soil respiration is one of the largest annual fluxes of carbon dioxide (CO_2) to the atmosphere. During the period of 1989 to 2008, global soil respiration has been estimated to increase by 0.1 Pg C yr^{-1} reaching 98 ± 12 Pg C yr^{-1} in 2008 (Bond-Lamberty and Thomson 2010b). As of 2018, the atmosphere contains over 850 Pg of carbon, meaning that every year the equivalent of more than 10% of atmospheric CO_2 cycles through soils.

Anthropogenic emissions of carbon were estimated to be 9.8 ± 0.5 Pg C yr^{-1} in 2014 (Le Quere et al. 2015), which is approximately the same size as the estimated uncertainty in global soil respiration and an order of magnitude lower than total global soil respiration. Therefore, small changes in soil respiration may have large effects on CO_2 concentrations thus radiative forcing of the atmosphere.

In general, little is known how future biotic and abiotic changes will affect soil respiration (Vicca et al. 2014). Soil respiration varies greatly on both spatial and temporal scales and climate projections must make assumptions about the sensitivity of soil respiration to changes in temperature, moisture, and organic matter input (Jobbágy and Jackson 2000). The majority of field data to inform these assumptions has been collected in temperate biomes. Data collected in under-sampled ecosystems is essential to improve estimates of this sensitivity. This chapter concentrates on tropical rainforests, which are one of the most important, yet poorly-sampled ecosystems.

Forests cover approximately 30% of land surface (FAO 2016) and represent an important sink of carbon (IPCC 2013) and 50% of forest land is in the tropics. Between aboveground and belowground stocks, tropical forests contain 55% of total forest carbon, approximately 471 ± 93 Pg C (Pan et al. 2011). Tropical forests have the highest annual soil respiration rates (Bond-Lamberty and Thomson 2010b) and

more than 25% of global soil respiration is estimated to be from broadleaf tropical rainforests (Raich et al. 2002).

While approximately twice as much land is covered by tropical forests than temperate forests based on a comprehensive soil respiration database compiled by Bond-Lamberty and Thomson (2010a), there are five times more annual soil respiration estimates from temperate forests sites than from tropical sites. This indicates that relative to temperate forests, much less is known about tropical soil respiration, which dominates annual soil flux rates. Therefore, increasing the number of field measurements of tropical soil respiration should be a priority.

One strategy to advance our understanding of soil respiration is to improve the way in which it is measured. There are several different methods of measuring and modeling soil respiration, each involving tradeoffs between scale, limitations, assumptions and cost. The main three methods are eddy covariance, chamber methods and gradient methods.

Eddy covariance (EC) can be used to estimate net ecosystem exchange by analyzing turbulent changes in vertical wind speed and CO_2 concentrations. These measurements are made on towers extending above an ecosystem's canopy. Carbon fluxes can be calculated within a footprint of the tower. This footprint can extend 100 m to 2 km from the tower depending on tower height, wind direction and speed and footprint estimation methodology (Hsieh et al. 2000, Kormann and Meixner 2001, Kljun et al. 2004). At night EC can be used to estimate soil respiration on large scales not possible with other techniques, greatly improving our understanding of carbon fluxes in a variety of ecosystems (Beer et al. 2010, Jung et al. 2010, Mahecha et al. 2010, Baldocchi 2014). However, there are limitations to using EC to estimate soil respiration. If the atmosphere is not turbulent enough, reliable soil respiration measurements cannot be made because too much CO_2 will be transported horizontally by advection rather than vertically by mixing. At night, surface cooling and low winds often produce a thin near-

surface boundary layer, resulting in poor agreement between EC based estimates of soil respiration and other methods (Barba et al. 2018). Building a tower that extends above the canopy and maintaining the instruments require substantial capital investments, especially in mature forests where towers must rise well above the tallest trees. In addition to high frequency CO_2 measurements, other ancillary data must be collected such as water vapor concentration, total solar radiation, three-dimensional wind vectors, CO_2 concentrations at multiple heights below the tower, among others. Data collection gaps can occur during power outages or when sensors in the sampling suite fail. Due to climate and location, tropical forest ecosystems of interest are likely to have both sensor failures and limited power availability. These constraints have limited the number of EC towers built and measurements made in the tropics.

Chamber methods (CMs) using an open bottom soil collar are the most common way to measure soil respiration. Some of the advantages of chambers are that they are portable, deployable to remote sites, and relatively inexpensive compared to eddy covariance methods. Most frequently, non-steady state chambers are used. To determine the soil efflux, the chamber is closed upon the soil ring and CO_2 in the headspace begins to accumulate above ambient concentrations. Because CO_2 is above ambient conditions, the concentration gradient within the headspace becomes distorted and can lead to sampling biases (Davidson et al. 2002). Other disadvantages include low sampling frequencies, the small area measured, inclusion or exclusion of litter and the collar causing changes in the soil micro-environment.

Automated chamber systems can improve the rate at which measurements are made but represent a fraction of published chamber-based soil respiration studies. There has been limited adoption of automated systems because they are expensive and have high power requirements. Similar to EC, high power requirements limit the locations and environments where automated systems can be deployed. Many automated systems rely on a central CO_2 analyzer which requires a network of tubes and manifolds to deliver headspace air to the analyzer. With limits on tubing length, chambers

connected to a central analyzer must be placed within a certain radius which may lead to pseudo-replication. Additionally, some automated systems cannot measure more than once an hour, but since some soil processes operate on sub hourly time scales (Lee et al. 2004), data collected may not accurately characterize soil responses.

The gradient method (GM) is based on measuring the soil CO_2 concentration gradient at several depths within the soil and calculating soil respiration using diffusion models. Most models assume that diffusion dominates gas transport and calculate the effective diffusivity from parameters such as soil moisture, soil temperature, air-filled porosity, bulk density and soil texture (Penman 1940, Marshall 1959, Millington and Quirk 1961, Moldrup et al. 1999). In the last two decades, rugged accurate sensors have been developed that allow long term in-situ measurements of soil CO_2, making GM more viable and popular (Tang et al. 2003).

GM also has the potential to avoid some limitations associated with eddy covariance and chamber methods. Assuming electricity is available for the relatively low-power sensors, data can be collected continuously and at rates comparable or faster than automated chambers. GM can generate soil respiration estimates when the atmosphere is too calm for eddy covariance and can potentially minimize problems associated with the chamber method such as changing the microclimate in the soil ring or changing the soil CO_2 concentration gradient. GM can provide additional information about the soil CO_2 depth profile while EC and chamber methods can only provide information about soil-air respiration fluxes.

GM can avoid some of the pitfalls of EC and CM, but there are still drawbacks. While GM creates less disturbance than CM, the installation and presence of CO_2 probes will still change the soil environment. Soil respiration is spatially heterogeneous. The CO_2 sensors used for gradient methods are relatively small and accurately sample a small area, areas which may not be representative of the larger

study area. This can be an advantage if small scale spatial heterogeneity is a central question. When estimating the mean soil respiration values from an environment, habitat or ecosystem using the gradient method, more replicates may be required, which is more costly than other methods. Moreover, electricity availability may be a limiting factor depending on the site.

Disturbance also plays a significant role in soil respiration; approximately 20% of the CO_2 that has been fluxed to the atmosphere is a result of disturbance via land use change (IPCC 2013), and much of that CO_2 originated as soil carbon. Changes in aboveground biomass through logging or thinning can result in altered soil respiration through changes in root biomass and inputs of litter and woody debris.

To explore patterns of tropical soil respiration and the importance of disturbance, we conducted two field campaigns in an upland, tropical, broadleaf rainforest within the Amazon basin in eastern Ecuador. Measurements were carried out in January 2010, the driest month of the year, and in May and June, the wettest months of the year. Soil respiration was compared between disturbed and pristine sites. We attempted to answer the following questions:

- How does disturbance affect soil respiration in an upland tropical broadleaf rainforest?
- How variable is soil respiration on spatial scales of several meters to tens of meters?
- How much does soil respiration vary on a diurnal and seasonal scales?
- How do soil respiration estimates from the gradient method compare with more traditional chamber methods?

4.2. Methods

Site

The study site is located in a lowland, broadleaf, tropical rainforest (0.6806°S, 76.4027°W, 240 meters (m)) within the Yasuni National Park and Biosphere Reserve in Ecuador. The site is within the Napo River basin and located south of the Tiputini River, both being tributaries of the Amazon River.

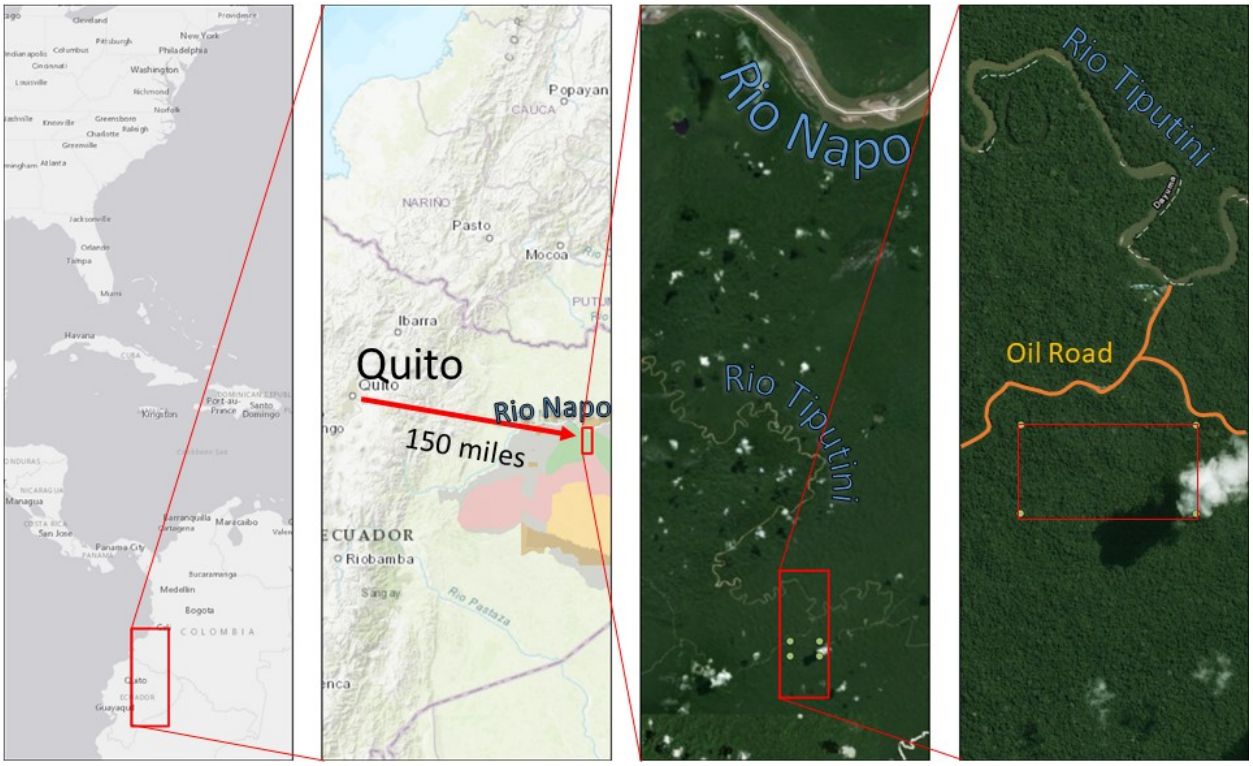

Figure 4-1: Location of diversity plot.

We conducted our experiment within a 25 hectare (ha) plant biodiversity and forest plot (Figure 4-1) established by the Catholic University of Ecuador, the Smithsonian Tropical Research Institute, and the University of Aarhus (Valencia et al. 2004). The forest plot is approximately 1 km south from the Yasuni Biological Station that is operated by the Catholic University of Ecuador. The forest plot is highly diverse, with over 1100 woody plant species (Molina et al. 2016). Our site is located on a hill in the southwest corner of the plot, 20 to 25 meters in elevation above a small floodplain, and within a non-

inundated, *terre firme* forest. In the southwest corner of the forest plot is a small disturbed area (described in more detail below). Half of our measurements occurred in this disturbed area and the remaining measurements were made in the adjacent undisturbed forest. Before discussing the soil CO_2 efflux measurements made at these sites, I will describe the climate and soil at the sites.

Temperature, Precipitation, and Seasonality

Climate and weather data have been collected at the station from May 2000, through February 2012. At the weather station, air temperature data was automatically measured multiple times each hour but is recorded as an hourly mean. The mean annual air temperature is 24.9 °C. While air temperatures do not vary much throughout the year, the hottest month is October with a mean air temperature of 25.6 °C, and the coolest month is June with a mean air temperature of 23.9 °C (Figure 4-2). Mean maximum and mean minimum air temperatures were computed by extracting the highest or lowest hourly temperature for each date available and then calculating the mean of all dates. The mean maximum air temperature (average high) was 30.8 °C (n=2928). The mean minimum air temperature (average low) was 21.2 °C (n=2928).

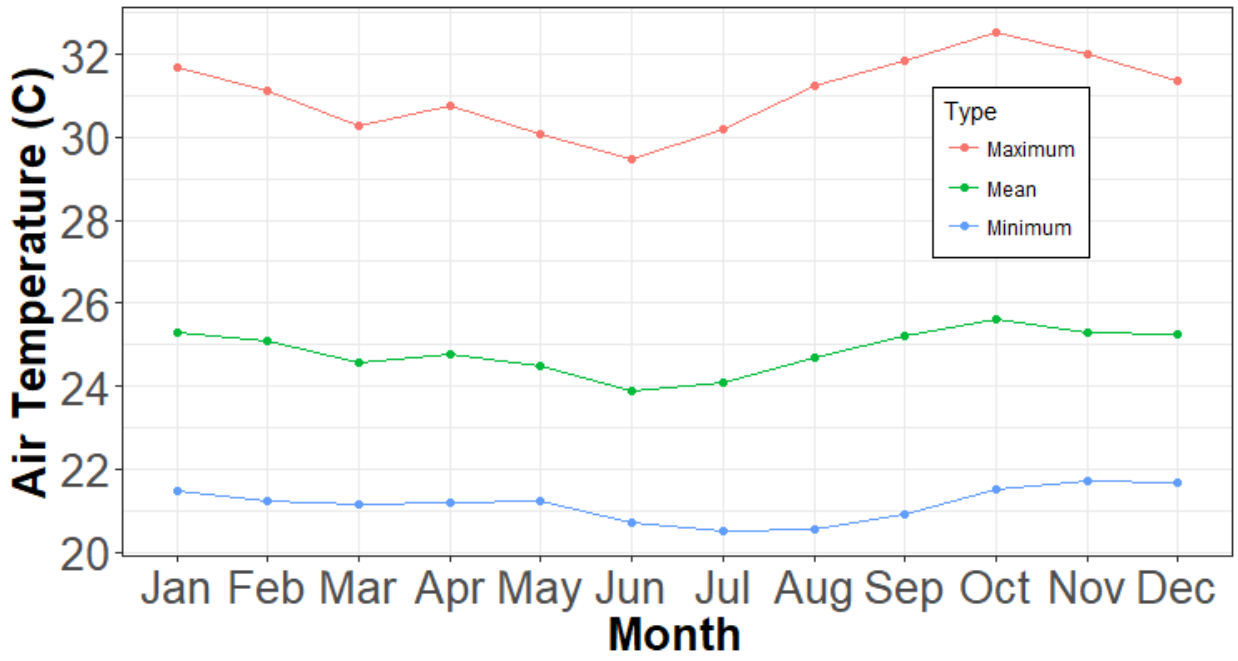

Figure 4-2: Mean, maximum and minimum air temperatures at Yasuni Biological Station for each month.

Mean annual precipitation is 3093 millimeters (mm). The forests in Yasuni National Park and Biosphere Reserve are not considered seasonal tropical forests because no months have average precipitation less than 150 mm (Figure 4-3). There are, however, two monthly peaks of precipitation; one in June and a smaller peak in October. With 396 mm of precipitation, June receives the most rainfall and January receives the least precipitation, with "only" 157 mm.

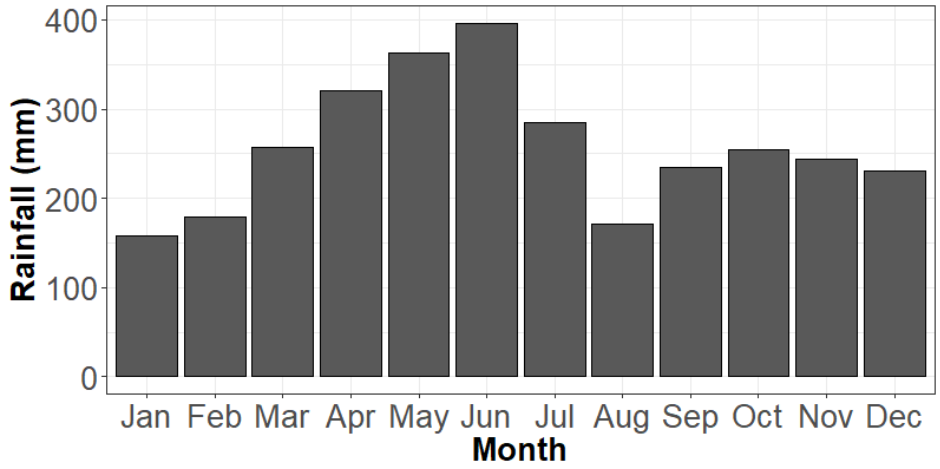

Figure 4-3: Mean monthly rainfall at the study site.

Soils

Soils in the Yasuni area are sparsely characterized. The soils within the larger forest plot are clayey, acidic, Udult Ultisols (John et al. 2007). The pH of the soil at our site is 4.1. Another study in the vicinity of our site measured the soil pH in the top 5 cm to be between 3.0 and 4.2 (Tuomisto et al. 2003).

For texture and bulk density measurements we took soil samples adjacent to each soil respiration measurement location. Soil texture was determined using a hydrometer method (Gee and Bauder 1986). Fifty grams of oven dried soil was added to 50 mL of water and 100 ml of sodium hexametaphosphate solution (50 g/L) to create a slurry. The soil particles in the slurry were dispersed by mixing for 5 minutes with an immersion blender (Conair Corp., Stamford, Connecticut, USA).

The dispersed soil mixture was transferred to a 1 L graduated cylinder and filled with water to 1000 mL mark. An agitation plunger was used to suspend the soil in solution by mixing with full strokes for 4 minutes. When the plunger was removed from the solution a timer was started and a hydrometer was placed into the cylinder. At 40 seconds and 2 hours solution density measurements were recorded along with temperature. Density measurements were corrected for solution temperature. Percent sand, silt, and clay were calculated using the following equations:

$$\%\, Sand = \frac{40\,\mathrm{sec}\, density\ measurement}{dry\ soil\ mass} \times 100$$

$$\%\, Clay = \frac{2\,\mathrm{hr}\, density\ measurement}{dry\ soil\ mass} \times 100$$

$$\%\, Silt = 100\% - \%\, Sand - \%\, Clay$$

The soils at our sites are primarily clay. In the undisturbed site the soil is composed of 7% sand, 24% silt and 69% clay. In the disturbed site the soil was composed of 3% sand, 22% silt and 75% clay. Other publications have found higher silt contents but may not have sampled the same locations or depths (Tuomisto et al. 2003, John et al. 2007).

We collected bulk density samples at each sampling location using 5 cm long and 5 cm diameter aluminum ring inserts (AMS Inc., American Falls, Idaho, USA) every 5 cm down to 20 cm. Each 5 cm section was collected individually due to unusually high compression observed in the upper soil profile when using a split-core sampler (AMS Inc., American Falls, Idaho, USA). For example, when collecting the 10-15 cm depth sample, the soil was excavated down to 10 cm, a flat surface was created, and the aluminum ring was pushed into the soil. The ring then had to be excavated and cut from the bottom so the entire soil core would remain within the ring. Soil samples were dried in an oven at 105 °C for several days or until sample mass stopped changing. Mean bulk density was 0.56 g cm^{-3}, 0.78 g cm^{-3}, 0.80 g cm^{-3}, and 0.87 g cm^{-3}, for 0-5 cm, 5-10 cm, 10-15 cm, and 15-20 cm respectively.

Experimental design

Our design took advantage of an accidental inclusion of a disturbed area within the larger forest plot, which itself is contained within a pristine rainforest forest (Figure 4-4A). The plot's northern boundary was established in 1995 and the southern corners were set later as the first census progressed. After the first census was completed in 2000 and over 150,000 individual woody plants had been surveyed, it was clear that a previously unknown disturbed area had been included within the plot (Valencia et al. 2004).

This disturbed area of approximately 50 meters in diameter was dominated by *Cecropia sciadophylla*. The *Cecropia* genus is known to be a fast-growing, shade intolerant, pioneer species that would normally be sparsely distributed within a mature forest (Alvarez-Buylla and Martinez-Ramos 1990). The density of *C. sciadophylla* within this area is uncharacteristically high compared to the rest of the plot. This indicates that a recent disturbance had created a clearing because over time other slower growth, shade tolerant tree species will out-compete *C. sciadophylla* for light and space. In addition, according to anecdotal evidence an oil exploration group worked in the area during the 1980's before

there was road access. It was common for these groups to clear a small hill of vegetation to create a rudimentary helicopter landing pad.

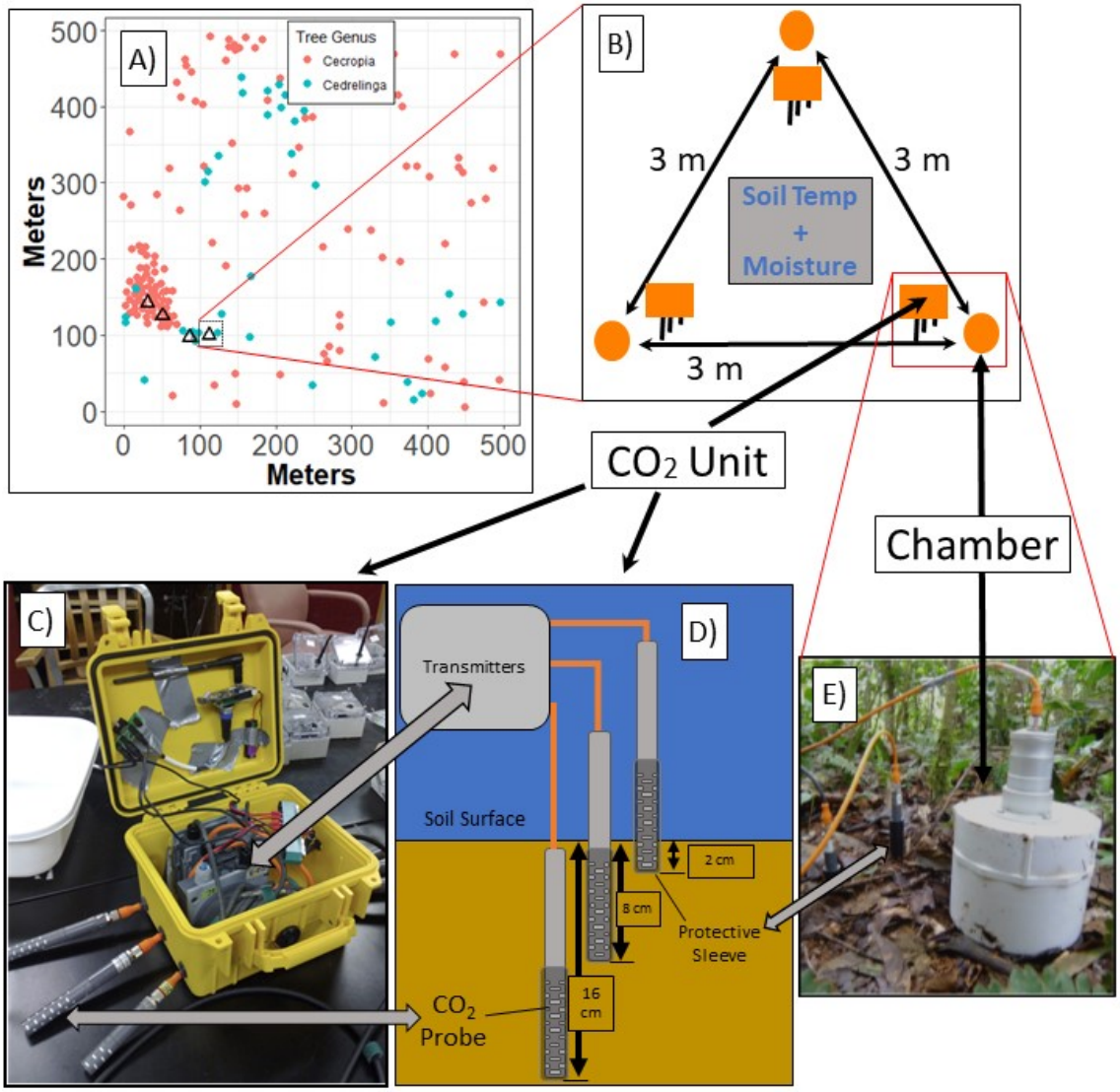

Figure 4-4: Experimental design. A) displays the distribution of Cecropia and Cedrelinga trees in the diversity plot. Black, open triangles represent the location of the four sites. Figure is modified from Valencia et al. (2004). B) is a diagram of each site. Each of the 12 sampling locations is at the corner of a 3 m triangle. Each corner has a soil ring for chamber measurements and three CO_2 probes used for the gradient method. C) shows the protective case for the CO_2 probe's transmitters. Wireless dataloggers were attached to the lid of the case. D) is a diagram of how the CO_2 probes were buried at each sampling location. The diagram is modified from Tang et al. (2003). E) is a photo of a sampling location with several CO_2 probes adjacent to a soil chamber.

Adjacent to this stand of *C. sciadophylla* are several *Cedrelinga catenaeformis*, an emergent tree species with one individual greater than 200 cm in diameter. Based on published growth rates, this individual has likely been growing for at least 150-200 years (Brienen and Zuidema 2006). With large

older trees adjacent to an unusually dense stand of young pioneer trees, we felt confident characterizing the *C. catenaeformis* area as undisturbed and the *C. sciadophylla* area as disturbed.

The experiment consisted of 12 soil respiration sampling locations, half in the disturbed forest and half in the undisturbed forest (Figure 4-4A). Within each forest, the sampling locations were arranged onto corners of an equilateral triangle with the dimensions of 3 m per side (Figure 4-4B). Each forest contained two triangles, a total of 6 sampling locations per area. The four triangles were arranged along an approximate 100 m east-west line, with 25 to 35 m between the centers of each triangle. The border of the disturbed and undisturbed area lay at the midpoint of the 100 m line.

Soil respiration was measured by two methods at each sampling location; the chamber method and the gradient method. At the corner of each 3 m equilateral triangle was one soil ring used for the chamber measurement and three soil CO_2 probes (Figure 4-4B), buried at specific depths, used for the gradient method. The soil ring and probes were adjacent to each other, within 20 cm (Figure 4-4E).

Chamber method

Soil respiration was measured using a non-steady-state chamber. Twelve soil rings, made of PVC with a height of 5 cm and a diameter of 15.2 cm, were inserted into the soil at each sampling location. Each had a beveled edge to assist in installation. The chamber enclosure was constructed from two PVC parts; a 6” adapter with a female socket and female threads (Part #4880K151, McMaster-Carr, Robbinsville, New Jersey, USA) and a 6” male threaded plug (Part #4880K151, McMaster-Carr, Robbinsville, New Jersey, USA). Carbon dioxide in the headspace of the chamber was monitored using a temperature corrected CO_2 probe (GMP343, Vaisala Corp., Vantaa, Finland). To mount the GMP343 to the chamber and create an airtight seal, a hole was drilled into the PVC plug using a 2.5” hole saw drill bit. A metal mounting flange (Vaisala Corp., Vantaa, Finland) was placed into the drilled hole, creating an airtight headspace, minus small capillary tube used for pressure relief.

To collect a soil respiration measurement, the chamber enclosure was placed upon a soil ring for 5-10 minutes while CO_2 concentrations were recorded. The GMP343 was connected to a small laptop running Windows XP through a serial to USB adapter (Figure 4-4E). The laptop communicated with the probe and logged data using Hyperterminal (Microsoft Corp., Redmond, Washington, USA). The GMP343 collected CO_2 concentration data every 2 seconds. Soil and air temperatures were recorded manually using a digital thermometer at each sampling location during each chamber measurement. Soil temperature was measured at 10 cm and air temperature was measured at 1.5 m.

When calculating the slope of CO_2 concentration change over time, we ignored the first 60 seconds of the observations, as those may produce false readings associated with pressure changes while lowering the enclosure onto the soil ring. The slope of gas concentration change was determined using the lm function in R v3.1.2 (R Core Team 2014). In every case, the slope was based on at least 120 observations.

Gas flux was calculated using the following equation:

$$F = \frac{d[CH_4]}{dt} \times \frac{PV}{ART} \quad (4.1)$$

where F is the flux in μmol m^{-2} s^{-1}, P is atmospheric pressure, T is the air temperature, R is the universal gas constant, A is the collar surface area and V is the volume of the air enclosed by the chamber. Air temperature is also measured simultaneous with concentration by the CO_2 probe. Atmospheric pressure was measured at the nearby weather station (<1 km away).

Gradient method

Each location used three CO_2 sensors buried vertically in the soil at depths of 2 cm, 8 cm and 16 cm (Figure 4-4D). We used ruggedized CO_2 sensors that can withstand the harsh soil environments (GM221 and GMT222, Vaisala Corp., Vantaa, Finland). The probe was open to air but protected from

moisture by a sleeve of Goretex™. The cavity and Goretex™ were protected from debris by an exterior plastic cover with slotted openings similar to a well screen. A plastic, cylindrical protective sleeve was placed around the cover so the top was sealed and the bottom was open to the soil at the target depth (Figure 4-4D). The GMT221 and GMT222 come in a variety of ranges and we had to use several to characterize the soil CO_2 concentration profile. We mostly used probes with ranges of 0-10,000 ppm (1%) and 0-20,000 ppm (2%) but at some depths and sampling locations we used probes with ranges as high as 0-30,000 ppm (3%) and 0-100,000 ppm (10%). A total of 36 CO_2 probes were deployed during each campaign, 3 per location, 6 locations in the undisturbed forest and 6 locations in the disturbed forest (Figure 4-4A and Figure 4-4B).

The CO_2 probes were calibrated before and after each field campaign using traceable standards. The GMT221 and GMT222 are powered by 24V direct current, so voltage-doublers were soldered to transmitter power inputs so the probes could be powered by 12V automotive batteries.

GMT220 sensor probes are watertight and were placed into the soil but the probe transmitter housing needed to be protected from the elements. For each sampling location, four holes were drilled into a watertight case (Pelican 1300 Protector Case, Pelican Products Inc., Torrance, California, USA); three holes for the GMT221 cables and one hole for the power cable (Figure 4-4C). A rubber grommet was placed into each hole and silicone caulk was used to seal any remaining voids between the cables, grommets, and drilled holes.

Soil temperature and soil moisture were measured at each soil CO_2 sampling depth to correct for CO_2 concentrations and to estimate diffusivity from temperature and volumetric water content. These measurements were made at the center of triangle; in between three sampling locations (B). Soil moisture was measured using a volumetric moisture content probe (ECHO EC-5, Meter, Pullman, Washington, USA). Soil temperature was measured using custom built thermistors.

Measurements from the CO_2 sensors, temperature and soil moisture sensors were recorded every 10 minutes on custom wireless dataloggers (Savva et al. 2013). The wireless dataloggers were each a node on a wireless sensor network which could be downloaded simultaneously in the field using a laptop to a local database. The local database could then be copied to a server when internet access was available.

Gradient Method Calculations

Soil respiration can be estimated from the flux of CO_2 diffusing from the soil. The flux can be calculated using models based on Fick's law:

$$F = -D_s \frac{dC}{dz} \quad (4.2)$$

Where F is the CO_2 efflux in in μmol m^{-2} s^{-1}, D_s is the CO_2 diffusion coefficient in the soil, and dC/dz in the vertical soil CO_2 concentration gradient. Soil CO_2 concentrations were collected every 10 minutes but averaged to 30 minute intervals when calculating the concentration gradient.

$$D_s = \xi D_a \quad (4.3)$$

Where ξ is the gas tortuosity factor, and D_a is the CO_2 diffusion coefficient in free air. Effects of temperature and pressure on D_a can be corrected by the following formula:

$$D_a = D_{a0} \left(\frac{T}{293.15}\right)^{1.75} \left(\frac{P}{101.3}\right) \quad (4.4)$$

Where D_{a0} is a reference value of D_a at 20 °C (293.15 °K) and 101.3 kPa and is given to be 14.7 mm^2 s^{-1} (Jones 1992). T is the soil temperature (K) adjacent to the CO_2 probes and P is the air pressure (kPa).

There are many models for calculating tortuosity (Penman 1940, Marshall 1959, Millington and Quirk 1961, Moldrup et al. 1997, Moldrup et al. 2000) but for this study a soil texture dependent model from Moldrup et al. (1999) was initially used:

$$\xi = \Phi^2 \left(\frac{\Phi - \theta}{\Phi}\right)^{\beta S} \quad (4.5)$$

where θ is volumetric soil water content, $\Phi = 1 - \rho b/\rho m$ is the porosity (where ρ_b is the bulk density and ρ_m is the particle density of mineral soil, using the common value for quartz sand of 2.65 g cm^{-3}), S is the percentage of sand and silt, and β is a constant determined by Moldrup et al. (1999) and is equal to 2.9. Because bulk density across the site was unusually low for the 0-5 cm samples, the mean bulk density of the 5-10 cm, 10-15 cm, and 15-20 cm cores were used to calculate the bulk density for each sampling location.

The measured soil CO_2 concentrations, at depths of 2, 8 and 16 cm, were used to construct concentration gradients and fluxes at intermediate depths, between the probe depths. Soil CO_2 fluxes were calculated at 5, 9 and 12 cm and were fit to a line, whose slope gives the size of the source, or sink, within the ground. The intercept where the soil depth is zero gives the surface flux. This methodology is similar to Tang and Baldocchi (2005) and is compared to other methods in Maier and Schack-Kirchner (2014).

Field Campaigns

In an attempt to capture seasonal changes, two field campaigns were conducted in 2010; one beginning in early January and the second beginning in late May. The first field campaign began on January 13th and ended on January 27th. The second campaign began on May 22nd and ended on June 7th. While the CO_2 sensors used in this experiment are relatively low power, the remoteness of the site

and closed canopy made battery power the only option. Maintaining charged batteries for the sensors proved labor intensive which is why each field campaign lasted several weeks.

Statistical analysis

Statistical analyses of flux data were conducted using R v3.1.2 (R Core Team 2014). Mixed linear models were fit using the lme4 package. Gradient fluxes were calculated using Matlab R2108a.

4.3. Results

Over the course of two field campaigns in 2010 a total of 234 manual chamber measurements were collected. In January, the mean soil respiration rate was 3.63 ± 0.10 µmol CO_2 m^{-2} s^{-1} (mean ± standard error) and 2.42 ± 0.08 µmol CO_2 m^{-2} s^{-1} from the undisturbed and disturbed forest, respectively. In May-June, the mean soil respiration rate was 3.36 ± 0.07 µmol CO_2 m^{-2} s^{-1} and 2.50 ± 0.10 µmol CO_2 m^{-2} s^{-1} from the undisturbed and disturbed forest, respectively. During January, soil respiration from the undisturbed forests was significantly higher ($P < 0.01$) than the disturbed forest Figure 4-5. During May-June, soil respiration from the undisturbed forests was significantly higher ($P < 0.02$) than the disturbed forest (Figure 4-5). There were no significant differences between the same forest in different seasons.

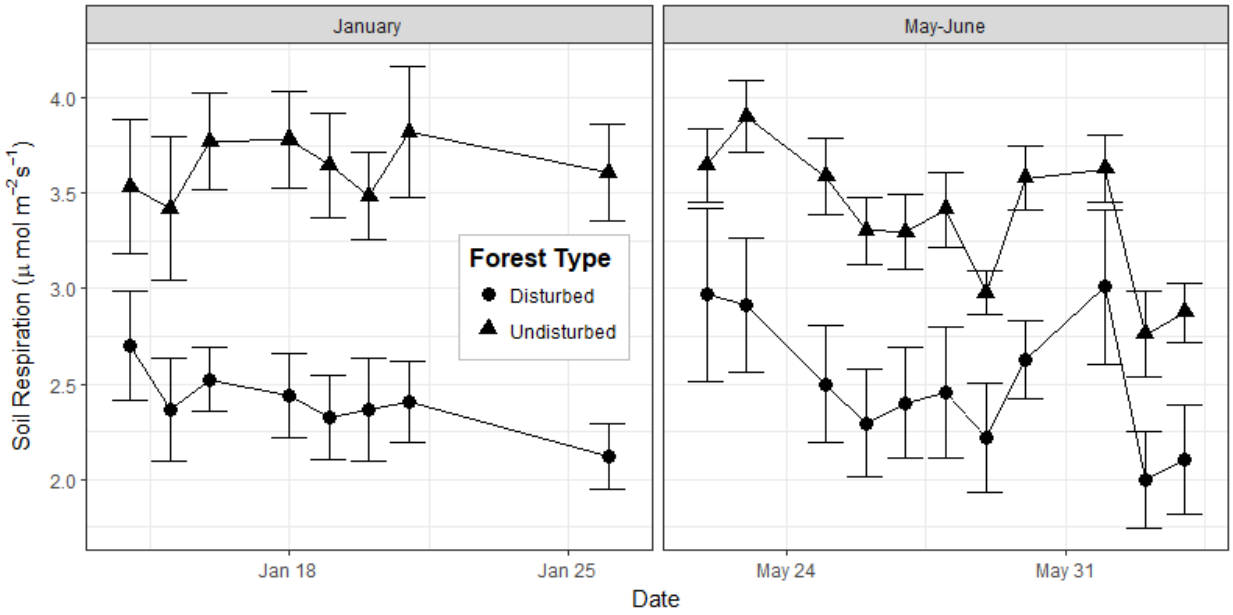

Figure 4-5: Soil Respiration during two field campaigns in both forests

Mean soil temperatures at all depths during both field campaigns ranged from 24.2 °C to 24.9°C. During the January field campaign mean soil temperatures were 24.2 ± 0.5 °C, 24.8 ± 0.3 °C and 24.5 ± 0.1 °C at depths of 2 cm, 8cm and 16 cm, respectively. The soil was slightly warmer at each depth in May and June, with a maximum difference at 2 cm of 0.4 °C. During the May-June field campaign mean soil temperatures were 24.6 ± 0.5 °C, 24.9 ± 0.3 °C and 24.6 ± 0.1 °C at depths of 2 cm, 8cm and 16 cm, respectively. Maximum and minimum observed soil temperatures were 26.3 °C and 22.9°C at a depth of 2 cm. Due to temperature sensor failures only one soil temperature dataset could be constructed so differences between the disturbed and undisturbed forest could not be assessed.

Soil moisture was higher during the May-June campaign. In the undisturbed forest, mean soil moisture among the depths was 28.9% during January and 35.6% during May-June. In the disturbed forest, mean soil moisture among the depths was 32.2% during January and 37.5% during May-June. During both field campaigns soil moisture was higher in the disturbed forest.

Mean soil CO_2 concentrations during the two campaigns, averaged by depth and forest type, ranged from 2259 ± 146 ppm at 2 cm in the undisturbed forest in January to 15006 ± 2932 ppm at 16 cm in the undisturbed forest in May-June (Figure 4-6A).

In January, soil CO_2 concentrations were higher in the disturbed forest. Within the undisturbed forest during January, mean soil CO_2 concentrations at 2 cm, 8 cm and 16 cm were 2259 ± 146 ppm (mean ± SE), 3893 ± 573 ppm and 9183 ± 1272 ppm, respectively (Figure 4-6A). Within the disturbed forest, mean soil CO_2 concentrations at 2 cm, 8 cm and 16 cm were 2845 ± 347 ppm, 5076 ± 713 ppm and 11488 ± 2301 ppm, respectively.

In May and June, soil CO_2 concentrations were generally higher in the disturbed forest, and soil CO_2 concentrations were higher and more variable compared to January (Figure 4-6B). Within the undisturbed forest during May and June, mean soil CO_2 concentrations at 2 cm, 8 cm and 16 cm were 6188 ± 2011 ppm, 8994 ± 2889 ppm and 15006 ± 2932 ppm, respectively. Within the disturbed forest during May and June, mean soil CO_2 concentrations at 2 cm, 8 cm and 16 cm were 6313 ± 1357 ppm, 10410 ± 1243 ppm and 13775 ± 1098 ppm, respectively.

Soil CO_2 concentrations were significantly higher during May-June in both forest types and all depths (Figure 4-6B). Except for 16 cm in the disturbed forest, variability was also higher during May-June in both forest types and all depths.

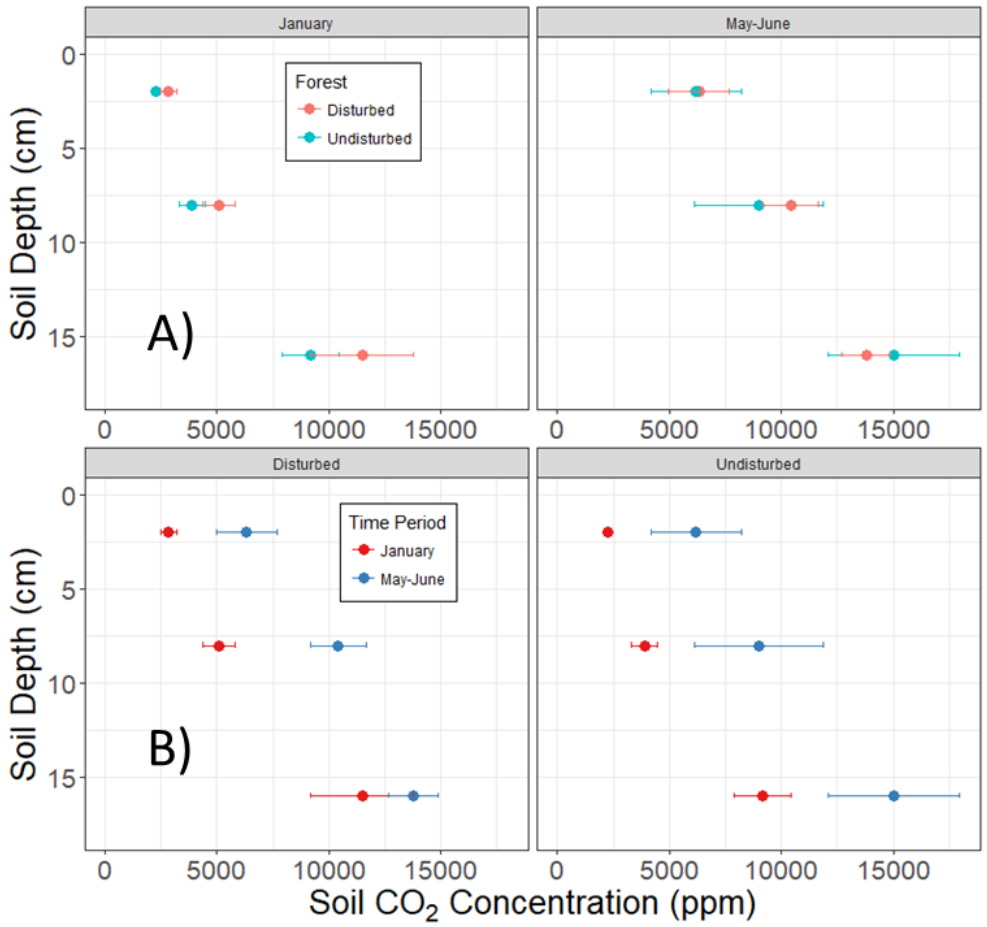

Figure 4-6: Soil CO_2 concentrations. A: Mean soil CO_2 concentrations at 2, 8 and 16 cm during each field campaign. B: Mean soil CO_2 concentrations at 2, 8 and 16 cm in each forest type. Each data point, n=6.

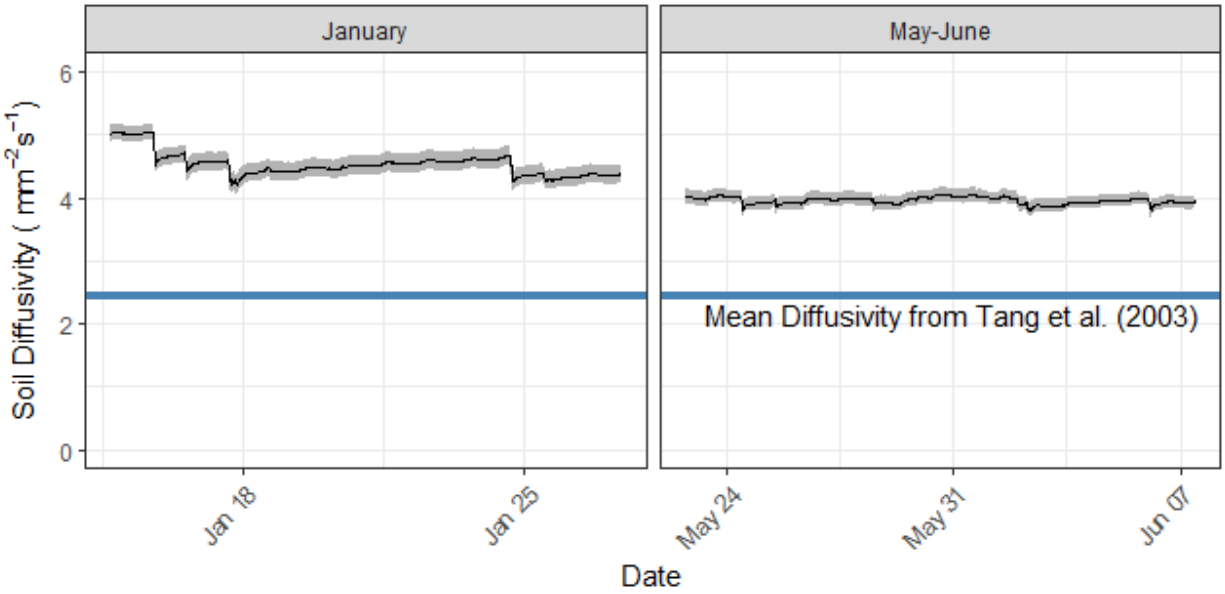

Figure 4-7: Mean Soil Diffusivity during the two field campaigns

Figure 4-7 displays the observed changes in soil diffusivity using Moldrup et al. (1999) during the two field campaigns. Mean diffusivity of all the sampling locations was 4.53 ± 0.19 $mm^2\ s^{-1}$ during January and 3.96 ± 0.05 $mm^2\ s^{-1}$ during May-June. The lower diffusivity during May-June is due to higher soil moisture. Variation of diffusivity was driven by changes in soil moisture and temperature (Figure 4-7). Large decreases in diffusivity were caused by rainfall events. Smaller variations were driven by temperature changes and evapotranspiration. The mean diffusivities during January and May-June were 86% and 63% higher, respectively, than the mean diffusivity that Tang et al. (2003) calculated at their site.

Using the gradient method, mean soil efflux was higher during the May-June field campaign (Figure 4-8). To calculate the mean soil efflux for each field campaign, all sampling locations, regardless of forest type were averaged together. During January, mean soil efflux from all sampling locations was estimated to be -1.09 ± 3.56 μmol $CO_2\ m^{-2}\ s^{-1}$ (mean ± standard deviation). During May-June, mean soil efflux from all sampling locations was estimated to be 8.84 ± 6.13 μmol $CO_2\ m^{-2}\ s^{-1}$ (mean ± standard deviation). Plotted on the same figure are the mean soil respiration values that were measured using the chamber method. Each point is the average of all sampling locations.

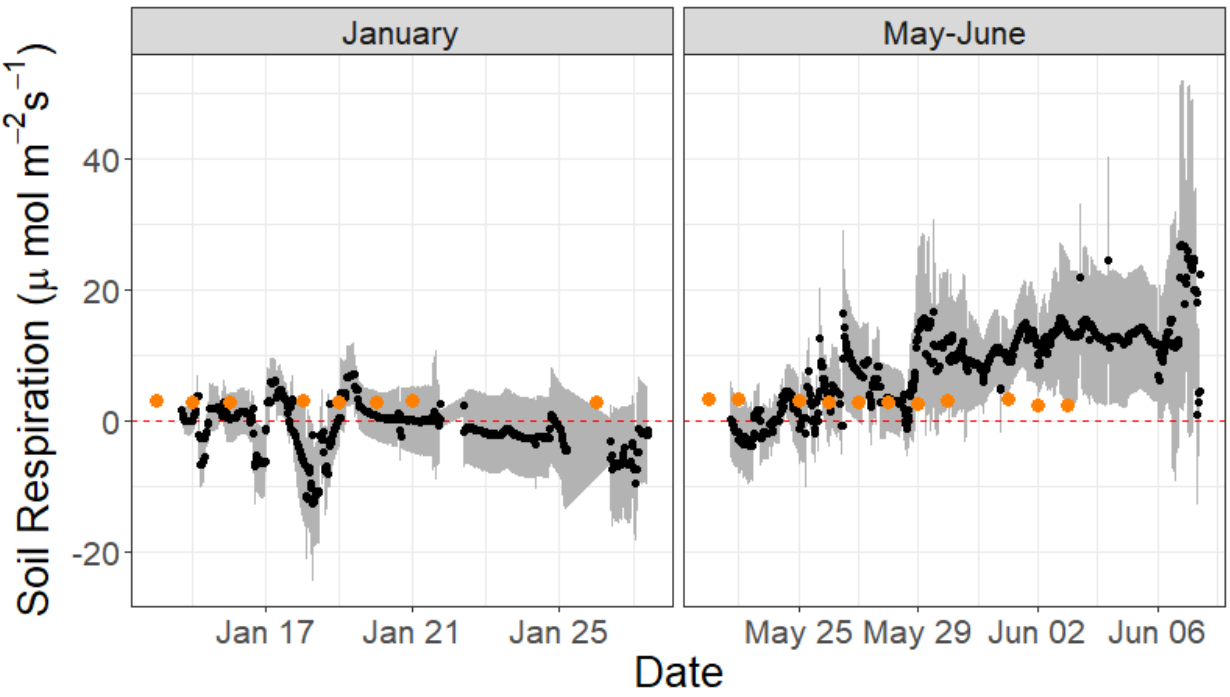

Figure 4-8: Mean soil efflux of all locations from the gradient method and the chamber method. Black circles are mean soil efflux from the gradient method. Orange circles are mean soil respiration from the chamber method.

4.4. Discussion

Fluxes estimated using the chamber method

Soil respiration measured using the chamber method was consistently higher in the undisturbed forest. Season did not have an effect within a given forest type. Soil respiration may be higher in the undisturbed forest due to higher aboveground biomass. Aboveground and belowground (root) biomass are highly correlated and higher aboveground biomass results in more leaf litter input to the forest floor (Bowden et al. 1993, Rustad et al. 2001). Higher root biomass will not only result in higher autotrophic respiration but can stimulate heterotrophic respiration (Scott-Denton et al. 2006).

Soil temperatures during both field campaigns were consistent and stable. Within the same depth, soil temperature was relatively stable between the two field campaigns with a maximum difference of with 0.4 °C at 2 cm. Soil temperature in a broadleaf tropical forest would not be variable compared to other ecosystems for two reasons; stable air temperatures and high canopy light

interception. During the two field campaigns, the average soil temperature at 8 cm was 24.8 ± 0.3 °C which is close to the average annual air temperature of 24.9 °C. The range in air temperatures between the warmest and coolest months at Yasuni is only 1.7 °C, which is small when compared to temperate climates where the average monthly temperature differences can be more than 15 °C. With negligible seasonal changes in air temperature, low variability in soil temperatures would also be expected. Minimal solar radiation reaches the forest floor in tropical evergreen broadleaf forests. The leaf area index (LAI) of tropical evergreen broadleaf forests can exceed 5 m^2 m^{-2} (Asner et al. 2003), particularly in forests that lack significant seasonality such as Yasuni. High foliar surface area results in high light interception and only 1-2% of the photosynthetically active radiation reaching the understory (Chazdon and Fetcher 1984, Montgomery and Chazdon 2001). With little direct or diffuse solar radiation reaching the soil surface, little temperature variation can occur, both on diurnal and seasonal timescales.

While temperature did not vary between the two periods, soil moisture did; it was 5-6% higher during May and June, historically the wettest months of the year. This higher soil moisture did not affect soil respiration. Studies have shown a "tipping point" of soil moisture as it relates to soil respiration (Wood et al. 2013). Peak soil respiration occurs around this "tipping point" and any increases of soil moisture will decrease soil respiration (Doff Sotta et al. 2004, Schwendenmann and Veldkamp 2006). At high soil moisture, pore spaces are closed for gaseous diffusion. With high water filled pore space, less oxygen can diffuse in to support respiration and less CO_2 can diffuse out.

Lower diffusion at higher soil moisture may also explain trends observed in soil CO_2 concentrations. Soil CO_2 was higher during May-June and higher in the disturbed forest. Soil respiration was not different in May-June but soil CO_2 concentrations were higher supporting the hypothesis that the soil CO_2 diffusion was restricted by high soil moisture in May-June. During both field campaigns, soil moisture was higher in the disturbed forest, which may partially explain the lower soil respiration.

Disagreement between the gradient and chamber methods

During January the gradient method tended to underestimate soil respiration while during May-June the gradient method tended to overestimate soil respiration. Additionally, the gradient method estimated negative soil efflux during January. Respiration at the soil atmosphere interphase should always be positive, unless a clear chamber is used in the presence of abundant herbaceous cover. Our chambers were dark and the forest floor had essentially no herbaceous vegetation, thus negative fluxes are indicative of the poor agreement between the chamber and gradient methods.

In Fick's Law-based models of soil respiration, flux is the product of the diffusivity coefficient and the concentration gradient. The diffusion coefficient can amplify or dampen the gradient derived from the concentration profile. We choose to use Moldrup et al. (1999) because it has been used with success by recent studies (Myklebust et al. 2008, Riveros-Iregui et al. 2008, Vargas and Allen 2008) and it includes a component that accounts for soil texture.

The mean diffusion coefficient at our site using Moldrup et al. (1999) was 4.22 $mm^2\ s^{-1}$, which is 74% higher than the soil diffusion coefficient that Tang et al. (2003) calculated using Millington and Quirk (1961), as seen in Figure 4-7. During their study, Tang et al. (2003) measured a soil temperature range of 32.6 - 38.3 °C and a soil moisture range of 5.9 - 6.5%, in a soil with 48% sand and 42% silt. Regardless of which diffusivity equation is used, it is intuitive that a hot, dry, silty sand soil should have a higher diffusion coefficient than a wet clay soil. Under those conditions, the pore spaces will be mostly open in the silty sand. Under conditions we observed in the clay soil at Yasuni, it would be expected that the pore spaces would be mostly closed. It is clear that relative to a sandy soil, the clay at Yasuni should have a lower diffusivity.

The other problem with the soil flux estimates we calculated using the gradient method relates to the concentration profile. We often measured higher soil CO_2 concentrations from shallow probes

than from deeper probes in the same location. When shallow concentrations are higher, the gradient method predicts negative fluxes between soil layers, and such fluxes are extrapolated to the soil surface, the resulting estimate will predict low or negative fluxes. So far as we could tell, these reversed gradients were not the result of instrumental error. Given that CO_2 is not uniformly produced in the soil and that diffusivity is not uniform throughout the soil, it is possible that shallow, high concentration areas exist. It is more likely that a clay soil with lower diffusivity will have areas where CO_2 can accumulate than a coarser textured soil. We believe this may explain why we did not always measure decreasing levels of soil CO_2 as we approached the soil surface.

As of 2018, only one study (Vargas and Allen 2008) has been published where the gradient method was used in a tropical forest to estimate soil respiration. Vargas and Allen (2008) found good agreement between chamber-based methods and the gradient method. It should be noted that the relative importance of soil forming factors were quite different from this study. Vargas and Allen (2008) measured soil respiration in shallow, alkaline, sandy soils (less than 25 cm) on young, calcareous bedrock (Natural-Resources-Conservation-Service 2016). This study was conducted on deep, acidic, clayey soils on highly, weathered sediments. Comparisons between the sites are challenging and highlights the variety of conditions found in tropical forests.

With an understanding of how a commonly implemented flux model was failing to estimate accurate CO_2 effluxes, we constructed two simple models that might better predict soil CO_2 fluxes at our site. For the two simple models, we chose to use only CO_2 concentration data from only one soil depth, 2 cm. The concentration gradient was calculated between the soil CO_2 concentration at 2 cm and a fixed value of 1000 ppm at the soil surface, thereby eliminating negative concentration gradients. For the first simple model we evaluated six commonly used diffusion models. The second simple model continued to use Moldrup et al. (1999) but the porosity was scaled down from the bulk and particle density derived 69%.

For the first simple efflux model, we evaluated all the most common diffusion models, similar to Pingintha et al. (2010), using our mean soil temperature of 24.4 °C at 2 cm, and mean soil moisture of 34 %. We continued to use a bulk density of approximately 0.80 g cm^{-3} which yields a porosity of 69%. Table 4-1 displays the results of the different diffusion models. Moldrup et al. (1997) output the lowest diffusivity of 0.51 mm^2 s^{-1}.

Model	Formula	Diffusivity (mm^2 s^{-1})
Moldrup et al. (1999)	$\xi = \Phi^2 \left(\frac{\Phi - \theta}{\Phi}\right)^{\beta S}$	4.21
Penman (1940)	$\xi = 0.66(\Phi - \theta)$	3.52
Marshall (1959)	$\xi = (\Phi - \theta)^{1.5}$	3.18
Millington and Quirk (1961)	$\xi = \frac{(\Phi - \theta)^{\frac{10}{3}}}{\Phi^2}$	1.03
Moldrup et al. (1997)	$\xi = 0.66(\Phi - \theta)\left(\frac{\Phi - \theta}{\Phi}\right)^3$	0.51
Moldrup et al. (2000)	$\xi = \frac{(\Phi - \theta)^{2.5}}{\Phi}$	1.65

Table 4-1: Soil diffusivities using six common models.

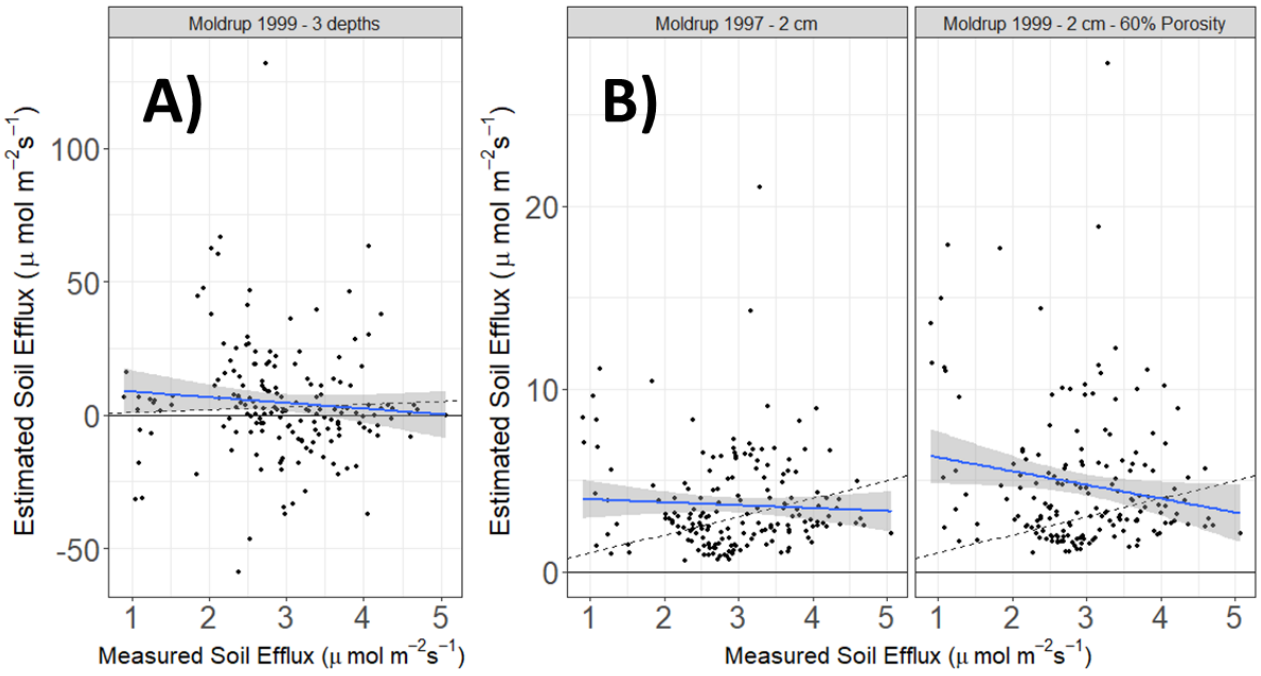

Figure 4-9: A) is the gradient method using three soil CO_2 depths and Moldrup et. al (1999). B) is the two simplified models using 2 cm soil CO_2 concentration data and different diffusion equations. Blue lines are linear regressions. Dashed lines are 1:1. X-axis is measured soil efflux using the chamber method. Y-axis is estimated soil efflux. Note each plot has different scales.

The second simple model used the diffusion model from Moldrup et al. (1999) but scaled the total porosity by a factor of 0.60. This reduced the mean porosity from 69% to 41%. Several scaling factors were tested but further reduction in the porosity would result in values lower than the soil moisture and unusable data.

The linear regression between chamber measurements and the soil efflux from the gradient method using Moldrup et al. (1999) and three concentration depths was not significant (Table 4-2) and both RMSE and MAE were relatively high.

The linear regression between the soil efflux from our simplified model using Moldrup et al. (1997) and chamber measurements was not significant (Table 4-2) but it did reduce error. The simplified model also did not estimate any negative soil effluxes (Figure 4-9). Both RMSE and MAE were almost an order of magnitude lower than the more complex Moldrup et al. (1999) based model. This indicates at

our site, the additional measurements of 8 and 16 cm soil CO_2 concentrations did not improve the estimation of soil efflux using a common implementation of the gradient method.

Table 4-2: Statistical parameters and error of different models

Model	Slope	R^2	p	F	RMSE	MAE	n
Moldrup 1999 – 3 depths	-2.124	0.00689	0.2775	1.187	21.53	14.20	173
Moldrup 1997 – 2 cm	-0.086	0.00073	0.7236	0.126	2.70	1.95	173
Moldrup 1999 – 2 cm – Scaled porosity	-0.754	0.02718	0.0302	4.778	3.81	2.68	173
Null (mean)	-	-	-	-	0.85	0.67	61

The linear regression between the chamber measurements and soil efflux from second simplified model using Moldrup et al. (1999) and scaled porosity was significant (Table 4-2). The slope, however, was negative. The RMSE and MAE of the second simplified model was higher than the first simplified model but lower than the three depth, Moldrup et al. (1999) gradient model.

Sixty-one chamber measurements could not be paired with concurrent gradient method soil efflux estimates. The mean of those 61 soil respiration measurements was 3.02 ± 0.79 µmol CO_2 m^{-2} s^{-1} and was used as our null model. The RMSE and MAE was approximately one third of the simplified models. This indicates that while simplified flux models reduced the overall error, they are less capable of predicting the temporal variation of chamber fluxes than is a mean of a subset of the chamber flux data.

The linear regressions between measured soil efflux and both simplified models, which only used the 2 cm soil CO_2 concentration, had negative slopes. Only the simplified model using scaled porosity and the diffusion equation from Moldrup et al. (1999) was significant but both models had lower RMSE and MAE than the three depth, Moldrup et al. (1999), gradient model. The negative slopes may indicate that higher soil CO_2 concentrations at 2 cm coincide with lower measured soil efflux. While this may seem counterintuitive, it may indicate that due to high clay content and relatively high soil moisture, CO_2 cannot diffuse from the soil to the atmosphere, and therefore accumulates in the soil.

Of the two simplified models, the fact that the model using the scaled porosity, reduced the error and the linear regression was significant demonstrate that the texture-based diffusion model from Moldrup et al. (1999) is not correctly parameterizing porosity in high clay soils. High clay soils often have low bulk density and therefore high total porosity (Jones 1983, Bernoux et al. 1998). But as our simplified model using scaled porosity shows, the effective porosity is likely lower.

The distance between the soil ring where soil efflux was measured using the chamber method and the soil CO_2 probes was less than 20 cm. It is possible that even at this relatively small distance, soil respiration is not consistently correlated to soil CO_2 concentrations, even the 2 cm probe in the case of our simplified model.

Logistical Challenges

Termites damage to the soil CO_2 probes proved to be an unforeseen and difficult problem. At several sampling locations after the CO_2 probe had been installed at the proper depth, ground or arboreal termites found the probe and chewed through the protective Gore-tex barrier then filled the sensor cavity with woody debris. The soil CO_2 probes have gold plated mirrors in the cavity and if they become soiled the probe is no longer useable. Several times the termites would chew through the silicone caulk, get inside the transmitters' protective 6.5 L Pelican case and overnight would fill it 10-25% with woody debris damaging the CO_2 probes transmitters.

Both the light source in the CO_2 probe and the transmitters inside the protective case give off some heat, which may create a favorable environment for termites. While we did not discover a method to deter termites from damaging the soil probe, we found that termites could be deterred from entering by placing small amounts of naphthalene-based moth balls within the protective case. However, moth balls contain naphthalene and other chemicals that have low vapor pressures, chemicals that may

damage some plastics. If using naphthalene, we recommend monitoring the transmitters so they are not damaged by the deterrent.

Data collection from temperature sensors proved problematic. By tracking when the temperature sensors failed, it was clear that rain events and the resulting moisture must have affected the electrical connections (data not shown). Even though they used the same 3.5 mm connections, the soil moisture sensors were relatively reliable. Further improvements should be made to the connections between the temperature sensors and dataloggers or, to compensate, more redundant temperature sensors could be installed. Because the soil temperature was stable, this was not as large of a problem as it would be in a temperate environment.

4.5. Conclusion

We measured soil respiration in a tropical broadleaf forest during two field campaigns using two different methodologies: 1) the well-established but labor intensive chamber method and 2) the less tested and less laborious gradient method. Soil respiration using the chamber method showed that an undisturbed forest had higher soil respiration than a disturbed forest. This was true during both the driest and wettest months of the year. However, within the undisturbed and disturbed forests, soil respiration was not significantly different between the two field campaigns. Finally, soil temperature was similar but soil moisture was 5-6% higher in the disturbed forest during the two field campaigns.

For researchers interested in measuring soil respiration in different biomes, based on this study and Pingintha et al. (2010), where relatively poor fits were found between chamber and gradient methods, the gradient method may not be suitable for high clay and wet soils. Other studies have shown this to be the case after rain events, even in xeric biomes. As true porosity decreases due to soil texture or soil moisture, two problems are likely to arise. First, it is more likely that the soil diffusivity will not be accurately represented by available empirical diffusion models. And second, there is a higher probability the soil CO_2 gradient will be abnormal.

The first problem may be remedied by making diffusion measurements on high clay, low bulk density soils over a range of soil moistures. These measurements could be used to update diffusion models, as they were not included by Moldrup et al. (1999). Abnormal soil CO_2 gradients may be an intractable problem with wet clays but it is possible that varying the CO_2 probe's depths, or measuring more depths would results in useable concentration gradients. Other studies show that gradient methods do perform well in lower moisture conditions and soils with higher sand and silt contents. Studies of soil respiration in biomes such as mesic grasslands could benefit from the gradient method, where solar power could assist in the collection of continuous data.

Acknowledgments

This study was supported by NSF (DEB-0423976), Microsoft Research, and the JHU EPS Summer Field Fund. Many thanks to Dr. Renato Valencia (Pontificia Universidad Católica del Ecuador) and to the staff at Yasuni Research Station. Many thanks to Chih-Han Chang, Michael Bernard, Doug Carlson, Jayant Gupchup, Andreas Terzis, Razvan Musaloiu-E, Alex Szalay, Jong Hyun Lim and Peter Houlihan. Thank you to Rodrigo Vargas for sharing the soil CO_2 efflux code for Matlab.

5. Conclusion

It is still unclear if the impacts of increasing CO_2 concentrations on biogeochemical cycling will result in positive feedbacks (more release of natural carbon dioxide and methane) or negative feedbacks (more uptake of carbon dioxide and decrease in CH_4 emission by the biosphere). Understanding the drivers of fluxes of CO_2 and CH_4 to the atmosphere is thus essential for improving our ability to predict future climates. Natural emissions of CO_2 are more variable and uncertain than anthropogenic emissions. Soil respiration is one of the largest natural fluxes of CO_2 to the atmosphere. Measuring and characterizing the biome specific responses of the soil system to abiotic factors remains a challenge. While *in-situ* monitoring of soil CO_2 concentrations and the gradient method have shown promise in predicting soil CO_2 efflux (Tang et al. 2003, Vargas and Allen 2008), results presented in the fourth chapter demonstrate that soils with high clay content are not suitable for the commonly implemented diffusion models. Further experiments with a larger range of soil textures and diffusivities are required to create more realistic empirical models. Chamber measurements, ideally automated chamber measurements, may be more suitable for tropical soils with high clay contents and may be a faster method for reducing soil respiration uncertainty.

Initial reports of novel CH_4 emissions from terrestrial plants(Keppler et al. 2006) were received skeptically (Dueck et al. 2007, Beerling et al. 2008) but have been since been proven to be caused by UV light, heart rot, and likely diffusion from belowground. Stem emissions have been demonstrated both in wetland and upland forests and in all three major biomes: boreal, temperate and tropical biomes. Other woody plant related emissions have also been identified, such as emissions from cryptic wetlands within the tree (Carmichael et al. 2014) and from plant (Martinson et al. 2010) and woody debris (Covey et al. 2016, Warner et al. 2017).

Many recent studies of CH_4 emissions from plants have been made possible by technological advancements in trace gas sensing. When I began measuring CH_4 fluxes in 2013, only gas chromatographs were available with precisions of approximately 100 ppb and detection limits above 500 ppb. In general, such level of precision is sufficient to measure CH_4 fluxes from wetland ecosystems but wetlands only cover a small fraction of the land surface. The currently available field-portable spectroscopic instruments, using high precision cavity ring down or off-axis integrated cavity output, can measure CH_4 with precisions of 2 ppb. These instruments can accurately and quickly measure very small flux rates seen in upland forests and allowed for the development of an automated system discussed in Chapter 2. Moreover, they cost less than the traditional gas chromatograph.

To better understand the contribution of trees to CH_4 emissions, more comprehensive studies must be conducted. Pangala et al. (2017) provides an excellent template for bridging the gap between bottom-up inventories and top-down estimates of regional CH_4 fluxes. After measuring thousands of stem CH_4 fluxes across a variety of seasonally flooded tropical forests in the Amazon basin, Pangala et al. (2017) reported flux rates that were more than two orders of magnitude larger than previously reported stem CH_4 emissions from wetland trees (Terazawa et al. 2007, Pangala et al. 2013, Pangala et al. 2015, Terazawa et al. 2015). In addition to stem CH_4 measurements, bi-weekly atmospheric concentration measurements of CH_4, CO, and SF_6 were made using aircraft during the same time. Using back-trajectory air mass and atmospheric mixing models, CH_4 fluxes could be estimated for the region. The regional CH_4 inventory based on field sampling and CH_4 fluxes from aircraft measurements were in agreement which reconciles methodological disagreements that have been observed (Frankenberg et al. 2008, Bergamaschi et al. 2009).

Though significant progress has been made in measuring and characterizing stem CH_4 emissions, many questions remain with regards to the drivers of observed patterns. I believe some of the most important questions are the following:

- Why do young tree stems release more CH_4 per unit area than mature trees in forested wetlands?
- What are the relative contributions of internal sources and belowground sources in different habitats?
- What is controlling diurnal variation in stem CH_4 fluxes and why are they not observed in some habitats?
- How does wood morphology and vascular physiology affect stem CH_4 emissions?

Answering these questions will help extrapolate results to other forested biomes, may inform existing findings regarding herbaceous plants and reduce uncertainty in the CH_4 budget.

In addition to presenting a current estimate of global CH_4 emissions, Saunois et al. (2016b) provided three suggestions for reducing uncertainty in future CH_4 budgets. First, reduce the high uncertainty in annual and decadal CH_4 emissions from natural wetlands and inland water. This can be accomplished by generating high frequency, high resolution maps of inland waters, developing mechanistic models for naturally emitting surfaces, and creating a network of flux measurements for CH_4, similarly to Fluxnet. Second, separate CH_4 sources and sinks into regions and processes by improving atmospheric observations. Possible solutions include extending the current observation network and including tracers such as ethane and isotopes of CH_4. Saunois et al. (2016b) recommended using high precision cavity ring down, off-axis integrated cavity output spectroscopic or quantum cascade laser instruments to measure CH_4 and its isotopes. Third, improve atmospheric transport and chemistry models, which they suggested could be accomplished by refining models' vertical and horizontal grids, improving hydroxyl fields, and more model inter-comparison. Finally, refining and

improving transport models will lead to more optimal placement of observation sites, which in turn will improve regional flux estimates and better separate local fluxes from distant transport.

These suggestions are generally sound. However, I would argue with the second point, i.e. extending the current observing network with high precisions instruments similar to Fluxnet. In my opinion, the signal to noise ratio of the currently available instruments is too high to identify different processes or sources using isotopic methods. This is likely the case because the precision of CH_4 concentration measurements of the best instruments is not low enough to measure the subtle CH_4 fluxes that occur in some biomes that cover relatively large areas. Kroon et al. (2010) used a flux tower with high precision, quantum cascade laser to measure CH_4 emissions from an intensely managed dairy farm located on peat soil. The flux system's lower detection limit was determined to be 196.8 μg m^{-2} h^{-1}. Pitz et al. (2018) found that in a temperate forest the upland soil's mean consumption rate was 64.8 ± 6.2 μg m^{-2} h^{-1}, (Figure 3-3) indicating that the existing flux tower systems may not be precise enough to measure CH_4 fluxes in some widespread biomes. The Amazonian sites measured by Pangala et al. (2017), however, had much higher emission rates, with the lowest emissions from the five sites totaling 3380 μg m^{-2} h^{-1}. These sites were seasonally flooded forests which makes establishing flux towers logistically challenging but the high flux rates make measurements technically feasible.

Studying sources and fluxes of CH_4 allows us to address climate change on a short time scales but the response of soil respiration to future climates could cause large changes in carbon pools. At the same time, methane's higher global warming potential and relatively short lifetime compared to CO_2, offers an opportunity to redirect current climate trajectories to lower warming scenarios such as RCP6 and RCP4.5. Therefore, understanding the processes that control CO_2 and CH_4 concentrations in the atmosphere should be a major focus for the biogeochemistry community.

References

Alvarez-Buylla, E. R., and M. Martinez-Ramos. 1990. Seed Bank Versus Seed Rain in the Regeneration of a Tropical Pioneer Tree. Oecologia **84**:314-325.

Anderson-Teixeira, K. J., S. J. Davies, A. C. Bennett, E. B. Gonzalez-Akre, H. C. Muller-Landau, S. Joseph Wright, K. Abu Salim, A. M. Almeyda Zambrano, A. Alonso, J. L. Baltzer, Y. Basset, N. A. Bourg, E. N. Broadbent, W. Y. Brockelman, S. Bunyavejchewin, D. F. R. P. Burslem, N. Butt, M. Cao, D. Cardenas, G. B. Chuyong, K. Clay, S. Cordell, H. S. Dattaraja, X. Deng, M. Detto, X. Du, A. Duque, D. L. Erikson, C. E. N. Ewango, G. A. Fischer, C. Fletcher, R. B. Foster, C. P. Giardina, G. S. Gilbert, N. Gunatilleke, S. Gunatilleke, Z. Hao, W. W. Hargrove, T. B. Hart, B. C. H. Hau, F. He, F. M. Hoffman, R. W. Howe, S. P. Hubbell, F. M. Inman-Narahari, P. A. Jansen, M. Jiang, D. J. Johnson, M. Kanzaki, A. R. Kassim, D. Kenfack, S. Kibet, M. F. Kinnaird, L. Korte, K. Kral, J. Kumar, A. J. Larson, Y. Li, X. Li, S. Liu, S. K. Y. Lum, J. A. Lutz, K. Ma, D. M. Maddalena, J.-R. Makana, Y. Malhi, T. Marthews, R. Mat Serudin, S. M. McMahon, W. J. McShea, H. R. Memiaghe, X. Mi, T. Mizuno, M. Morecroft, J. A. Myers, V. Novotny, A. A. de Oliveira, P. S. Ong, D. A. Orwig, R. Ostertag, J. den Ouden, G. G. Parker, R. P. Phillips, L. Sack, M. N. Sainge, W. Sang, K. Sri-ngernyuang, R. Sukumar, I. F. Sun, W. Sungpalee, H. S. Suresh, S. Tan, S. C. Thomas, D. W. Thomas, J. Thompson, B. L. Turner, M. Uriarte, R. Valencia, M. I. Vallejo, A. Vicentini, T. Vrška, X. Wang, X. Wang, G. Weiblen, A. Wolf, H. Xu, S. Yap, and J. Zimmerman. 2015. CTFS-ForestGEO: a worldwide network monitoring forests in an era of global change. Global Change Biology **21**:528-549.

Angel, R., P. Claus, and R. Conrad. 2012. Methanogenic archaea are globally ubiquitous in aerated soils and become active under wet anoxic conditions. Isme Journal **6**:847-862.

Asner, G. P., J. M. O. Scurlock, and J. A. Hicke. 2003. Global synthesis of leaf area index observations: implications for ecological and remote sensing studies. Global Ecology and Biogeography **12**:191-205.

Aydin, M., K. R. Verhulst, E. S. Saltzman, M. O. Battle, S. A. Montzka, D. R. Blake, Q. Tang, and M. J. Prather. 2011. Recent decreases in fossil-fuel emissions of ethane and methane derived from firn air. Nature **476**:198-201.

Baird, A. J., I. Stamp, C. M. Heppell, and S. M. Green. 2010. CH_4 flux from peatlands: a new measurement method. Ecohydrology **3**:360-367.

Baldocchi, D. 2014. Measuring fluxes of trace gases and energy between ecosystems and the atmosphere – the state and future of the eddy covariance method. Global Change Biology **20**:3600-3609.

Barba, J., A. Cueva, M. Bahn, G. A. Barron-Gaffordd, B. Bond-Lamberty, P. J. Hanson, A. Jaimes, L. Kulmala, J. Pumpanen, R. L. Scott, G. Wohlfahrt, and R. Vargas. 2018. Comparing ecosystem and soil respiration: Review and key challenges of tower-based and soil measurements. Agricultural and Forest Meteorology **249**:434-443.

Beer, C., M. Reichstein, E. Tomelleri, P. Ciais, M. Jung, N. Carvalhais, C. Rödenbeck, M. A. Arain, D. Baldocchi, G. B. Bonan, A. Bondeau, A. Cescatti, G. Lasslop, A. Lindroth, M. Lomas, S. Luyssaert, H. Margolis, K. W. Oleson, O. Roupsard, E. Veenendaal, N. Viovy, C. Williams, F. I. Woodward, and D. Papale. 2010. Terrestrial Gross Carbon Dioxide Uptake: Global Distribution and Covariation with Climate. Science **329**:834.

Beerling, D. J., T. Gardiner, G. Leggett, A. McLeod, and W. P. Quick. 2008. Missing methane emissions from leaves of terrestrial plants. Global Change Biology **14**:1821-1826.

Bergamaschi, P., C. Frankenberg, J. F. Meirink, M. Krol, M. G. Villani, S. Houweling, F. Dentener, E. J. Dlugokencky, J. B. Miller, L. V. Gatti, A. Engel, and I. Levin. 2009. Inverse modeling of global and

regional CH_4 emissions using SCIAMACHY satellite retrievals. Journal of Geophysical Research-Atmospheres **114**.

Bernoux, M., C. Cerri, D. Arrouays, C. Jolivet, and B. Volkoff. 1998. Bulk Densities of Brazilian Amazon Soils Related to Other Soil Properties. Soil Science Society of America Journal **62**:743-749.

Bond-Lamberty, B., and A. Thomson. 2010a. A global database of soil respiration data. Biogeosciences **7**:1915-1926.

Bond-Lamberty, B., and A. Thomson. 2010b. Temperature-associated increases in the global soil respiration record. Nature **464**:579-U132.

Bowden, R. D., K. J. Nadelhoffer, R. D. Boone, J. M. Melillo, and J. B. Garrison. 1993. Contributions of Aboveground Litter, Belowground Litter, and Root Respiration to Total Soil Respiration in a Temperature Mixed Hardwood Forest. Canadian Journal of Forest Research-Revue Canadienne De Recherche Forestiere **23**:1402-1407.

Brienen, R. J. W., and P. A. Zuidema. 2006. Lifetime growth patterns and ages of Bolivian rain forest trees obtained by tree ring analysis. Journal of Ecology **94**:481-493.

Brown, M. J., and G. G. Parker. 1994. Canopy Light Transmittance in a Chronosequence of Mixed-Species Deciduous Forests. Canadian Journal of Forest Research-Revue Canadienne De Recherche Forestiere **24**:1694-1703.

Brush, G. S., C. Lenk, and J. Smith. 1980. The Natural Forests of Maryland - an Explanation of the Vegetation Map of Maryland. Ecological Monographs **50**:77-&.

Bushong, F. W. 1907. Composition of Gas from Cottonwood Trees. Transactions of the Kansas Academy of Science (1903-) **21**:53.

Carmichael, M. J., E. S. Bernhardt, S. L. Brauer, and W. K. Smith. 2014. The role of vegetation in methane flux to the atmosphere: should vegetation be included as a distinct category in the global methane budget? Biogeochemistry **119**:1-24.

Chazdon, R. L., and N. Fetcher. 1984. Photosynthetic Light Environments in a Lowland Tropical Rain-Forest in Costa-Rica. Journal of Ecology **72**:553-564.

Conrad, R. 2007. Microbial ecology of methanogens and methanotrophs. Advances in Agronomy, Vol 96 **96**:1-63.

Correll, D. L., T. E. Jordan, and D. E. Weller. 2000. Dissolved silicate dynamics of the Rhode River watershed and estuary. Estuaries **23**:188-198.

Covey, K. R., C. P. B. de Mesquita, B. Oberle, D. S. Maynard, C. Bettigole, T. W. Crowther, M. C. Duguid, B. Steven, A. E. Zanne, M. Lapin, M. S. Ashton, C. D. Oliver, X. Lee, and M. A. Bradford. 2016. Greenhouse trace gases in deadwood. Biogeochemistry **130**:215-226.

Covey, K. R., S. A. Wood, R. J. Warren, X. Lee, and M. A. Bradford. 2012. Elevated methane concentrations in trees of an upland forest. Geophysical Research Letters **39**.

Curry, C. L. 2007. Modeling the soil consumption of atmospheric methane at the global scale. Global Biogeochemical Cycles **21**.

Dacey, J. W. H., and M. J. Klug. 1979. Methane Efflux from Lake-Sediments through Water Lilies. Science **203**:1253-1255.

Davidson, E. A., E. Belk, and R. D. Boone. 1998. Soil water content and temperature as independent or confounded factors controlling soil respiration in a temperate mixed hardwood forest. Global Change Biology **4**:217-227.

Davidson, E. A., K. Savage, L. V. Verchot, and R. Navarro. 2002. Minimizing artifacts and biases in chamber-based measurements of soil respiration. Agricultural and Forest Meteorology **113**:21-37.

De Simone, O., E. Muller, W. J. Junk, and W. Schmidt. 2002. Adaptations of central Amazon tree species to prolonged flooding: Root morphology and leaf longevity. Plant Biology **4**:515-522.

Dlugokencky, E. J., K. A. Masarie, P. M. Lang, and P. P. Tans. 1998. Continuing decline in the growth rate of the atmospheric methane burden. Nature **393**:447-450.

Dlugokencky, E. J., E. G. Nisbet, R. Fisher, and D. Lowry. 2011. Global atmospheric methane: budget, changes and dangers. Philosophical Transactions of the Royal Society a-Mathematical Physical and Engineering Sciences **369**:2058-2072.

do Carmo, J. B., M. Keller, J. D. Dias, P. B. de Camargo, and P. Crill. 2006. A source of methane from upland forests in the Brazilian Amazon. Geophysical Research Letters **33**.

Doff Sotta, E., P. Meir, Y. Malhi, A. Donato nobre, M. Hodnett, and J. Grace. 2004. Soil CO_2 efflux in a tropical forest in the central Amazon. Global Change Biology **10**:601-617.

Dueck, T. A., R. de Visser, H. Poorter, S. Persijn, A. Gorissen, W. de Visser, A. Schapendonk, J. Verhagen, J. Snel, F. J. M. Harren, A. K. Y. Ngai, F. Verstappen, H. Bouwmeester, L. A. C. J. Voesenek, and A. van der Werf. 2007. No evidence for substantial aerobic methane emission by terrestrial plants: a C-13-labelling approach. New Phytologist **175**:29-35.

Dutaur, L., and L. V. Verchot. 2007. A global inventory of the soil CH(4) sink. Global Biogeochemical Cycles **21**.

Etheridge, D. M., L. P. Steele, R. J. Francey, and R. L. Langenfelds. 1998. Atmospheric methane between 1000 AD and present: Evidence of anthropogenic emissions and climatic variability. Journal of Geophysical Research-Atmospheres **103**:15979-15993.

Etminan, M., G. Myhre, E. J. Highwood, and K. P. Shine. 2016. Radiative forcing of carbon dioxide, methane, and nitrous oxide: A significant revision of the methane radiative forcing. Geophysical Research Letters **43**:12614-12623.

FAO. 2016. State of the World's Forests 2016. Rome, Italy.

Frankenberg, C., P. Bergamaschi, A. Butz, S. Houweling, J. F. Meirink, J. Notholt, A. K. Petersen, H. Schrijver, T. Warneke, and I. Aben. 2008. Tropical methane emissions: A revised view from SCIAMACHY onboard ENVISAT. Geophysical Research Letters **35**.

Frankenberg, C., J. F. Meirink, M. van Weele, U. Platt, and T. Wagner. 2005. Assessing methane emissions from global space-borne observations. Science **308**:1010-1014.

Fung, I., E. Matthews, and J. Lerner. 1987. Atmospheric Methane Response to Biogenic Sources - Results from a 3-D Atmospheric Tracer Model. Abstracts of Papers of the American Chemical Society **193**:6-Geoc.

Garnet, K. N., J. P. Megonigal, C. Litchfield, and G. E. Taylor. 2005. Physiological control of leaf methane emission from wetland plants. Aquatic Botany **81**:141-155.

Gauci, V., D. J. G. Gowing, E. R. C. Hornibrook, J. M. Davis, and N. B. Dise. 2010. Woody stem methane emission in mature wetland alder trees. Atmospheric Environment **44**:2157-2160.

Gee, G. P., and J. W. Bauder. 1986. Particle-size Analysis. 2 edition. American Society of Agronomy, Madison, WI.

Hagedorn, F., and P. Bellamy. 2011. Hot spots and hot moments for greenhouse gas emissions from soils. Soil Carbon in Sensitive European Ecosystems: From Science to Land Management:13-32.

Herrmann, V., S. M. McMahon, M. Detto, J. A. Lutz, S. J. Davies, C. H. Chang-Yang, and K. J. Anderson-Teixeira. 2016. Tree Circumference Dynamics in Four Forests Characterized Using Automated Dendrometer Bands. Plos One **11**.

Higman, D. 1968. An Ecologically Annotated Checklist of the Vascular Flora at the Chesapeake Bay Center for Field Biology, with Keys.*in* O. o. E. S. Institution, editor., Washington DC.

Hothorn, T., F. Bretz, and P. Westfall. 2008. Simultaneous inference in general parametric models. Biometrical Journal **50**:346-363.

Hsieh, C. I., G. Katul, and T. Chi. 2000. An approximate analytical model for footprint estimation of scaler fluxes in thermally stratified atmospheric flows. Advances in Water Resources **23**:765-772.

IPCC. 2013. Climate Change 2013: The Physical Science Basis. Contribution of Working Group I to the Fifth Assessment Report of the Intergovernmental Panel on Climate Change. Cambridge University Press, Cambridge, United Kingdom and New York, NY, USA.

Jackson, R. B., L. A. Moore, W. A. Hoffmann, W. T. Pockman, and C. R. Linder. 1999. Ecosystem rooting depth determined with caves and DNA. Proceedings of the National Academy of Sciences of the United States of America **96**:11387-11392.

Jobbágy, E. G., and R. B. Jackson. 2000. THE VERTICAL DISTRIBUTION OF SOIL ORGANIC CARBON AND ITS RELATION TO CLIMATE AND VEGETATION. Ecological Applications **10**:423-436.

John, R., J. W. Dalling, K. E. Harms, J. B. Yavitt, R. F. Stallard, M. Mirabello, S. P. Hubbell, R. Valencia, H. Navarrete, M. Vallejo, and R. B. Foster. 2007. Soil nutrients influence spatial distributions of tropical tree species. Proceedings of the National Academy of Sciences of the United States of America **104**:864-869.

Jones, C. A. 1983. Effect of Soil Texture on Critical Bulk Densities for Root Growth. Soil Science Society of America Journal **47**:1208-1211.

Jones, H. G. 1992. Plants and Microclimate: A Quantitative Approach to Environmental Plant Physiology. Cambridge University Press.

Jung, M., M. Reichstein, P. Ciais, S. I. Seneviratne, J. Sheffield, M. L. Goulden, G. Bonan, A. Cescatti, J. Chen, R. de Jeu, A. J. Dolman, W. Eugster, D. Gerten, D. Gianelle, N. Gobron, J. Heinke, J. Kimball, B. E. Law, L. Montagnani, Q. Mu, B. Mueller, K. Oleson, D. Papale, A. D. Richardson, O. Roupsard, S. Running, E. Tomelleri, N. Viovy, U. Weber, C. Williams, E. Wood, S. Zaehle, and K. Zhang. 2010. Recent decline in the global land evapotranspiration trend due to limited moisture supply. Nature **467**:951.

Keppler, F., J. T. G. Hamilton, M. Brass, and T. Rockmann. 2006. Methane emissions from terrestrial plants under aerobic conditions. Nature **439**:187-191.

Keppler, F., J. T. G. Hamilton, W. C. McRoberts, I. Vigano, M. Brass, and T. Rockmann. 2008. Methoxyl groups of plant pectin as a precursor of atmospheric methane: evidence from deuterium labelling studies. New Phytologist **178**:808-814.

Kirschke, S., P. Bousquet, P. Ciais, M. Saunois, J. G. Canadell, E. J. Dlugokencky, P. Bergamaschi, D. Bergmann, D. R. Blake, L. Bruhwiler, P. Cameron-Smith, S. Castaldi, F. Chevallier, L. Feng, A. Fraser, M. Heimann, E. L. Hodson, S. Houweling, B. Josse, P. J. Fraser, P. B. Krummel, J. F. Lamarque, R. L. Langenfelds, C. Le Quere, V. Naik, S. O'Doherty, P. I. Palmer, I. Pison, D. Plummer, B. Poulter, R. G. Prinn, M. Rigby, B. Ringeval, M. Santini, M. Schmidt, D. T. Shindell, I. J. Simpson, R. Spahni, L. P. Steele, S. A. Strode, K. Sudo, S. Szopa, G. R. van der Werf, A. Voulgarakis, M. van Weele, R. F. Weiss, J. E. Williams, and G. Zeng. 2013. Three decades of global methane sources and sinks. Nature Geoscience **6**:813-823.

Kljun, N., P. Calanca, M. W. Rotach, and H. P. Schmid. 2004. A simple parameterisation for flux footprint predictions. Boundary-Layer Meteorology **112**:503-523.

Kormann, R., and F. X. Meixner. 2001. An analytical footprint model for non-neutral stratification. Boundary-Layer Meteorology **99**:207-224.

Kozlowski, T. T. 1997. Responses of woody plants to flooding and salinity. Tree Physiology Monograph **1**.

Kroon, P. S., A. Hensen, H. J. J. Jonker, H. G. Ouwersloot, A. T. Vermeulen, and F. C. Bosveld. 2010. Uncertainties in eddy covariance flux measurements assessed from CH_4 and N2O observations. Agricultural and Forest Meteorology **150**:806-816.

Kuzyakov, Y., and E. Blagodatskaya. 2015. Microbial hotspots and hot moments in soil: Concept & review. Soil Biology & Biochemistry **83**:184-199.

Le Quere, C., R. Moriarty, R. M. Andrew, J. G. Canadell, S. Sitch, J. I. Korsbakken, P. Friedlingstein, G. P. Peters, R. J. Andres, T. A. Boden, R. A. Houghton, J. I. House, R. F. Keeling, P. Tans, A. Arneth, D. C. E. Bakker, L. Barbero, L. Bopp, J. Chang, F. Chevallier, L. P. Chini, P. Ciais, M. Fader, R. A. Feely, T. Gkritzalis, I. Harris, J. Hauck, T. Ilyina, A. K. Jain, E. Kato, V. Kitidis, K. K. Goldewijk, C. Koven, P. Landschutzer, S. K. Lauvset, N. Lefevre, A. Lenton, I. D. Lima, N. Metzl, F. Millero, D. R. Munro, A. Murata, J. E. M. S. Nabel, S. Nakaoka, Y. Nojiri, K. O'Brien, A. Olsen, T. Ono, F. F. Perez, B. Pfeil, D. Pierrot, B. Poulter, G. Rehder, C. Rodenbeck, S. Saito, U. Schuster, J. Schwinger, R. Seferian, T. Steinhoff, B. D. Stocker, A. J. Sutton, T. Takahashi, B. Tilbrook, I. T. van der Laan-Luijkx, G. R. van der Werf, S. van Heuven, D. Vandemark, N. Viovy, A. Wiltshire, S. Zaehle, and N. Zeng. 2015. Global Carbon Budget 2015. Earth System Science Data **7**:349-396.

Lee, X., H. J. Wu, J. Sigler, C. Oishi, and T. Siccama. 2004. Rapid and transient response of soil respiration to rain. Global Change Biology **10**:1017-1026.

Lenhart, K., M. Bunge, S. Ratering, T. R. Neu, I. Schuttmann, M. Greule, C. Kammann, S. Schnell, C. Muller, H. Zorn, and F. Keppler. 2012. Evidence for methane production by saprotrophic fungi. Nature Communications **3**.

Lenhart, K., B. Weber, W. Elbert, J. Steinkamp, T. Clough, P. Crutzen, U. Pöschl, and F. Keppler. 2015. Nitrous oxide and methane emissions from cryptogamic covers. Global Change Biology:n/a-n/a.

Machacova, K., J. Bäck, A. Vanhatalo, E. Halmeenmäki, P. Kolari, I. Mammarella, J. Pumpanen, M. Acosta, O. Urban, and M. Pihlatie. 2016. Pinus sylvestris as a missing source of nitrous oxide and methane in boreal forest. Scientific Reports **6**:23410.

Mahecha, M. D., M. Reichstein, N. Carvalhais, G. Lasslop, H. Lange, S. I. Seneviratne, R. Vargas, C. Ammann, M. A. Arain, A. Cescatti, I. A. Janssens, M. Migliavacca, L. Montagnani, and A. D. Richardson. 2010. Global Convergence in the Temperature Sensitivity of Respiration at Ecosystem Level. Science **329**:838.

Maier, M., K. Machacova, F. Lang, K. Svobodova, and O. Urban. 2017. Combining soil and tree-stem flux measurements and soil gas profiles to understand CH_4 pathways in Fagus sylvatica forests. Journal of Plant Nutrition and Soil Science:n/a-n/a.

Maier, M., and H. Schack-Kirchner. 2014. Using the gradient method to determine soil gas flux: A review. Agricultural and Forest Meteorology **192**:78-95.

Marshall, T. J. 1959. The Diffusion of Gases through Porous Media. Journal of Soil Science **10**:79-82.

Martinson, G. O., F. A. Werner, C. Scherber, R. Conrad, M. D. Corre, H. Flessa, K. Wolf, M. Klose, S. R. Gradstein, and E. Veldkamp. 2010. Methane emissions from tank bromeliads in neotropical forests. Nature Geoscience **3**:766-769.

Matthews, E., and I. Fung. 1987. Methane Emission from Natural Wetlands: Global Distribution, Area, and Environmental Characteristics of Sources. Global Biogeochemical Cycles **1**:61-86.

Mayer, H. P., and R. Conrad. 1990. Factors Influencing the Population of Methanogenic Bacteria and the Initiation of Methane Production Upon Flooding of Paddy Soil. Fems Microbiology Ecology **73**:103-111.

McClain, M. E., E. W. Boyer, C. L. Dent, S. E. Gergel, N. B. Grimm, P. M. Groffman, S. C. Hart, J. W. Harvey, C. A. Johnston, E. Mayorga, W. H. McDowell, and G. Pinay. 2003. Biogeochemical hot spots and hot moments at the interface of terrestrial and aquatic ecosystems. Ecosystems **6**:301-312.

Megonigal, J. P., W. H. Conner, S. Kroeger, and R. R. Sharitz. 1997. Aboveground production in Southeastern floodplain forests: A test of the subsidy-stress hypothesis. Ecology **78**:370-384.

Megonigal, J. P., and A. B. Guenther. 2008. Methane emissions from upland forest soils and vegetation. Tree Physiology **28**:491-498.

Megonigal, J. P., M. E. Hines, and P. T. Visscher. 2004. Anaerobic Metabolism: Linkages to Trace Gases and Aerobic Processes. Pages 317-424 *in* W. H. Schlesinger, editor. Biogeochemistry. Elsevier-Pergamon, Oxford, UK.

Millington, R., and J. P. Quirk. 1961. Permeability of Porous Solids. Transactions of the Faraday Society **57**:1200-&.

Moldrup, P., T. Olesen, J. Gamst, P. Schjonning, T. Yamaguchi, and D. E. Rolston. 2000. Predicting the gas diffusion coefficient in repacked soil: Water-induced linear reduction model. Soil Science Society of America Journal **64**:1588-1594.

Moldrup, P., T. Olesen, D. E. Rolston, and T. Yamaguchi. 1997. Modeling diffusion and reaction in soils .7. Predicting gas and ion diffusivity in undisturbed and sieved soils. Soil Science **162**:632-640.

Moldrup, P., T. Olesen, T. Yamaguchi, P. Schjonning, and D. E. Rolston. 1999. Modeling diffusion and reaction in soils: IX. The Buckingham-Burdine-Campbell equation for gas diffusivity in undisturbed soil. Soil Science **164**:542-551.

Molina, P. X., G. P. Asner, M. F. Abadia, J. C. O. Manrique, L. A. S. Diez, and R. Valencia. 2016. Spatially-Explicit Testing of a General Aboveground Carbon Density Estimation Model in aWestern Amazonian Forest Using Airborne LiDAR. Remote Sensing **8**.

Montgomery, R. A., and R. L. Chazdon. 2001. Forest structure, canopy architecture, and light transmittance in tropical wet forests. Ecology **82**:2707-2718.

Moyano, F. E., S. Manzoni, and C. Chenu. 2013. Responses of soil heterotrophic respiration to moisture availability: An exploration of processes and models. Soil Biology & Biochemistry **59**:72-85.

Myklebust, M. C., L. E. Hipps, and R. J. Ryel. 2008. Comparison of eddy covariance, chamber, and gradient methods of measuring soil CO_2 efflux in an annual semi-arid grass, Bromus tectorum. Agricultural and Forest Meteorology **148**:1894-1907.

Natural-Resources-Conservation-Service. 2016. Web Soil Survey.

Neubauer, S. C., and J. P. Megonigal. 2015. Moving Beyond Global Warming Potentials to Quantify the Climatic Role of Ecosystems. Ecosystems **18**:1000-1013.

Nisbet, E. G., E. J. Dlugokencky, M. R. Manning, D. Lowry, R. E. Fisher, J. L. France, S. E. Michel, J. B. Miller, J. W. C. White, B. Vaughn, P. Bousquet, J. A. Pyle, N. J. Warwick, M. Cain, R. Brownlow, G. Zazzeri, M. Lanoiselle, A. C. Manning, E. Gloor, D. E. J. Worthy, E. G. Brunke, C. Labuschagne, E. W. Wolff, and A. L. Ganesan. 2016. Rising atmospheric methane: 2007-2014 growth and isotopic shift. Global Biogeochemical Cycles **30**:1356-1370.

Pan, Y. D., R. A. Birdsey, J. Y. Fang, R. Houghton, P. E. Kauppi, W. A. Kurz, O. L. Phillips, A. Shvidenko, S. L. Lewis, J. G. Canadell, P. Ciais, R. B. Jackson, S. W. Pacala, A. D. McGuire, S. L. Piao, A. Rautiainen, S. Sitch, and D. Hayes. 2011. A Large and Persistent Carbon Sink in the World's Forests. Science **333**:988-993.

Pangala, S. R., A. Enrich-Prast, L. S. Basso, R. B. Peixoto, D. Bastviken, E. R. C. Hornibrook, L. V. Gatti, H. Marotta, L. S. B. Calazans, C. M. Sakuragui, W. R. Bastos, O. Malm, E. Gloor, J. B. Miller, and V. Gauci. 2017. Large emissions from floodplain trees close the Amazon methane budget. Nature **552**:230-+.

Pangala, S. R., D. J. Gowing, E. R. C. Hornibrook, and V. Gauci. 2014. Controls on methane emissions from Alnus glutinosa saplings. New Phytologist **201**:887-896.

Pangala, S. R., E. R. C. Hornibrook, D. J. Gowing, and V. Gauci. 2015. The contribution of trees to ecosystem methane emissions in a temperate forested wetland. Global Change Biology:n/a-n/a.

Pangala, S. R., S. Moore, E. R. C. Hornibrook, and V. Gauci. 2013. Trees are major conduits for methane egress from tropical forested wetlands. New Phytologist **197**:524-531.

Parker, G. G., and D. J. Tibbs. 2004. Structural phenology of the leaf community in the canopy of a Liriodendron tulipifera L. forest in Maryland, USA. Forest Science **50**:387-397.

Penman, H. L. 1940. Gas and vapour movements in the soil I. The diffusion of vapours through porous solids. Journal of Agricultural Science **30**:437-462.

Pingintha, N., M. Y. Leclerc, J. P. Beasley, G. S. Zhang, and C. Senthong. 2010. Assessment of the soil CO_2 gradient method for soil CO_2 efflux measurements: comparison of six models in the calculation of the relative gas diffusion coefficient. Tellus Series B-Chemical and Physical Meteorology **62**:47-58.

Pitz, S., and J. P. Megonigal. 2017. Temperate forest methane sink diminished by tree emissions. New Phytologist:n/a-n/a.

Pitz, S. L., J. P. Megonigal, C. H. Chang, and K. Szlavecz. 2018. Methane fluxes from tree stems and soils along a habitat gradient. Biogeochemistry **137**:307-320.

Pulliam, W. M. 1992. Methane Emissions from Cypress Knees in a Southeastern Floodplain Swamp. Oecologia **91**:126-128.

R Core Team. 2014. R: A language and environment for statistical computing. R Foundation for Statistical Computing, Vienna, Austria.

Raich, J. W., C. S. Potter, and D. Bhagawati. 2002. Interannual variability in global soil respiration, 1980-94. Global Change Biology **8**:800-812.

Rice, A. L., C. L. Butenhoff, M. J. Shearer, D. Teama, T. N. Rosenstiel, and M. A. K. Khalil. 2010. Emissions of anaerobically produced methane by trees. Geophysical Research Letters **37**.

Riveros-Iregui, D. A., B. L. McGlynn, H. E. Epstein, and D. L. Welsch. 2008. Interpretation and evaluation of combined measurement techniques for soil CO_2 efflux: Discrete surface chambers and continuous soil CO_2 concentration probes. Journal of Geophysical Research-Biogeosciences **113**.

Rusch, H., and H. Rennenberg. 1998. Black alder (Alnus glutinosa (L.) Gaertn.) trees mediate methane and nitrous oxide emission from the soil to the atmosphere. Plant and Soil **201**:1-7.

Rustad, L. E., J. L. Campbell, G. M. Marion, R. J. Norby, M. J. Mitchell, A. E. Hartley, J. H. C. Cornelissen, J. Gurevitch, and Gcte-News. 2001. A meta-analysis of the response of soil respiration, net

nitrogen mineralization, and aboveground plant growth to experimental ecosystem warming. Oecologia **126**:543-562.

Ryan, M. G. 1990. Growth and Maintenance Respiration in Stems of Pinus-Contorta and Picea-Engelmannii. Canadian Journal of Forest Research-Revue Canadienne De Recherche Forestiere **20**:48-57.

Saunois, M., P. Bousquet, B. Poulter, A. Peregon, P. Ciais, J. G. Canadell, E. J. Dlugokencky, G. Etiope, D. Bastviken, S. Houweling, G. Janssens-Maenhout, F. N. Tubiello, S. Castaldi, R. B. Jackson, M. Alexe, V. K. Arora, D. J. Beerling, P. Bergamaschi, D. R. Blake, G. Brailsford, V. Brovkin, L. Bruhwiler, C. Crevoisier, P. Crill, K. Covey, C. Curry, C. Frankenberg, N. Gedney, L. Hoglund-Isaksson, M. Ishizawa, A. Ito, F. Joos, H. S. Kim, T. Kleinen, P. Krummel, J. F. Lamarque, R. Langenfelds, R. Locatelli, T. Machida, S. Maksyutov, K. C. McDonald, J. Marshall, J. R. Melton, I. Morino, V. Naik, S. O'Doherty, F. J. W. Parmentier, P. K. Patra, C. H. Peng, S. S. Peng, G. P. Peters, I. Pison, C. Prigent, R. Prinn, M. Ramonet, W. J. Riley, M. Saito, M. Santini, R. Schroeder, I. J. Simpson, R. Spahni, P. Steele, A. Takizawa, B. F. Thornton, H. Q. Tian, Y. Tohjima, N. Viovy, A. Voulgarakis, M. van Weele, G. R. van der Werf, R. Weiss, C. Wiedinmyer, D. J. Wilton, A. Wiltshire, D. Worthy, D. Wunch, X. Y. Xu, Y. Yoshida, B. Zhang, Z. Zhang, and Q. Zhu. 2016a. The global methane budget 2000-2012. Earth System Science Data **8**:697-751.

Saunois, M., R. B. Jackson, P. Bousquet, B. Poulter, and J. G. Canadell. 2016b. The growing role of methane in anthropogenic climate change. Environmental Research Letters **11**.

Savva, Y., K. Szlavecz, D. Carlson, J. Gupchup, A. Szalay, and A. Terzis. 2013. Spatial patterns of soil moisture under forest and grass land cover in a suburban area, in Maryland, USA. Geoderma **192**:202-210.

Schaefer, H., S. E. M. Fletcher, C. Veidt, K. R. Lassey, G. W. Brailsford, T. M. Bromley, E. J. Dlugokencky, S. E. Michel, J. B. Miller, I. Levin, D. C. Lowe, R. J. Martin, B. H. Vaughn, and J. W. C. White. 2016. A

21st-century shift from fossil-fuel to biogenic methane emissions indicated by (CH_4)-C-13. Science **352**:80-84.

Schenk, H. J., and R. B. Jackson. 2002. Rooting depths, lateral root spreads and below-ground/above-ground allometries of plants in water-limited ecosystems. Journal of Ecology **90**:480-494.

Schlesinger, W. H. 2013. Biogeochemistry : an analysis of global change.*in* E. S. Bernhardt, editor.

Schwendenmann, L., and E. Veldkamp. 2006. Long-term CO_2 production from deeply weathered soils of a tropical rain forest: evidence for a potential positive feedback to climate warming. Global Change Biology **12**:1878-1893.

Schwietzke, S., O. A. Sherwood, L. M. P. B. Ruhwiler, J. B. Miller, G. Etiope, E. J. Dlugokencky, S. E. Michel, V. A. Arling, B. H. Vaughn, J. W. C. White, and P. P. Tans. 2016. Upward revision of global fossil fuel methane emissions based on isotope database. Nature **538**:88-91.

Scott-Denton, L. E., T. N. Rosenstiel, and R. K. Monson. 2006. Differential controls by climate and substrate over the heterotrophic and rhizospheric components of soil respiration. Global Change Biology **12**:205-216.

Shoemaker, J. K., T. F. Keenan, D. Y. Hollinger, and A. D. Richardson. 2014. Forest ecosystem changes from annual methane source to sink depending on late summer water balance. Geophysical Research Letters **41**:673-679.

Siegenthaler, A., B. Welch, S. R. Pangala, M. Peacock, and V. Gauci. 2016. Technical Note: Semi-rigid chambers for methane gas flux measurements on tree stems. Biogeosciences **13**:1197-1207.

Simpson, I. J., M. P. S. Andersen, S. Meinardi, L. Bruhwiler, N. J. Blake, D. Helmig, F. S. Rowland, and D. R. Blake. 2012. Long-term decline of global atmospheric ethane concentrations and implications for methane. Nature **488**:490-494.

Sorz, J., and P. Hietz. 2006. Gas diffusion through wood: implications for oxygen supply. Trees-Structure and Function **20**:34-41.

Spahni, R., R. Wania, L. Neef, M. van Weele, I. Pison, P. Bousquet, C. Frankenberg, P. N. Foster, F. Joos, I. C. Prentice, and P. van Velthoven. 2011. Constraining global methane emissions and uptake by ecosystems. Biogeosciences **8**:1643-1665.

Sundqvist, E., P. Crill, M. Molder, P. Vestin, and A. Lindroth. 2012. Atmospheric methane removal by boreal plants. Geophysical Research Letters **39**.

Suseela, V., R. T. Conant, M. D. Wallenstein, and J. S. Dukes. 2012. Effects of soil moisture on the temperature sensitivity of heterotrophic respiration vary seasonally in an old-field climate change experiment. Global Change Biology **18**:336-348.

Tang, J. W., and D. D. Baldocchi. 2005. Spatial-temporal variation in soil respiration in an oak-grass savanna ecosystem in California and its partitioning into autotrophic and heterotrophic components. Biogeochemistry **73**:183-207.

Tang, J. W., D. D. Baldocchi, Y. Qi, and L. K. Xu. 2003. Assessing soil CO_2 efflux using continuous measurements of CO_2 profiles in soils with small solid-state sensors. Agricultural and Forest Meteorology **118**:207-220.

Terazawa, K., S. Ishizuka, T. Sakatac, K. Yamada, and M. Takahashi. 2007. Methane emissions from stems of Fraxinus mandshurica var. japonica trees in a floodplain forest. Soil Biology & Biochemistry **39**:2689-2692.

Terazawa, K., K. Yamada, Y. Ohno, T. Sakata, and S. Ishizuka. 2015. Spatial and temporal variability in methane emissions from tree stems of Fraxinus mandshurica in a cool-temperate floodplain forest. Biogeochemistry **123**:349-362.

Teskey, R. O., A. Saveyn, K. Steppe, and M. A. McGuire. 2008. Origin, fate and significance of CO_2 in tree stems. New Phytologist **177**:17-32.

Tiner, R. W., and D. G. Burke. 1995. Wetlands of Maryland. Page 193 *in* E. S. US Fish and Wildlife Service, Region 5, editor. US Fish and Wildlife Service, Ecological Services, Region 5, Hadley, MA and Maryland Department of Natural Resources, Annapolis, MD.

Topp, E., and E. Pattey. 1997. Soils as sources and sinks for atmospheric methane. Canadian Journal of Soil Science **77**:167-178.

Tuomisto, H., A. D. Poulsen, K. Ruokolainen, R. C. Moran, C. Quintana, J. Celi, and G. Canas. 2003. Linking floristic patterns with soil heterogeneity and satellite imagery in Ecuadorian Amazonia. Ecological Applications **13**:352-371.

Ullah, S., and T. R. Moore. 2011. Biogeochemical controls on methane, nitrous oxide, and carbon dioxide fluxes from deciduous forest soils in eastern Canada. Journal of Geophysical Research-Biogeosciences **116**.

Valencia, R., R. B. Foster, G. Villa, R. Condit, J. C. Svenning, C. Hernandez, K. Romoleroux, E. Losos, E. Magard, and H. Balslev. 2004. Tree species distributions and local habitat variation in the Amazon: large forest plot in eastern Ecuador. Journal of Ecology **92**:214-229.

Vann, C. D., and J. P. Megonigal. 2003. Elevated CO_2 and water depth regulation of methane emissions: Comparison of woody and non-woody wetland plant species. Biogeochemistry **63**:117-134.

Vargas, R., and M. F. Allen. 2008. Diel patterns of soil respiration in a tropical forest after Hurricane Wilma. Journal of Geophysical Research-Biogeosciences **113**.

Vicca, S., M. Bahn, M. Estiarte, E. E. van Loon, R. Vargas, G. Alberti, P. Ambus, M. A. Arain, C. Beier, L. P. Bentley, W. Borken, N. Buchmann, S. L. Collins, G. de Dato, J. S. Dukes, C. Escolar, P. Fay, G. Guidolotti, P. J. Hanson, A. Kahmen, G. Kroel-Dulay, T. Ladreiter-Knauss, K. S. Larsen, E. Lellei-Kovacs, E. Lebrija-Trejos, F. T. Maestre, S. Marhan, M. Marshall, P. Meir, Y. Miao, J. Muhr, P. A. Niklaus, R. Ogaya, J. Penuelas, C. Poll, L. E. Rustad, K. Savage, A. Schindlbacher, I. K. Schmidt, A. R. Smith, E. D. Sotta, V. Suseela, A. Tietema, N. van Gestel, O. van Straaten, S. Wan, U. Weber,

and I. A. Janssens. 2014. Can current moisture responses predict soil CO_2 efflux under altered precipitation regimes? A synthesis of manipulation experiments. Biogeosciences **11**:2991-3013.

Vigano, I., H. van Weelden, R. Holzinger, F. Keppler, A. McLeod, and T. Rockmann. 2008. Effect of UV radiation and temperature on the emission of methane from plant biomass and structural components. Biogeosciences **5**:937-947.

von Fischer, J. C., and L. O. Hedin. 2002. Separating methane production and consumption with a field-based isotope pool dilution technique. Global Biogeochemical Cycles **16**.

von Fischer, J. C., and L. O. Hedin. 2007. Controls on soil methane fluxes: Tests of biophysical mechanisms using stable isotope tracers. Global Biogeochemical Cycles **21**.

Wang, Z. P., Q. Gu, F. D. Deng, J. H. Huang, J. P. Megonigal, Q. Yu, X. T. Lu, L. H. Li, S. Chang, Y. H. Zhang, J. C. Feng, and X. G. Han. 2016. Methane emissions from the trunks of living trees on upland soils. New Phytologist **211**:429-439.

Warner, D. L., S. Villarreal, K. McWilliams, S. Inamdar, and R. Vargas. 2017. Carbon Dioxide and Methane Fluxes From Tree Stems, Coarse Woody Debris, and Soils in an Upland Temperate Forest. Ecosystems:1-12.

Wood, T. E., M. Detto, and W. L. Silver. 2013. Sensitivity of Soil Respiration to Variability in Soil Moisture and Temperature in a Humid Tropical Forest. Plos One **8**.

Yesilonis, I., K. Szlavecz, R. Pouyat, D. Whigham, and L. Xia. 2016. Historical land use and stand age effects on forest soil properties in the Mid-Atlantic US. Forest Ecology and Management **370**:83-92.

Yu, K. W., S. P. Faulkner, and M. J. Baldwin. 2008. Effect of hydrological conditions on nitrous oxide, methane, and carbon dioxide dynamics in a bottomland hardwood forest and its implication for soil carbon sequestration. Global Change Biology **14**:798-812.

Zeikus, J. G., and J. C. Ward. 1974. Methane Formation in Living Trees: A Microbial Origin. Science **184**:1181-1183.

Biography

Scott Pitz was born in 1982 in Pennsylvania, USA.

Scott completed is undergraduate work at Johns Hopkins University in 2004, returned in 2008 as a research assistant and in 2009 began his PhD. When he started working for Dr. Katalin Szlavecz in April of 2008 the department van, a 1998 Ford Econoline 350, had only 57,000 miles on it. He has, conservatively, put 40,000 miles on the van's odometer while traveling to and from the field, making him the all-time record holder of… Earth and Planetary Sciences van driving. As of the date of this submission, it still runs like a dream. He is sorry about the carbon footprint and will try to make it up somehow in his next job but will miss all the good conversations had while stuck in traffic on I-97.